

Dissertation zur Erlangung des Doktorgrades
der Fakultät für Chemie und Pharmazie
der Ludwig-Maximilians-Universität München

**Role of the RNA-binding protein Roquin in
immune homeostasis and autoimmunity**

Arianna Bertossi

aus

Udine, Italy

2011

Erklärung

Diese Dissertation wurde im Sinne von § 13 Abs. 3 bzw. 4 der Promotionsordnung vom 29. Januar 1998 (in der Fassung der sechsten Änderungssatzung vom 16. August 2010) von Herrn Prof. Dr. Reinhard Fässler betreut.

Ehrenwörtliche Versicherung

Diese Dissertation wurde selbständig, ohne unerlaubte Hilfe erarbeitet.

München, am 05.11.2011

(Arianna Bertossi)

Dissertation eingereicht am 10.11.2011
1. Gutachter: Prof. Dr. Reinhard Fässler
2. Gutachter: Prof. Dr. Ludger Klein
Mündliche Prüfung am 07.12.2011

Table of contents

TABLE OF CONTENTS	I
LIST OF PUBLICATIONS	II
ABBREVIATION	III
SUMMARY	V
INTRODUCTION	1
1 THE RNA-BINDING PROTEIN ROQUIN	1
1.1 OVERVIEW OF ROQUIN	1
1.2 THE SANROQUE MOUSE STRAIN	3
1.3 CONTROL OF mRNA STABILITY IN THE IMMUNE SYSTEM	5
1.3.1 Pathways of mRNA degradation	5
1.3.2 Control of mRNA stability in the immune system	9
2 TOLERANCE AND AUTOIMMUNITY	11
2.1 T CELL TOLERANCE	11
2.1.1 T cell development in the thymus	11
2.1.2 Central T cell tolerance	12
2.1.3 Peripheral T cell tolerance	14
2.1.3.1 T cell intrinsic mechanisms of peripheral T cell tolerance	14
2.1.3.2 T cell extrinsic mechanisms of peripheral tolerance	16
2.2 B CELL TOLERANCE	17
2.2.1 B cell development and tolerance in the bone marrow	17
2.2.2 B cell maturation and peripheral B cell tolerance	20
2.2.2.1 B cell maturation	20
2.2.2.2 Peripheral mechanisms of B cell tolerance	21
3 ANTIBODY- AND CELL-MEDIATED IMMUNITY	22
3.1 MATURE B CELL DIFFERENTIATION	22
3.2 THE GERMINAL CENTER REACTION	23
3.3 CELL-MEDIATED RESPONSES	25
4 SYSTEMIC LUPUS ERYTHEMATOSUS	28
4.1 SYSTEMIC LUPUS ERYTHEMATOSUS IN GENERAL	28
4.2 THE ETIOLOGY OF SYSTEMIC LUPUS ERYTHEMATOSUS	30
AIM OF THE THESIS	32
BRIEF SUMMARIES OF THE PUBLICATIONS	33
ACKNOWLEDGEMENT	35
CURRICULUM VITAE	36
REFERENCES	37
SUPPLEMENTS	47

List of publications

The thesis is based on the following publications which are referred to in the text by their Roman numerals (I–II):

- I. Yuanyuan Chu, J. Christoph Vahl, Dilip Kumar, Klaus Heger, **Arianna Bertossi**, Edyta Wójtowicz, Valeria Soberon, Dominik Schenten, Brigitte Mack, Miriam Reutelshöfer, Rudi Beyaert, Kerstin Amann, Geert van Loo and Marc Schmidt-Supprian

B cells lacking the tumor suppressor TNFAIP3/A20 display impaired differentiation and hyperactivation and cause inflammation and autoimmunity in aged mice.

Blood (2011) vol. 117 (7) pp. 2227-36

- II. **Arianna Bertossi**, Martin Aichinger, Paola Sansonetti, Maciej Lech, Frauke Neff, Martin Pal, F. Thomas Wunderlich, Hans-Joachim Anders, Ludger Klein and Marc Schmidt-Supprian

Loss of Roquin induces early death and immune deregulation but not autoimmunity.

Journal of Experimental Medicine (2011) pp. 1-15

Abbreviation

Aa	aminoacid	FasL	Fas ligand
Ago	argonaute	FcR	Fc receptor
AICD	activation induced cell death	Fc γ R	Fc receptor for IgG
AID	activation-induced cytidine deaminase	FDC	follicular dendritic cell
AIRE	autoimmune regulator	FO	follicular
AKT	protein kinase B	GC	germinal center
ALPS	autoimmune lymphoproliferative syndrome	GDP	guanosine diphosphate
AMD	ARE-mediated decay	GEF	guanine nucleotide exchange factor
ANA	anti-nuclear antibody	GM-CSF	granulocyte-macrophage colony-stimulating factor
AP1	activator binding protein 1	GTP	guanosine triphosphate
APC	antigen presenting cell	HLA	human leukocyte antigen
ARE	AU-rich element	ICOS	T cell inducible co-stimulator
ARE-BP	ARE-binding protein	ICOSL	ICOS ligand
BAFF	B cell activator factor	Ig	immunoglobulin
BAFF-R	BAFF receptor	IGF	insulin-like growth factor
BCR	B cell receptor	IKK1	I κ B kinase-1/ α
CBL-B	casitas B-lineage lymphoma	IL	interleukin
CCL	CC-chemokine ligand	INF	interferon
CCR	CC-chemokine receptor	IPEX	immune dysregulation, polyendocrinopathy, enteropathy, X-linked syndrome
CD40L	CD40 ligand	I κ B	inhibitor of NF- κ B
CMP	common myeloid precursors	LPS	lipopolysaccharide
CSR	class switch recombination	LT-HSC	long term-hematopoietic stem cell
cTEC	cortical thymic epithelial cell	LT- α	lymphotoxin- α
CTL	cytotoxic T lymphocyte	mAb	monoclonal antibody
CTLA-4	cytotoxic T-lymphocyte-associated antigen 4	MAPK	mytogen-activated protein kinase
CXCL	CXC-chemokine ligand	MBL	mannose-binding lectin
CXCR	CXC-chemokine receptor	MHC	major histocompatibility complex
DAMP	damage associated molecular patterns	miRNA	microRNA
DC	dendritic cell	Mnab	membrane-associated nucleic acid binding protein
DN	double negative	MPEC	memory precursors effector cell
DNA	deoxyribonucleic acid	MPP	multipotent progenitor
DP	double positive	mRNA	messenger RNA
ds-DNA	double-stranded DNA	mRNP	mRNA-protein complexes
ds-siRNA	double-stranded siRNA	mTEC	medullary thymic epithelial cell
EBV	epstein-barr virus	MZ	marginal zone
eIF4G	eukaryotic initiation factor 4G	ncRNA	non coding RNA
EJC	exon-junction complex	NF- κ B	nuclear factor- κ B
ENU	ethylnitrosourea		
ERK	extracellular signal-regulated kinase		

Abbreviations

NFAT	nuclear factor of activated T cells	SL-HSC	short-lived hematopoietic stem cell
NK	natural killer	SLC	surrogate light chain
NMD	nonsense-mediated decay	SLE	systemic lupus erythematosus
Nt	nucleotide	SLEC	short-lived effector cell
PAMP	pathogen associated molecular pattern	snRNA	small nuclear RNA
PB	P-body	SOS	son of sevenless
PD-1	programmed death 1	SP	single positive
PI3K	phosphoinositide-3 kinase	T _{CM}	T central memory
PKC	protein kinase C	TCR	T cell receptor
PRR	pattern-recognition receptor	Tcra	T cell receptor locus α
RAG	recombination-activating gene	Tcrb	T cell receptor locus β
RISC	RNA-induced silencing complex	TD	thymus-dependent
RNA	ribonucleic acid	T _{EM}	T effector memory cell
RNAi	RNA interference	T _{FH}	T follicular helper cell
San	sanroque	T _h	T helper cell
SG	stress granule	T _h 2	CD4 T helper type 2 cell
SHM	somatic hypermutation	TI	thymus-independent
siRNA	short-interfering RNA	TLR	toll-like receptor
		TNF	tumor necrosis factor
		T _{reg}	T regulatory cell
		TTP	tristetraprolin
		UTR	untranslated region

Summary

The immune system of mammals and birds has the potential to generate millions of cellular receptors that can sense invading pathogens. On lymphocytes, this large range of specificities has the potential to recognize components of the own organism, and several self-tolerance mechanisms have evolved to control the activity of the autoreactive cells. Defects in tolerance pathways have been described in several autoimmune diseases. Systemic lupus erythematosus is a multi-organ autoimmune disorder which has been linked with defects in several components of the immune system and several genetic alterations have been shown to predispose to lupus in humans. Recently, abnormal expansion of the follicular helper T cell subset in humans has been associated with systemic lupus erythematosus, and in mice the RNA-binding protein Roquin was proposed to exert an important role in preventing aberrant activation of these cells.

To examine its precise mechanism-of-action in the immune system we generated a Roquin conditional knockout allele (Paper II). Complete loss of Roquin caused perinatal lethality with spinal cord defects and insufficiently ventilated lungs. Surprisingly, loss of Roquin specifically in the T cell compartment, in the entire hematopoietic system, or in the whole organism, did not lead to autoimmunity. This result is in contrast to the sanroque mouse model, in which a point mutation in the Roquin gene causes aberrant follicular helper T cell expansion and development of a lupus-like autoimmune disorder. Specific ablation of Roquin in T and in B cells, however, caused specific perturbations in the immune homeostasis. Loss of Roquin in T lymphocytes leads to expansion of effector-like CD8 T cells which phenotypically resemble short-lived effector cells. Moreover, expansion of eosinophils and macrophages/monocytes was also observed following deletion of Roquin in T cells. Furthermore, we analyzed the effects of Roquin ablation in the B cell compartment. In these mice immune homeostasis was impaired. In particular, expansion of total B, regulatory T, activated CD4 and CD8 T, and germinal center B cells was described. These results indicate that in the hematopoietic system Roquin is instrumental in maintaining immune homeostasis, and that loss of Roquin alone is not sufficient to break tolerance to self.

Recently, polymorphisms and mutations in the gene encoding for A20 (*Tnfaip3*), a negative regulator of NF- κ B pathway, have been described in lupus patients. To study B cell intrinsic functions of A20 during B cell development and activation, and to understand its possible role in preventing autoimmune manifestations, we employed a conditional *Tnfaip3* knockout mouse model (Paper I). Ablation of A20 in

B lymphocytes reduced their activation threshold and increased their proliferation and survival in response to pathogenic stimuli. Furthermore, together with autoimmune pathology and inflammation, we observed increased levels of class-switched auto-antibodies in old A20 B cell specific knock out mice. In conclusion, specific loss of A20 in B cells is sufficient to cause an inflammatory syndrome and to break tolerance to self.

Introduction

1 The RNA-binding protein Roquin

Control of mRNA stability has emerged as a key mechanism to control gene expression, and RNA-binding proteins play important roles in maintaining immune homeostasis. Vinuesa and colleagues [5], [6], [7] described the RNA-binding protein Roquin [8], a novel RING-type E3 ubiquitin ligase family member that also contains a CCCH-type zinc finger domain. A mouse strain harboring a single point mutation in Roquin, the sanroque mouse, is characterized by a severely compromised immune system and it develops a spontaneous lupus-like autoimmune syndrome at young age. In the sanroque mice, the hypomorphic mutant of Roquin (Roquin^{san}) fails to control the expression of the T cell inducible co-stimulator ICOS [6], an important regulator of T lymphocyte activation. Ectopic expression of ICOS on naive T cells was proposed to induce spontaneous differentiation and/or expansion of follicular helper T (T_{FH}) cells. The T_{FH} cells in turn trigger germinal center B cell responses to self-antigens with ensuing autoantibody production and autoimmunity [5], [6], [9]. According to this model, inhibiting ICOS expression on naive T cells represents a key checkpoint in the maintenance of immunological tolerance.

1.1 Overview of Roquin

Roquin is a 1130aa long intracellular protein. It is highly conserved from invertebrates to mammals and its transcript has been ubiquitously detected in different organs [5]. The gene encoding for Roquin, *Rc3h1*, is located on chromosome 1 in both humans and mice. The amino-terminus of the protein harbors a RING finger domain suggesting E3-ubiquitin ligase activity. Carboxy-terminal to the RING-finger follow a so-called ROQ domain and the CCCH-zinc finger domains responsible for Roquin's ability to bind RNA [8]. The ROQ domain is a ~ 200 aa long, highly conserved domain (94% identity at the protein level) present only in Roquin and its paralogue membrane-associated nucleic acid binding protein (Mnab, encoded by *Rc3h2*). In mammals the two proteins share a very similar amino-terminus, while they are characterized by divergent carboxy-termini (Figure 1). The carboxy-terminus of Mnab contains a hydrophobic region which is completely absent from Roquin and which might target the protein to the plasmamembrane [10]. The carboxy-terminus of

Roquin instead is characterized by the presence of a coiled-coil domain being a potential site for homo/heteroligomerization (Figure 1).

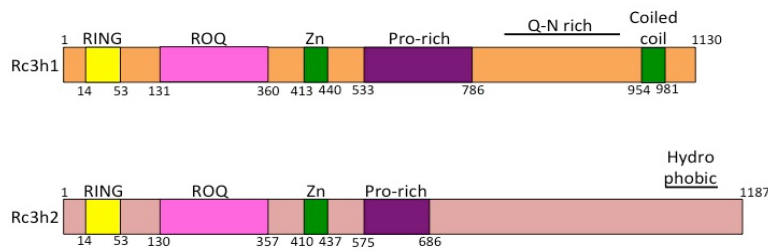


Figure 1 : comparison of the domain organization of Roquin (*Rc3h1*, upper schematic drawing, transcript ID ENSMUST00000161609) and Mnab (*Rc3h2*, lower schematic drawing, transcript ID ENSMUST00000100143) proteins. Numbers indicate aa according to Ensembl annotation.

Recently it has been demonstrated that Roquin can interact with components of both the P-bodies (PB) and stress granule (SG) pathways [8]. Processing bodies (PB) are cytoplasmic foci which are sites of mRNA degradation [11] and translational repression [12]. These foci contain high concentrations of proteins involved in mRNA degradation and microRNA components, while stress granules are structures containing mRNAs that are translationally arrested in response to a wide range of environmental stresses [13]. Roquin overexpressed in *ex vivo* isolated CD4 T cells colocalizes with Rck protein, which is a marker for PBs. However, arsenite-treatment of CD4 T cells leads to formation of SGs in the cytoplasm, and in this case Roquin mainly colocalizes with SGs while it remains associated with PBs only in 5.5% of the stressed cells [8]. Interestingly, the carboxy-terminus of Roquin showed a high frequency of glutamine and asparagine residues. As reported for other PB-components [14], this region of Roquin is important for its correct localization to the PBs, but not to arsenite-induced SGs.

PBs are structures highly enriched for proteins involved in mRNA decay, including the decapping complex Dcp1/Dcp2, the enhancer of decapping Edc4, the RNA helicase Rck, the exonuclease Xrn1 and the deadenylase Ccr4. Moreover they contain proteins involved in the nonsense-mediated decay (NMD) and the microRNA pathways (see chapter 1.3.1). It has been shown that Roquin can interact with several of these components, namely Rck, Edc4 and Dcp1a, and this physical interaction has been proposed to be important for ICOS repression [8].

Roquin's ability to bind RNA and to localize to PBs, but not SGs, is necessary to allow Roquin to destabilize ICOS mRNA by binding to its 3'UTR inducing mRNA decay [6, 8]. A binding site of Roquin to the ICOS mRNA has been identified in the region between 100 and 200 base pairs downstream of the stop codon of ICOS.

However, the degree of ICOS repression by Roquin increased with length of the ICOS 3'UTR, indicating that multiple sites on ICOS 3'UTR might be necessary to induce full repression by Roquin [8].

The precise mechanism-of-action of Roquin has not been precisely elucidated yet. A previous report indicated that Roquin induces mRNA degradation in a miR-101 dependent manner [6]. A more recent publication, however, demonstrates that Roquin's action on ICOS mRNA is independent of miRNAs or miRISC formation, since Roquin can still induce the downregulation of ICOS mRNA or ICOS 3'UTR in *Dicer*^{-/-} mouse embryonic fibroblasts (MEFs) and in mouse *Ago1-4*^{-/-} embryonic stem cell lines [8].

Roquin and Mtab also contain a RING-finger domain which might mediate E3 ubiquitin ligase activity. In mammals a function for Roquin or Mtab as E3 ubiquitin ligases has not yet been demonstrated. In *C. elegans*, however, the Rc3h1 homolog RLE-1 has been found to regulate the lifespan of the worm by ubiquitinating and inducing the degradation of the transcriptional activator DAF-16 [15]. DAF-16, the homolog of mammalian Foxo3a, is a transcriptional activator that regulates longevity and stress resistance in *C.elegans* and is highly regulated at the post-translational level. Activation of AKT by the Insulin/IGF pathway induces phosphorylation of DAF-16 preventing its nuclear translocation and transcriptional activity. Moreover, DAF-16 proteins levels are controlled through the proteasome pathway. RLE-1 can physically interact with DAF-16 through its carboxy-terminus, while the RING finger domain mediates ubiquitination of DAF-16 inducing its degradation thereby shortening *C. elegans* lifespan.

1.2 The sanroque mouse strain

The autoimmune sanroque mouse strain [5] is characterized by the presence of a single point mutation leading to the exchange of methionine 199 for arginine (M199R) in the ROQ domain of Roquin. This strain was generated by treating C57BL/6 mice with ethylnitrosourea (ENU), a chemical compound that introduces point mutations into the germline of mice at a frequency of one mutation per 0.5 megabases.

Sanroque homozygous mice develop an autoimmune syndrome, which resembles systemic lupus erythematosus (SLE) in human patients. Rc3h1^{san/san} animals develop anti-nuclear antibodies (ANAs) at an age of 6-7 (females) or 8-16 (males) weeks. The mice display also other features typical of SLE, for example the production of high affinity anti-dsDNA antibodies, focal proliferative glomerulonephritis, necrotizing hepatitis, anemia, autoimmune thrombocytopenia, splenomegaly and lymphadenopathy. Moreover, sanroque mice develop high titers of immunoglobulins

of all T-dependent isotypes. Despite normal T and B cell development, effector-like CD4 and CD8 T cells accumulate in the periphery of adult mice.

In the Rc3h1^{san/san} mice the M199R is a hypomorphic rather than null mutation, since forced expression of Rc3h1^{M199R} in san/san T cells induced an intermediate downregulation of ICOS on the cell surface compared to Roquin^{wt} [5]. The M199R substitution most likely disturbs the predicted alpha-helical structure of the ROQ domain by introducing a positively charged arginine residue, but it does not destabilize the protein, since normal levels of Roquin have been detected by western blot in *ex vivo* isolated san/san thymocytes [5]. The analysis of the sanroque mouse strain revealed the critical function of Roquin and its ROQ domain in regulating ICOS expression on the T cell surface [5]. However, the M199R mutation does not impair the ability of Roquin to bind ICOS mRNA, but it rather increases it [16]. It has been instead suggested that the M199R substitution alters the ability of Roquin to interact with as yet unknown critical effector proteins [7].

Mice homozygous for the sanroque mutation display increased levels of ICOS on their T cells. This deregulation was proposed to cause accumulation of T cells within the B cell follicle and to induce germinal center reactions to self-antigens. Moreover, the sanroque mice are characterized by an overrepresented T_{FH} compartment within the CD4⁺ T cells. Both increased ICOS expression and T_{FH} expansion were shown to be caused by a T cell intrinsic defect of Roquin [9]. T^{san/san} cells inappropriately provide help to self-reactive B cells within the GC reaction (see chapter 3.2). Formation of spontaneous GC is critical for the pathogenesis of the autoimmune syndrome in sanroque mice, since loss of one allele of the GC master regulator Bcl6, which significantly prevents the development of the germinal centers, reduces the lupus-like phenotype [9]. Moreover, impaired CD4 T cell help to GC B cells caused by ablation of SAP, an adaptor protein downstream of the T cell receptor (TCR), also prevents GC formation and ameliorates the autoimmune phenotype of the sanroque mice. In particular, impaired GC formation in Rc3h1^{san/san}SAP^{-/-} mice rescued autoantibodies production (including ANA and anti-dsDNA antibodies) and immunocomplex deposition in the kidneys ameliorating the renal pathology. However, features of the sanroque mice like hypergammaglobulinemia, splenomegaly and lymphadenopathy are not rescued by loss of GC formation, indicating that a non-T_{FH} mediated mechanism contributes to the disease development in these animals [9].

CD28 is a T cell-surface receptor that delivers signals required for full activation of naive T cells in addition to TCR engagement by antigen. The ligands of CD28, B7.1 and B7.2 are only upregulated on antigen-presenting cells in response to infections, thereby preventing T cell activation by innocuous or self-antigens. Interestingly, *Icos*

emerged by duplication of the more ancient *Cd28* gene and both are highly similar in protein sequence. Moreover, both CD28 and ICOS activate PI3K signaling and sustain TCR-induced gene expression and cytokine synthesis [17]. Under normal physiological conditions the CD28 and ICOS pathways have sequential and distinct functions, since ICOS is only expressed on activated T cells. In T cells with intact Roquin function ICOS is inducibly expressed subsequent to TCR/CD28 co-stimulation and can then be triggered through its constitutively expressed ligand (ICOSL). In sanroque mice, however, ectopically expressed ICOS receives the co-stimulatory signal through binding ICOSL and can therefore substitute for CD28 signaling on naive T cells. These events eliminate a critical checkpoint designed to discriminate between self and non-self. It has been proposed that, by regulating ICOS mRNA stability, Roquin prevents ICOS to bypass the requirement for CD28 during the early phase of an immune response, including primary antibody responses and GC formation. Roquin's main function was therefore proposed to ensure that the overlapping functions of *Cd28* and *Icos* are well compartmentalized [18].

1.3 Control of mRNA stability in the immune system

1.3.1 Pathways of mRNA degradation

In eukaryotes different pathways of RNA degradation remove RNA molecules from the cells. These pathways determine the physiological mRNA turnover, enable processing of RNA precursors and ensure quality control of the transcripts. RNA processing is essential for the maturation of many different classes of cellular RNAs that are synthesized as larger precursors, as microRNAs (miRNAs) or small nuclear RNAs (snRNAs) [19]. Pathways of quality control instead recognize incorrectly synthesized mRNAs or ncRNAs both in the nucleus and cytoplasm. In the nucleus, mRNA-protein complexes (mRNPs), which assemble immediately after transcription, are subjected to surveillance. Aberrant mRNAs are recognized and are either degraded by the nuclear exosome complex from the 3' end or by 5' to 3' exoribonucleases. In the cytoplasm, instead, the best studied mRNA quality control system is represented by the nonsense-mediated decay (NMD) pathway. The NMD-pathway identifies the formation of premature stop codons. In particular, the NMD machinery recognizes the presence of a stop codon in a position that is located 5' to exon-exon junction complexes (EJCs). EJCs are ribonucleoprotein complexes that are deposited on mRNAs during splicing at the junction of two exons. Translation of mRNAs terminates at the stop codon, which in appropriate transcripts is not followed by an EJC.

Two main classes of enzymes mediate mRNA degradation, the endoribonucleases and the exoribonucleases. The former enzymes cleave mRNAs internally, while the latter degrade mRNAs either from the 5' or the 3' end. Both ends of eukaryotic mRNAs are normally protected from exoribonuclease activity by specific terminal structures: a m⁷GpppN cap at the 5' end and a poly(A) tail at the 3' end. Removal of these terminal modifications requires the activation of specific deadenylating and decapping enzymes, and these processes are rate limiting for the mRNA decay pathway [20].

Three main pathways of mRNA decay have been described: 1) Deadenylation-dependent mRNA decay; 2) Deadenylation-independent mRNA decay; 3) Endoribonuclease-mediated mRNA decay (Figure 2).

Most of the transcripts undergo deadenylation-dependent mRNA decay. Deadenyating enzymes, as the CCR4-NOT complex, shorten the poly(A) tail of the transcript [21]. Only when this process is complete, the exosome, which in eukaryotes is a complex composed of 9 different proteins, can completely degrade the mRNA from the 3' end through its 3' to 5' exoribonuclease activity [22]. Alternatively, removal of the 5' cap on the mRNA by the decapping machinery, represented by the Dcp1/Dcp2 complex which hydrolyzes the m⁷GpppN cap into m⁷GDP and a monophosphate 5' RNA end, exposes an unprotected 5' end allowing the 5' to 3' exoribonuclease Xrn1 to degrade the RNA. In this case, the decapping machinery is recruited to the targeted mRNA through interaction with the LSM1-7 complex which binds partially deadenylated mRNA [23]. The exoribonuclease Xrn1, however, can degrade some mRNA substrates without prior deadenylation, giving rise to the deadenylation-independent mRNA decay pathway [24]. In yeasts, Rps28b regulates the half-life of its own mRNA by interacting with secondary structures of the 3' untranslated region (3' UTR) and with the enhancer of decapping Edc3. In this case the process of decapping is not induced by deadenylation but by the presence of Edc3, which recruits the decapping machinery to the targeted mRNA [25].

The third pathway of mRNA decay is mediated by endonucleases [26]. Endoribonucleases can hydrolyze ester-bonds within the RNA creating two fragments which lack the m⁷GpppN cap or the poly(A) tail and are then susceptible to exoribonuclease activity. Since both cap and poly(A) tail are structures necessary to initiate translation, none of the fragments generated by these different decay pathways should be efficiently translated into aberrantly truncated and potentially harmful proteins [20].

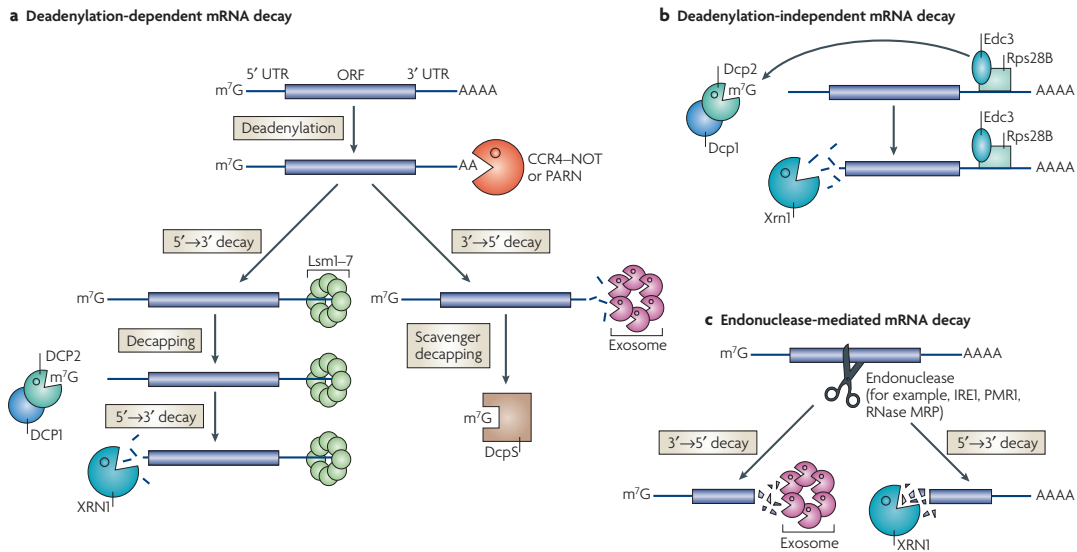


Figure 2: Different pathways of mRNA decay. a) Deadenylation-dependent mRNA decay. Removing of the poly(A) tail is mediated by CCR4-NOT or PARN complexes and is the rate limiting step of the pathway. Following deadenylation the targeted mRNA can be alternatively degraded by 3' to 5' exoribonucleases or by 5' to 3' exoribonucleases as Xrn1 following removal of the m⁷GpppN cap by the Lsm1-7 induced decapping enzymes Dcp1/Dcp2. b) Deadenylation-independent mRNA decay. In rare cases the decapping machinery can be recruited to the targeted mRNA without previous deadenylation by enhancers of decapping as Edc3. Rps28B directly interact with Edc3 to promote decapping of its own mRNA autoregulating its half-life. c) Endonuclease-mediated mRNA decay. Endonucleases are enzymes that cut the mRNA internally, leading to formation of two RNA fragments, one of which lacks the poly(A) tail and is degraded by the exosome, while the other fragment, since it lacks the m⁷GpppN cap, is degraded by Xrn1. The cartoon is taken from [4].

Roquin is a RNA-binding protein, and it can interact with target mRNAs through its ROQ and CCCH-zinc finger domains, thereby regulating their stability and turnover. mRNA stability is regulated by the presence of specific sequences within the mRNA itself. Such regulatory elements are often located in the 3'UTR, as in the case of ICOS mRNA's control by Roquin, but are also found in the coding sequence [27] or in the 5'UTR [28]. Well-known regulatory sequences are represented by the AU-rich elements (AREs), which are located in the 3'UTRs of various mRNAs [29]. ARE sequences are approximately 50 nt in length and contain several copies of an AUUUA pentamer. Three different ARE's classes characterized by different deadenylation kinetics have been identified. Class II AREs contain 4 to 7 copies of the AUUUA pentamer within an U-rich context and are the most potent ones, compared to class I AREs (they contain only few pentamer elements) or class III AREs (they do not contain AUUUA sequences) [30]. ARE-induced mRNA degradation is mediated by both the exosome [31], and in agreement with this model ARE binding proteins directly interact with subunits of the exosome, and the decapping-Xrn1 pathway [32]. Moreover, AREs can also mediate inhibition of

translation of the target mRNA [33]. Further regulation of mRNA stability is achieved through modification of the ARE-binding proteins (ARE-BPs). p38 MAPK [34] and ERK [35] kinases have been shown to phosphorylate ARE-BPs modulating their ability to bind ARE sequences and to destabilize the target mRNA. Phosphorylation of HuR by protein kinase C (PKC), instead, shifts the cellular localization of HuR from the nucleus to the cytoplasm, where HuR can physically interact with its target mRNAs [36].

mRNA stability and gene expression is regulated also by small noncoding RNA molecules with sequence complementarity with their target transcripts through the process of RNA interference (RNAi). Elements of the RNAi pathway that control mRNA turnover can be both short-interfering RNAs (siRNAs) or microRNAs (miRNAs). Ds-siRNA are ~ 21nt in length and are characterized by the presence of two nucleotides 3' overhangs and phosphorylated 5' ends [37]. One strand of the duplex is incorporated into the RNA induced silencing complex (RISC) and is loaded onto Argonaute (Ago) proteins, whereas the passenger strand behaves as a RISC substrate and is cleaved by the endonuclease activity of Ago2 [38]. The RISC-loaded guide strand drives the RISC to complementary target RNA molecules. In mammals, the endonuclease Ago2 cleaves the siRNA-targeted transcript and the generated fragments are removed from the cell by different cellular degradation pathways [39]. miRNAs, instead, are ~ 22nt RNA's molecules which are characterized by partial complementarity with their target mRNAs. Approximately 25% of the human genes were estimated to contain miRNA-binding sites [40]. miRNAs are transcribed in the nucleus by the RNA polymerase II as larger polyadenylated and capped precursors, the pri-miRNAs [37]. These transcripts are processed by the RNase III enzyme Drosha to release a ~ 70nt long pre-miRNA precursor [19]. The pre-miRNA is shuttled by the Exportin5-RanGTP complex from the nucleus to the cytoplasm [41], where a different RNase III enzyme, Dicer, releases a 22 nt long miRNA-miRNA duplex [42]. After unwinding of the transient duplex, one strand is loaded on the miRNA-associated multiprotein RNA induced silencing complex (miRISC) in association with the Ago proteins. The mechanism of post-transcriptional gene regulation by the RNAi pathway depends on the degree of complementarity of the miRNA's seed region and its target. Imperfect complementarity is typical for miRNAs and leads to translational repression and shuttling of the repressed mRNA into P-bodies, where it can be stored or degraded through mRNA-decay pathways [43] [44]. Ago and GW182 proteins, which are loaded on the miRISC, are major effectors of miRNA-mediated mRNA decay. The eukaryotic initiation factor 4G (eIF4G) binds to the poly(A)-binding protein PABPC1 leading to circularization of the mRNA to

increase translation efficiency [45]. GW182, by directly competing with eIF4G for binding to PABPC1, interferes with circularization of the transcript repressing translation and favouring the access of decapping and deadenylation machineries to their targets [46].

1.3.2 Control of mRNA stability in the immune system

Tight control of protein levels in the immune system is particularly important to allow efficient immune and inflammatory reactions. Post-transcriptional regulation of mRNA stability is widely used in the innate and adaptive immune systems to control the expression of many signaling and effector genes.

ARE-mediated mRNA decay (AMD) in the immune system is particularly important to regulate the stability of mRNAs encoding for cytokines, chemokines and intercellular secreted factors [30]. Tristetraprolin (TTP) is a RNA-BP containing two CCCH-zinc finger domains which recognizes with high specificity ARE elements within 3' UTRs of target genes [47]. TTP binds to AREs of several different genes, as TNF- α , CCL-2, CCL-3, GM-CSF, IL-2, IL-6 and INF- γ , inducing fast degradation of their mRNAs. TTP, by limiting the half-life of these cytokine transcripts, has mainly an anti-inflammatory function in the immune system [30]. However, it has been shown that TTP can also act as pro-inflammatory molecule since it can target immune-suppressive IL-10 mRNA for degradation in macrophages [48]. Furthermore, TTP targets the transcription factor E47, which regulates expression of the activation-induced cytidine deaminase (AID). AID is critically involved in two central processes of the germinal center reaction, namely somatic hypermutation and class-switch recombination. Aged B cells are characterized by impaired class switch recombination and this process has been linked to the increased levels of TTP [34]. In rare cases ARE-containing mRNAs can be stabilized by ARE-BPs. The main example of stabilizing ARE-BPs is represented by HuR. IL-3 mRNA contains AREs elements which can be recognized by both HuR and TTP proteins, which compete for the same binding site on the target transcript [49].

miRNAs have also a major role in the regulation of the immune system. miRNA-155 is the best studied miRNA in the adaptive immune system. Several lymphocytes effector functions were shown to be regulated by miR-155. In TCR-stimulated naive T cell, miR-155 skews T helper (Th) cell differentiation towards a Th1 rather than a Th2 profile. Mir-155 contributes also in maintaining peripheral T cell tolerance by promoting survival and proliferation of regulatory T (T_{reg}) cells (see chapter 2.1.3.2) Moreover, loss of miR-155 in mice has been shown to impair T-cell dependent antibody responses by regulating B cell secretion of TNF and lymphotoxin- α (LT-

α)[50]. Finally, mir-155 regulates Pu.1, a transcription factor with different functions in B cells and dendritic cells (DCs). In B cells, miR-155 induced degradation of Pu.1 is important to promote class switching to IgG1 [51]. In DCs, instead, upregulation of miR-155 during the switch from antigen uptake to antigen presentation function in DCs is important to activate phagocytosis [52].

As previously anticipated, endonucleases have also been recently demonstrated to play important roles in the regulation of the immune system. The CCCH-zinc finger containing protein Zc3h12a binds to the 3' UTR of IL-6 and through its endoribonuclease domain cleaves IL-6 mRNA. Additional targets of Zc3h12a as IL-1b and IL-12b mRNAs have also been suggested [53].

In general, control of the mRNA stability of genes involved in immune and inflammatory reactions is characterized by high degree of cooperativity, which probably increases the efficiency of the RNA degradation pathway. The same miRNAs, as mir-155, or the same ARE-BP, as TTP, can target and control the transcript stability of several different genes, as it has been previously described. Moreover, the highly unstable IL-6 mRNA represent a nice example of how a single mRNA molecule can be regulated in its stability through different mRNA decay pathways. In addition to the Zc3h12a binding site present in the 3' UTR, IL-6 mRNA also contains an ARE [54] and a binding site for miR-26 [55]. Several different mRNA degradation pathways can then join the forces and cooperatively regulate the stability of single mRNA molecules tightly and efficiently controlling the final protein concentration.

The process of mRNA degradation is highly compartmentalized and mainly takes place in the P-bodies. In conditions of cellular stresses, however, the SGs cooperate with PBs in regulating mRNA stability and turnover. Recently, it has been suggested that also the formation of SGs is highly important in the context of T lymphocyte biology. Even if transcription at a cytokine locus starts within a few hours after initial priming of naive T cells [56], secretion of effector cytokines is not abundant at this time and can be detected only after a second TCR stimulation. An interesting model that has been proposed to explain this phenomenon suggests that delayed cytokine secretion might be caused by the induction of an integrated stress response upon initial priming of the naive T cells, during which mRNAs coding for effector cytokines are stalled in translation and stored into SGs. In contrast, restimulation of the primed T cell through the TCR might release translation from the stress response leading to ribosomal mRNA loading and cytokine secretion [57].

2 Tolerance and Autoimmunity

The immunological specificity of the B and the T cell receptors is the result of the process of somatic recombination of the immunoglobulin (Ig) locus in B lymphocytes or of the TCR β and α loci in T lymphocytes. This process can generate millions of different TCRs and BCRs, and owing to its random nature also leads to the emergence of receptors that potentially recognize components of the same organism (= "self"). The term tolerance summarizes a variety of processes that eliminate or neutralize such autoreactive lymphocytes. A breakdown of these mechanisms, which act on lymphocytes both in primary (central tolerance) or secondary (peripheral tolerance) lymphoid organs, can lead to the development of autoimmune pathologies.

2.1 T cell tolerance

2.1.1 T cell development in the thymus

T lymphocytes belong to the hematopoietic system, and derive from multipotent bone marrow precursors which enter the thymus, the non-self renewing hematopoietic organ where thymocytes are generated, at the cortico-medullary junction [58]. The thymus is subdivided into two different regions, an outer part, containing mainly immature thymocytes and called cortex, and an inner part, containing mature thymocytes and called medulla [59]. Once the progenitors have undergone commitment to the T cell lineage, they differentiate into double negative 1 (DN1) cells and progressively lose their potential for B [60] or NK cell differentiation [61]. The double negative stage (DN; CD4⁻CD8⁻) can be subdivided on the basis of CD25 and CD44 expression into DN1 (CD25⁻CD44⁺), DN2 (CD25⁺CD44⁺), DN3 (CD25⁺CD44⁻) and DN4 (CD25⁻CD44⁻) [62]. Upon opening of the chromatin configuration of the T-cell receptor β chain (Tcrb) locus and expression of recombination-activating genes (RAGs), which catalyze somatic rearrangements, cells at the DN2 or DN3 stages rearrange their Tcrb locus. The TCR β locus contains numerous variable (V β), diversity (D β) and joining (J β) regions as well as one constant (C) region. While the rearranged VDJ region of the TCR encodes for the antigen binding site of the receptor, the constant region encodes for the transmembrane domain and the short cytoplasmic tail of the TCR. A productively rearranged TCR β chain pairs with the invariant pre-TCR α chain to form the pre-TCR which transduces a signal for further differentiation towards the DN4 and double positive (DP) stages [63]. Cells that do not produce rearrangements encoding a functional receptor die at the CD44⁻CD25⁺ stage of development during a process called β selection [64] [65] [66]. Pre-TCR

signaling induces allelic exclusion, a process that blocks recombination of the second TCR β allele, ensuring that every cell expresses only a single TCR β product [67]. During the transition from DN3 to DN4 the Tcrb locus becomes inaccessible and the cells undergo extensive proliferation during which RAG1 and RAG2 genes become inactive [1].

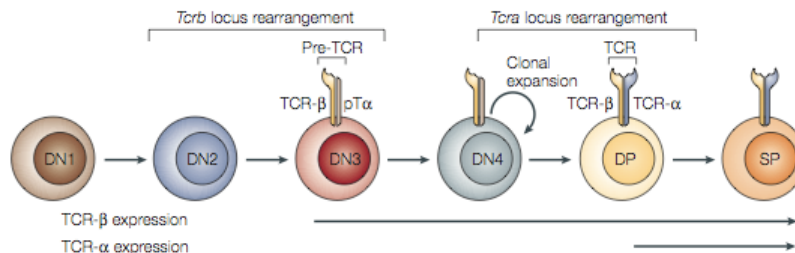


Figure 3: T cell development in the thymus, showing timing of Tcrb and Tcra locus rearrangement. The cartoon is taken from [1]

Upon further thymocyte maturation, RAG genes are re-activated and the TCR α locus becomes accessible leading to the rearrangement of the α chain of the TCR (see Figure 3). In contrast to the TCR β locus, TCR α lacks diversity genes, and it is composed only of V α and J α gene segments. The newly-formed TCR α chain pairs with the TCR β chain to form the TCR. Allelic exclusion at the TCR α locus is less stringent than at the TCR β locus. Indeed, cells that express on their surface a non-functional TCR do not downregulate RAG genes as in the case of cells expressing a non-functional pre-TCR. This phenomenon allows the immature lymphocytes to undergo several rounds of rearrangements at the α locus to increase the probability to generate a functional TCR [68]. At this stage, the thymocytes also start to express the co-receptors CD4 and CD8 forming the double positive (DP) $\alpha\beta$ -TCR-expressing immature cells, which represent about 90% of the lymphoid compartment in the thymus of young organisms.

2.1.2 Central T cell tolerance

One major mechanism of tolerance in T lymphocytes is represented by the deletion of autoreactive T lymphocytes in the thymus, a process which has been named central tolerance. More than 95% of thymocytes are lost during the stringent process of positive and negative selection that takes place in the thymus [69]. Approximately 90% of DP thymocytes undergo death by neglect, a passive form of cell death caused by the failure of a $\alpha\beta$ TCR expressed by the thymocyte to engage a peptide-MHC complex expressed on the cell surface of epithelial cells in the thymic cortex [70]. This process enriches the T cell compartment also for autoreactive cells, most

of which however are deleted through a process called negative selection that eliminates lymphocytes expressing a TCR which binds with very high affinity to a peptide-MHC complex. Two major mechanisms of negative selection have been described: 1) clonal deletion and 2) anergy.

It has been proposed that about 5% of thymocytes, corresponding to at least 50% of positively selected T cells, are removed by clonal deletion [59]. Positively selected T cells that can recognize with high affinity a ligand-MHC molecule complex undergo apoptosis (clonal deletion), while only DP thymocytes that express TCRs with low affinity for self-peptide-MHC ligands differentiate into CD4 or CD8 SP thymocytes (positive selection) and leave the thymus to populate the periphery. The effector pathways responsible for apoptosis during negative selection have not been fully understood yet. However, typical mediators of apoptosis in T lymphocytes in the periphery such as Fas [71] or caspase-1, 2, 3, 8, 9 and 11 [72] are, when deleted one-by-one, dispensable for deletion of self-reactive T lymphocytes. A different pathway which is known to control apoptosis depends on members of the BCL-2 protein family. The BH3-only Bcl-2 family member Bim is required to instruct proper deletion of autoreactive lymphocytes in the thymus, and Bim-deficient animals [73] are characterized by impaired negative selection. The thymic medulla may be the predominant site where clonal deletion takes place because it is enriched with two different types of APCs, the dendritic cells (DC) [74] and the medullary epithelial cells (mTEC) [75], which are both important for the process of negative selection. Moreover mTECs are sites of promiscuous gene expression, i.e. they transcribe a large array of genes that are otherwise only expressed in distinct peripheral tissues [76]. The transcription factor AIRE (autoimmune regulator) is required for ectopic expression of peripheral antigens in mTECs, and if mutated leads to the development of the autoimmune polyendocrine syndrome type 1 in humans [77]. Mice deficient for AIRE develop an autoimmune syndrome similar to the human disease [78], confirming the importance of mTECs in negative selection. Clonal deletion, however, has been proposed to take place in the cortex as well. cTECs are non-professional APCs and do not express co-stimulatory molecules. It has been proposed that cTECs can present MHC-ligand peptides, but since they lack costimulation they can not efficiently induce apoptosis [79]. It has been instead suggested that cTECs mark a DP T lymphocyte in the cortex as self-reactive, and a subsequent stimulus from DCs induces efficient clonal deletion [80].

The second non-deletional mechanism of central tolerance is represented by induction of anergy, which is a state of unresponsiveness. Also in this case thymic epithelial cells that present MHC-ligand peptide can induce a state of

unresponsiveness in the immature T cells which are unable to respond to further stimulation [81].

Although central tolerance is a highly efficient process, it cannot eliminate all the T cells which express an auto-reactive TCR on their surface. For this reason mature T cells leaving the thymus are controlled by peripheral tolerance mechanisms, and they induce lymphocytes at their first encounter with the self-antigen in the periphery to become tolerant.

2.1.3 Peripheral T cell tolerance

Healthy individuals are characterized by the presence of self-reactive thymocytes in the periphery. Since high affinity thymocytes are deleted in the thymus, most likely these autoreactive lymphocytes express a low-affinity TCR for self-antigens [82]. Outside the thymus self-reactive T lymphocytes are controlled through mechanisms of peripheral tolerance, which can be both T cells intrinsic, acting directly on the self-reactive T cell like ignorance, anergy, phenotypic skewing or apoptosis, or T cell extrinsic, acting on the auto-reactive T cell via additional cells like regulatory T cells (T_{reg}) or tolerogenic dendritic cells.

2.1.3.1 T cell intrinsic mechanisms of peripheral T cell tolerance

To achieve tolerance of autoreactive T lymphocytes in the periphery the simplest scenario is the ignorance of self antigens by the T cells. This is possible in two different ways. The first one is when the T cells and the respective auto-antigens are physically separated into two different compartments. This happens when the self antigens are sequestered into sites which are not easily accessible to the blood/lymph borne immune system [83]. A second way to induce tolerance by ignorance in the periphery is to prevent activation of a T cell in response to a stimulus which is too weak, for instance when the amount of antigen does not reach the threshold required to trigger a T cell response [84].

As in the thymus, T cells can become anergic in the periphery as well, maintained in a state of reduced cellular proliferation and unable to produce cytokines in response to second stimulation. Anergy is induced by ligation of the TCR on the surface of mature T cells without costimulation [85] and at the same time signaling through alternative receptors as cytotoxic T-lymphocyte-associated antigen 4 (CTLA-4) [86] or programmed cell death 1 (PD-1) [87]. Signaling downstream of the TCR leads to calcium flux and NFAT nuclear translocation and activation. Both these events are required also for induction of anergy. In anergic cells, however, DNA binding by the activator binding protein 1 (AP1), a heterodimer composed of Fos and Jun, is

reduced, due to defective activation of the MAPK pathway [88]. Ras proteins, which belong to the superfamily of monomeric GTPases, are located on the inner surface of the plasmamembrane. Activation of the costimulatory pathway leads to the activation of guanine exchange factor (GEF) son of sevenless (SOS) which is linked to the receptor through the adaptor protein Grb2 [89]. Activation of SOS following CD28 engagement leads to the exchange of GDP bound to the inactive form of Ras with GTP, inducing Ras activation and then efficient signaling through the MAPK pathway. In anergic cells, however, deregulation of MAPK activation is caused by a defect in the GTP loading of Ras. Defective MAPK activation and AP1 formation, together with intact NFAT nuclear translocation in anergic cells, leads for instance to impaired IL-2 production, a hallmark of anergic T lymphocytes [90]. Moreover, the presence of NFAT in the cell nucleus of activated T lymphocytes without contribution from other MAPK-regulated transcription factors in anergic T cells, has been recently linked also to the ubiquitination pathway. Transcription of three E3 ubiquitin ligases, CBL-B, GRAIL and ITCH is induced in response to tolerogenic signals. Casitas B-lineage lymphoma (CBL-B) is activated by phosphorylation following TCR engagement and it can downmodulate peripheral T cell activation by regulating the Rho-family GEF Vav1 [91]. Mice lacking CBL-B develop autoimmunity with autoantibody production and resting T cells are hyperproliferative and secrete higher amounts of IL-2 in response to antigenic stimulation. Moreover, in *cbl-b*^{-/-} mice proliferation and secretion of IL-2, as well as regulation of Vav1, are not dependent on CD28 costimulation anymore [92].

Even if a self-reactive T cell is fully activated tolerance can still be maintained if the immune response does not induce pathogenic effects. In this scenario autoimmune tissue damage is prevented by skewing the profile of the activated T cells towards a non pathogenic profile in terms of which cytokines and chemokine receptors they express. An important example is represented by CXCR5, a chemokine receptor that mediates migration of activated T cells to the B cell follicle. Optimal expression of CXCR5 by the T cells is achieved following activation of CD28 pathway, which is defective during presentation of self-peptides to T lymphocytes. Therefore tolerogenic signals can stimulate T cells to proliferate but migration to B cell areas of secondary lymphoid organs is impaired [93].

The last mechanism of T cell intrinsic peripheral tolerance is represented by the activation induced cell death (AICD). Repetitive encounter of the mature T cell with self-proteins leads to activation of apoptotic mechanisms mainly through the activation of the Fas-FasL pathway. The importance of this mechanism in maintaining peripheral tolerance is revealed by the observations that defects in the

FasL pathway in humans cause the autoimmune lymphoproliferative syndrome (ALPS) [94], while in mice defects in Fas or FasL, respectively in MRL/lpr and gld mouse strains, lead to lymphoproliferative lupus-like syndromes [95].

2.1.3.2 T cell extrinsic mechanisms of peripheral tolerance

In the periphery DCs are the most important type of professional APCs and they mediate both immune responses and induction of tolerance. To achieve complete T cell activation the APC needs to transmit two different signals: 1) presenting peptide-antigen on their MHC molecule to the TCR expressed on the T cell surface; 2) activation of dendritic cells leads to the expression of co-stimulatory molecules that engage CD28 on the T cells. Presentation of a self-peptide by an APC is not associated with activation of co-stimulatory pathways and in this case the APC transmits a tolerogenic signal. This phenomenon has been explained by two complementary models. The first model was proposed by Janeway [96] in 1992. His model suggests the presence of a distinctive recognition event involving the binding of conserved receptors on the APC's surface to evolutionarily conserved pathogens components. Support to this theory came in 1997, with the discovery of the pattern-recognition receptors (PRRs). Toll-like receptors (TLRs) are PRRs which can recognize pathogen associated molecular patterns (PAMPs) such as lipopolysaccharide (LPS), lipoproteins, peptidoglycans or DNA-containing unmethylated CpG motifs [97]. To date many different PRRs have been discovered, some of which are signaling PRRs as TLRs and CD14, which promote the ability of TLR4 to respond to LPS on the surface of macrophages, while others are secreted signaling PRRs found in plasma and tissue fluids as the mannose-binding lectin (MBL) which binds mannose-rich glycans on microbes in order to activate the lectin complement pathway. The third type of PRRs is represented by the endocytic PRRs like the mannose receptor, the scavenger receptor, the N-formyl Met receptor or the opsonin receptor which are expressed on the surface of phagocytes and promote the attachment of pathogens to these cells. The second model suggested was developed by Matzinger in 1994. This model proposes that the immune system does not discriminate between self and non-self, but the driving force of the immune system is the possible danger coming from invading pathogens [98]. The second signal necessary to activate the APCs in this view is represented by intracellular components of the attacked cells of the host which are representative of the damage. Molecules as heat shock proteins or mitochondrial components, which are released by necrotic cells but not by apoptotic cells which undergo normal turnover, can be

defined as damage associated molecular patterns (DAMPs) and as the PAMPs can instruct APCs to provide a full stimulus to T lymphocytes.

The second mechanism of T cell extrinsic peripheral tolerance is represented by the presence of regulatory T cells (T_{reg}) in the secondary lymphoid organs. T_{reg} cells act in a dominant and trans-acting way and are characterized by suppressor activity which is induced upon TCR ligation, but once they are activated their suppressor function is completely unspecific [99]. T_{reg} cells are constantly produced in the thymus [100] and they originate from thymocytes which express on their surface a TCR which bind self-peptides presented in the thymus with intermediate/high affinity [101]. It is not clear yet how a T lymphocyte bearing a TCR with intermediate/high affinity for self peptides is instructed towards negative selection in the thymus or towards a regulatory T cell fate [102]. The key transcription factor controlling T_{reg} development is FoxP3 which is also the most reliable marker for the identification of T_{reg} cells in humans and mice [103]. Mutations in the FoxP3 gene have been shown to cause the immune dysregulation, polyendocrinopathy, enteropathy, X-linked syndrome (IPEX). IPEX is an immunodeficiency syndrome that results in severe organ-specific autoimmune disease, confirming the important role that functional T_{reg} cells play in maintaining immune homeostasis in the periphery preventing the development of autoimmunity [104].

2.2 B cell tolerance

The development of B lymphocytes until the immature B cell stage takes place in the bone marrow. Immature or transitional B cells exit the bone marrow and migrate to secondary lymphoid organs such as the spleen, where they differentiate into mature peripheral B cells. B lymphocyte development is controlled through several checkpoints in both the primary and secondary organs. Breakdown of B cell tolerance is an important event in the development of autoimmune diseases.

2.2.1 B cell development and tolerance in the bone marrow

In mice B cell development takes place in the liver during fetal development and in the bone marrow after birth starting from hematopoietic precursors. According to the model established by the Weissman group long-term hematopoietic stem cells (LT-HSC) develop into short-lived hematopoietic stem cells (SL-HSC) and further into multipotent progenitors (MPP). MPPs, which have lost self-renewing potential, can differentiate into both common myeloid precursors (CMP) or common lymphoid precursors (CLP), the latter giving rise to T, B, NK and dendritic cells [105]. Commitment of the precursors to the B cell lineage is dependent on the transcription

factor Pax5, which instructs the B lineage and suppresses alternative lineage choices [106]. The first B lineage restricted cells are found in the pro-B cell stage. Upon expression of the RAG genes recombination of the immunoglobulin heavy chain (IgH) locus takes place, starting with the joining of one D_H and one J_H gene and concluding with the joining of a V_H segment to the preformed D_HJ_H complex [107]. The $V_H D_H J_H$ -encoded μ chain protein associates with the surrogate light chain (SLC) composed of $\lambda 5$ and VpreB to form the pre-BCR [108]. At the pro-B cells stage also the $Ig\alpha/Ig\beta$ molecules start to be expressed in a complex with the chaperone molecule calnexin. The presence of the $Ig\alpha/Ig\beta$ signaling molecules is indispensable for further differentiation of B cells, since the developmental block at the pro-B cells stage seen in $RAG^{-/-}$ mice can be overcome by treatment of the mice with an α - $Ig\beta$ mAb [109]. The first checkpoint of B cell development takes place at the pre-B cell stage. It has been postulated that only μ chains which can associate with the SLC to form a functional pre-BCR can promote cell proliferation and progression to later stages of development [110]. Signaling through the pre-BCR leads also subsequently to downregulation of the SLC and the RAG genes, limiting proliferation of the B cell clones and preventing recombination of the second allele of the Igh locus (allelic exclusion) [111]. The pre-BCR might also play a role in negative selection, since mice lacking the SLC develop higher titers of anti-nuclear DNA antibodies [112]. Small post-mitotic pre-B cells rearrange their light chain loci upon expression of a functional pre-BCR [113]. V to J recombination leads to expression of a κ or λ chain which pairs with the preformed μ chain. Expression of a functional light and heavy chain complex (IgM) on the surface of the cell is a feature of immature B lymphocytes (see Figure 4).

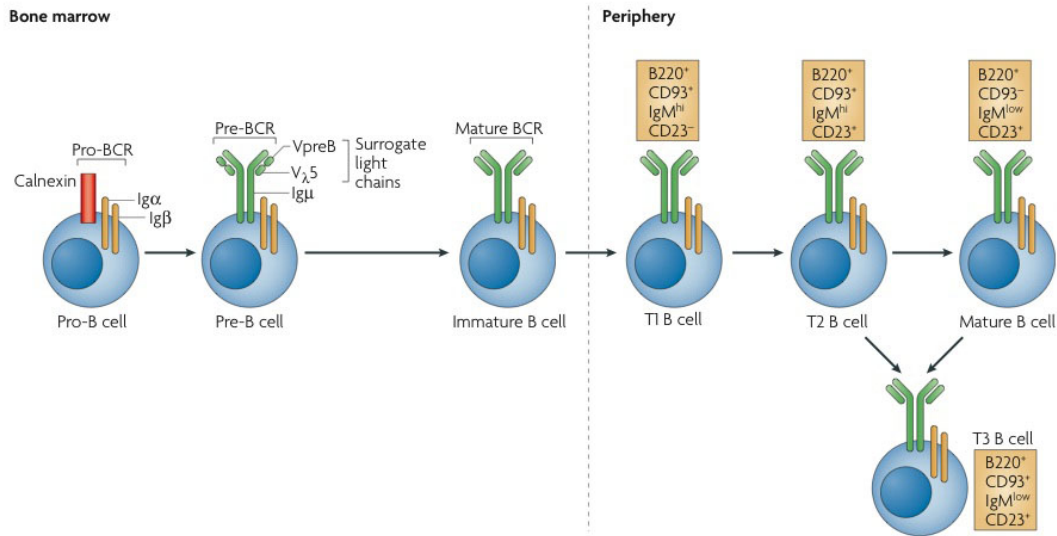


Figure 4: B cell development in the bone marrow and in the periphery. Committed pro-B cells, upon expression of the RAG machinery, rearrange the IgH locus, leading to production a μ chain which, if able to pair with the SLC, forms the pre-BCR on the surface of the pre-B cells. At this stage both negative and positive selection takes place. Upon productive rearrangement of the light chain locus the pre-B cells progress to the stage of Immature B cells, which express on the surface a complex of light and heavy chains, the IgM. Immature B cells leaving the bone marrow enter the periphery and become Transitional B cells. Expression of different markers on the surface of different transitional B cell subtypes in the periphery is shown. Cartoon from [3].

Immature B cells undergo selection prior to be exported in the periphery. From the immature B cell stage onwards, the process of clonal selection is Ag-dependent. Negative selection of self-reactive B lymphocytes is mediated by two different mechanisms: clonal deletion [114] and receptor editing [115]. It has been proposed that the site of first encounter of the antigen defines which mechanism of negative tolerance is utilized. In the bone marrow, autoreactive immature B cells undergo BCR editing, because of signals delivered by the microenvironment that block apoptosis favour RAG re-expression [116]. BCR editing involves secondary Ig genes rearrangements to develop a new BCR which is not reactive to self-peptides. Receptor editing takes place mainly at the light chain locus, leading to expression of a new light chain which might change specificity of the BCR [117]. Clonal deletion instead functions predominantly in bone marrow immature B lymphocytes that exhausted their editing potential [118]. Immature B cells in the periphery, instead, lack the signals from the bone marrow and the main mechanism of negative selection is therefore apoptosis as result of BCR engagement [116].

2.2.2 B cell maturation and peripheral B cell tolerance

2.2.2.1 B cell maturation

Immature B cells that survive negative selection in the bone marrow are released into the periphery where they differentiate into transitional B cells. Transitional B cells are characterized by high expression of IgM and CD24 and three different subtypes have been described: T1 (which express no or low levels of L-selectin, IgM, CD23 and CD21), T2 (which express high levels of L-selectin, IgM, CD23 and CD21) and T3 (which differ from T2 by lower expression of IgM on the surface) (Figure 4).

A small fraction of transitional cells differentiate towards mature peripheral follicular (FO) and marginal zone (MZ) B cells. A complex network of interactions between BCR- and nonBCR-mediated signaling pathways dictate the fate of the transitional B lymphocytes. Using a monoclonal BCR mouse line specific for the self-peptide Thy1/CD90 it has been demonstrated that BCR-crosslinking by low doses of self-antigen induces cell survival of immature transitional B lymphocytes [119], indicating that positive selection happens in the periphery as well. Together with a previous publication, [120], this study provides support to a model according to which increasing the strength of the stimulation through the BCR leads to differentiation of the transitional B cells towards MZ (intermediate BCR signal) rather than FO B cells (weak BCR signal). Other signals, however, participate, together with BCR engagement, in the decision between survival or death of the transitional B cells. The tumor necrosis factor family member B cell activation factor (BAFF) has major effects on B cell development. It is secreted by radioresistant stromal cells and myeloid cells. Binding of BAFF to BAFF-R, one of its three receptors, ensures the survival of transitional B cells and allows them to differentiate to FO and MZ B cells. Signaling through the other two BAFF receptors TACI and BCMA is dispensable for this purpose [121]. Several transcription factors control B cell development and tolerance in the periphery. The transcription factor family NF- κ B is activated by both BCR engagement, through its canonical pathway, and BAFF-R signaling, through its alternative pathway. BCR engagement is linked to the activation of the canonical NF- κ B pathway through the trimolecular complex CARMA1-Bcl10-MALT1 [122]. Mice lacking CARMA1 [123], Bcl10 [124] and MALT1 [125] are characterized by reduced numbers of MZ B cell, while the FO subset was minimally affected. Establishment of the FO compartment, however, is still highly dependent on the activation of the canonical NF- κ B pathway, since loss of Nemo, master regulator of canonical NF- κ B activation downstream of CARMA1-Bcl10-MALT1, in developing B cells leads to

defective differentiation of MZ and FO B cells [126]. Blockade of the alternative NF- κ B pathway also leads to reduced numbers of peripheral mature B lymphocytes, as assessed in irradiated chimeras reconstituted with I κ B Kinase-1/ $\alpha^{-/-}$ fetal liver cells [127]. BAFF $^{-/-}$ and BAFF-R $^{-/-}$ animals, however, show a more pronounced loss of peripheral mature B cells compared to the reconstituted IKK1 $^{-/-}$ chimeras, indicating an NF- κ B independent mechanism of action by BAFF signaling.

2.2.2.2 Peripheral mechanisms of B cell tolerance

Despite the control checkpoints in the bone marrow, some autoreactive B cell clones can escape central tolerance and migrate to the secondary lymphoid organs. In the periphery, however, several mechanisms prevent these cells to become pathogenic. For a few days after release from the bone marrow, these immature-transitional B lymphocytes, unlike mature B cells, are sensitive to BCR-induced apoptosis or to anergy, a state of unresponsiveness during which the cells lose the ability to be activated by antigenic stimulation. In this way autoreactive B cells that escape central negative selection can be deleted in the periphery upon encounter with the self-antigen [128]. Therefore, upon BCR crosslinking, immature and mature B cells respond in different ways. While *in vitro* sIgM stimulation of immature B lymphocytes results in cell death, the same stimulus applied to mature B cells leads to activation and proliferation [129]. The process of maturation of the transitional B cells causes changes in the properties of the cells to allow different responses to BCR engagement. Upon cross-linking in mature B cells, for instance, the BCR immediately translocates into lipid drafts and it is rapidly internalized into the cell, while in immature B cells BCR's compartmentalization into lipid drafts is impaired [130] due to lower membrane's levels of unesterified cholesterol [131].

A different mechanism of peripheral tolerance at later stages of B cell maturation is represented by downmodulation of BCR signaling through expression of inhibitory co-receptors such as CD32 (Fc γ RIIb) [132]. Activatory signals delivered through the BCR are usually counterbalanced by simultaneous cross-linking of the Fc γ RIIb receptor on GC B cells. In this way, only B cells with sufficient affinity for the antigen can overcome the inhibitory block mediated by Fc γ RIIb [133]. Exclusion of self-reactive clones from GCs was also shown to prevent development of autoimmune pathologies in humans [134]. Despite the self-reactive VH4-34 B cell clone being positively selected and well represented in the naive pool of B lymphocytes, it is excluded from the germinal centers and prevented from differentiating towards antibody-producing plasma cells. Moreover, full activation of B cells during T-cell

dependent processes can be achieved only in the presence of co-stimulation by T lymphocytes through CD40 engagement and cytokines, preventing the activation of B cells upon self-antigen presentation (see chapter 3.2).

As described in chapter 2.2.2.1, survival of mature B cells depends on signals transmitted through BAFF-R. Competition for BAFF limits B cell numbers and represent an other important checkpoint during B cell maturation.

3 Antibody- and cell-mediated immunity

The term “immune system” describes a diverse group of mechanisms which have evolved to protect the organisms from invading pathogens. The most primitive immune system is the innate immune system. Its mechanism of protection relies on the expression of germline encoded receptors which can recognize conserved patterns on different classes of pathogens and which can trigger an inflammatory response. Only later during evolution the adaptive immune system has evolved. In contrast to innate immunity, adaptive immunity relies on cells which can diversify their receptors through somatic recombination in order to specifically respond to pathogen-derived antigens. Generation of a vast repertoire of cells which can clonally expand and differentiate upon activation is than essential for the generation of an efficient adaptive immune system.

3.1 Mature B cell differentiation

Stimulation of a mature B cell leads to activation, proliferation and differentiation rather than anergy or apoptosis as seen in immature B cells (see chapter 2.2.2.2). However, proliferation and activation of naive B cells is dependent on the presence of helper T (T_H) cells, their cytokines or other activation signals like TLR-ligands [135]. Depending on the nature of these signals, a mature B cell can enter three different developmental pathways after activation, it can become a short-lived antibody-secreting plasma cell, a memory B cell, or it can enter a germinal center reaction.

Upon immunization of mice with a thymus-dependent (TD) antigen, two different populations of B cells originating from the same original clone are observed in the spleen: the extrafollicular and the germinal center B cell population [136]. When recirculating B cells in the blood recognize an antigen [137], they migrate to the T-cell-rich zone in the secondary lymphoid organs following upregulation of CCR7, the receptor for the T-zone chemokines CCL19 and CCL21 [138]. Extrafollicular plasma cells develop after migration of the activated clones to the extrafollicular areas at the junction between red pulp and T-cell zone. In the T-cell zone primed T cells interact with antigen-stimulated B cells resulting in cell cycle entry and plasma cell

commitment induced by upregulation of the transcription factor B lymphocyte induced maturation protein-1 (Blimp-1) [139]. These plasma cells produce an early wave of low affinity antibodies. Most of them are short-lived and die by apoptosis [140], but a small percentage can compete to enter into long-lived niches [141]. During an extrafollicular antibody response B cells do not undergo somatic hypermutation. Other B blasts can remain in the follicles and enter the germinal center reaction undergoing affinity maturation (see chapter 3.2). It is not completely clear yet why some B cells enter the GC reaction while others enter the plasma cells development pathway directly. It has been proposed that the strength of BCR engagement determines the fate of the B cells, with high affinity B cells preferentially enrolled into the extrafollicular plasma cell developmental pathway [142]. The third pathway of differentiation of mature B cells leads to formation of low-affinity memory B cells. Most of the memory B cells in mice derive from germinal center reactions and have been shown to be somatically hypermutated. However, unmutated memory B cells have been detected in $Bcl6^{-/-}$ mice, which can not develop GC, confirming that memory B cells can be generated independently of somatic hypermutation and GC formation [143].

3.2 The Germinal Center reaction

The germinal centers are dynamic structures which develop in secondary lymphoid organs of birds and mammals during an immune response to infectious organisms. During the germinal center reaction activated B cells can mutate their BCR specificity and undergo affinity maturation, which leads to production of high-affinity antibodies and long-lived memory B cells. GCs are characteristic of TD immune responses, but they can also be generated in a thymus-independent (TI) manner in response to some TI antigens like the bacterial polysaccharide $\alpha(1-6)$ dextran [144] [145], even if in this case the efficiency of the reaction is reduced.

Activated B cells that mature into GC-precursors migrate to the primary follicle, where the B cells start to proliferate forming a GC. The structure of the germinal centers has been subdivided by histological examination into the dark zone, which mostly consists of highly proliferating centroblasts, and the light zone, in which non-dividing centrocytes are situated within a mesh of follicular dendritic cells (FDCs), T cells and macrophages [146].

Germinal centers B cells can be detected 4-5 days after immunization [136]. Proliferating centroblasts in the dark zone downregulate surface expression of Ig and start somatic hypermutation (SHM) upon activation of the activation-induced cytidine deaminase (AID) [147]. The process of SHM modifies the variable region of BCR by

introducing single nucleotide substitutions, small deletions or duplications into the rearranged sequence [148]. After the process of SHM the cells (centrocytes) stop to divide and re-express the hypermutated receptor.

Migration of the B cells between the dark and the light zone in the GCs is mediated by chemokine gradients generated by the stromal cells. Centroblasts are characterized by high expression of CXCR4 and migrate towards the CXCL12 chemokine highly expressed in the dark zone, while CXCR5 directs the cells towards the light zone abundant for CXCL13 [149].

A stringent process of selection rescues high-affinity B cells from apoptosis during which a specific subset of T_h cells called follicular helper T (T_{FH}) cells play a critical role [150]. GC B cells are naturally prone to undergo apoptosis and it has been shown that they lack anti-apoptotic factors as Bcl-2 and its family members, while they are rich in pro-apoptotic molecules [151]. B cells in which mutations in the newly formed immunoglobulin lead to production of non-functional or non-binding antibodies undergo rapid cell death because of the pro-apoptotic program of the GC B cells. T_{FH} cells represent then a critical checkpoint to maintain tolerance in the germinal centers.

Differentiation of $CD4^+$ T cells into the T_{FH} subset has been shown to require strong or prolonged signals through the TCR [152]. Upon expression of the CXCR5 receptor and migration into the CXCL-13-rich B cell follicles [153], T_{FH} cells can provide instructive signals for B cell differentiation [154]. Survival signals transmitted by the activated T_{FH} cells comprise both activation of costimulatory pathways and cytokine secretion. Transient expression of CD40L (CD154) on the surface of activated CD4 T cells, which can interact with constitutively expressed CD40 on the B cell surface, has been shown to transmit a crucial survival signal to B cells, since mice lacking CD40 or CD40L can not mount normal germinal center reactions [155]. Moreover, signaling through CD40 stimulates B cell proliferation and facilitates cytokine-induced class switching [156]. The inducible T cell costimulator (ICOS) is also expressed at high levels on activated T_{FH} cells [157] upon activation of the CD28 pathway [158]. ICOS ligand (ICOSL) instead, is constitutively expressed on B cells, and ICOS-ICOSL engagement provides critical signals to T_{FH} cells required for initiation and maintenance of GC reactions [159]. Complete activation of T_{FH} cells induces production of specific cytokines, which control B cell survival, proliferation and Ig class switch recombination (CSR). IL-21 production enforces the generation of T_{FH} cells upon binding to the IL-21R expressed on T cells, but it also promotes differentiation of centrocytes by binding to IL-21R on B cells in the GC [160]. Plasma cell differentiation was indeed impaired in IL-21^{-/-} and IL-21R^{-/-} mice, and Ig V gene

mutation and selection were attenuated [161]. Moreover, B cell proliferation was also diminished during the late GC response in these mice. T_{FH} cells have also been shown to secrete the cytokine IL-4 in response to T_H2 polarizing pathogens and in these conditions, IL-4 secretion is critical to induce B cell maturation and expansion [162].

Upon BCR stimulation and activation of co-stimulatory signals, high affinity centrocytes are selected and rescued from cell death. In the light zone of the germinal centers, selected centrocytes undergo the process of CSR, by which B cells switch their Ig class expression from IgM or IgD to other classes with different effector functions.

Terminal differentiation of B cells as a result of the GC reactions leads to development of high-affinity plasma cells and memory B cells. However, the signals that induce B cells to become a plasma cell or a memory B cell are still largely unknown, even if there are some indications that expression of a high affinity BCR skews B cells differentiation towards plasma cells [163]. The regulation of several transcription factors have been shown to be crucial to allow plasma cell differentiation. Loss of Pax-5 represent the first-step towards formation of plasma cells [164], while downregulation of Bcl-6 releases the repression of Blimp-1 allowing plasma cell differentiation [165].

Together with the previously described tolerance checkpoints (see chapter 2), further tolerance mechanisms also control the accumulation and function of T_{FH} cells in the GC reaction. The lifespan of T_{FH} cells is tightly controlled. T_{FH} cells express higher levels of Fas on their surface, and are more sensitive to cell death after TCR stimulation compared to naive or memory helper T cells [166]. Accumulation of T_{FH} cells in sanroque mice plays also an important role in the development of the autoimmune phenotype, since sanroque mice deficient for SAP can not accumulate T_{FH} cells nor form GCs and they are protected from the lupus-like disease [9] (see chapter 1.2). T_{reg} cells in the GC reactions can also suppress T_{FH} function limiting provision of help to B lymphocytes [167]. Maintaining normal numbers and function of T_{FH} cells in the GC reaction is then fundamental to enable T_{FH} cell-mediated selection of high affinity GC B cells which are non-self reactive.

3.3 Cell-mediated responses

Immunity to intracellular pathogens relies on induction of specific cell-mediated rather than antibody-mediated immunity. The main effectors against pathogens located in the cytoplasm of host cells are the $CD8^+$ cytotoxic T lymphocytes (CTL). Their activation requires presentation of antigens in association with MHC class I (MHC I)

molecules on the surface of APCs in association with co-stimulatory and cytokine signals [168]. Upon activation of the CD8 T cell, an initial phase of expansion and acquisition of effector functions, such as cytotoxicity and cytokine secretion, is followed by a contraction phase during which the majority of reactive T cells undergoes apoptosis and the memory compartment is generated. The exact mechanism of differentiation from naive to effector and memory CD8 T cells has not been identified yet, but several models have been proposed (see Figure 5). The uniform potential model proposes that memory CD8 T cells arise directly from effector T cells. Support to this theory comes from the observation that memory T cells derive from cells that previously displayed effector functions as Granzyme B promoter activity [169]. Moreover, precursors of the memory T cell compartment, characterized by high expression of $IL7R\alpha$, have been identified within the effector CD8 T cells [170]. Memory T cells, however, display many characteristics typical of naive rather than effector T cells. Alternative models have been proposed to explain this discrepancy. The straight to memory differentiation model proposes that naive T cells can directly differentiate towards memory cells. In this scenario cytokines play an important role, since it has been shown that the presence of inflammatory cytokines (as IL-12) [171], INF-type-I [172] and IL-21 [173] favours differentiation towards effector cells, while antigen/costimulation alone leads to memory T cell formation [174]. The third proposed model of CD8 T cell differentiation is named decreasing potential model. According to this model, effector T cells progressively lose their memory potential during the immune response and are pushed towards terminal effector cell differentiation [175].

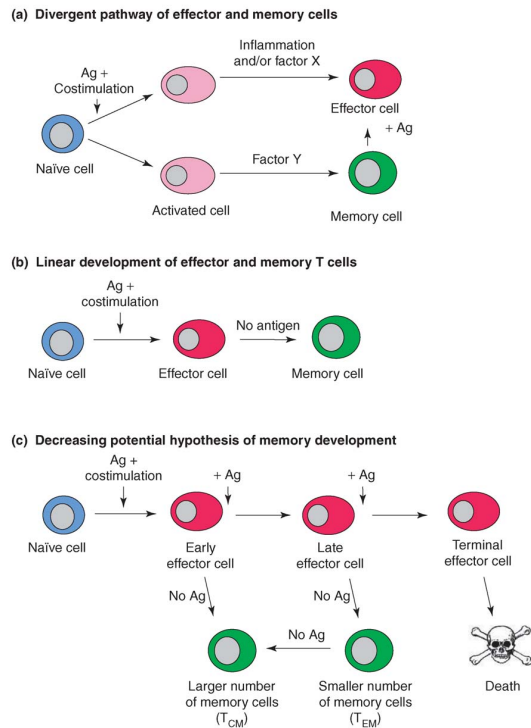


Figure 5: three different models of CD8 T cell differentiation have been proposed. a) Straight-to-memory model: cytokines as IL-12 and IL-21 or type I INF play an important role in determining the fate of a naive T cell activated through antigen+co-stimulation. b) Uniform potential model: memory T cells derive directly from effector T cells during the contraction phase of the response. c) Decreasing potential model: activated T cells progressively loose their ability to differentiate towards memory T cells. Duration and level of antigen stimulation largely determin the effector/memory ratio. Cartoon from [2]

On the basis of cell surface protein expression and proliferative capacity, two different subsets of effector CD8 T cells have been described. Short-lived effector cells (SLECs) are identified as $CD8^+CD44^{hi}KLRG1^{hi}IL7R\alpha^{lo}$ cells and are characterized by direct cytotoxic activity but low proliferative potential. Memory precursors effector cells (MPECs), instead, are recognized as $CD8^+CD44^{hi}KLRG1^{lo}IL7R\alpha^{hi}$ cells and can give rise to long-lived memory cells [176]. MPECs represent the precursors of two different CD8 memory cells, the T-central-memory (T_{CM}) and the T-effector-memory (T_{EM}) cells [170]. T_{CM} cells are found predominantly in lymph nodes, and accordingly they express high levels of the lymph node homing receptor CD62L. T_{CM} cells represent the cells with the highest proliferative capacity upon re-encounter with the antigen and they rapidly develop an effector phenotype, but they have reduced cytotoxicity. T_{EM} cells, instead, do not express CD62L and are mostly found in non-lymphoid tissues where they can survive for long periods [177]. Moreover, T_{EM} cells are characterized by pronounced cytolytic potential and can rapidly secrete high amounts of cytokines upon re-stimulation [178] and can rapidly control invading pathogen at the site of their entry into the organism.

Upon encounter with an antigen, naive CD8 T cells clonally expand and differentiate towards CTLs. The effector functions of these cells comprise both cytolysis of the infected cells, and production of cytokines, chemokines or microbicidal molecules. Cytolysis of infected cells can be mediated by two different pathways. The first one is

the granule exocytosis pathway and it depends on the pore-forming molecule perforin and granzymes. Stimulation of the CTL leads to activation of a Ca^{++} -dependent degranulation process which releases perforin and granzymes from intracellular granules into the localized space between the CTL and the target cell [179]. Secreted perforin and granzyme B have complementary roles in inducing lysis of a target cell, since perforin lyses the target cells, while granzyme B fragmentizes the DNA [180]. The second cytolytic mechanism of CTLs depends on upregulation of FasL on the lymphocyte surface which can initiate programmed-cell death upon ligation of Fas (CD95) on target cells [181]. Activated CD8 T cells, however, can also secrete cytokines such as $\text{TNF}\alpha$, and chemokines, which recruit effector cells as neutrophils or macrophages to the site of infection [182]. Moreover, the calcium influx induced by TCR stimulation induces NFAT1 protein which transactivates $\text{INF}\gamma$ gene promoter leading to secretion of $\text{INF}\gamma$ by effector CD8 T cells [183].

4 Systemic lupus erythematosus

4.1 Systemic lupus erythematosus in general

Systemic lupus erythematosus (SLE) is an autoimmune disease characterized by the presence of autoantibodies due to breakdown of tolerance affecting multiple organs, including the skin, hematopoietic and lymphoreticular organs, joints, kidney, lung and cardiovascular structures. The incidence of SLE in Northern Europe is around 40 cases every 100,000 persons and up to 200 cases per 100,000 persons among blacks [184]. 90% of patients with lupus are females; during the reproductive years the ratio of diagnosis between females and males is 10 : 1, suggesting a potential pathogenic role of female hormones [185].

The disease is characterized by chronic inflammation in different organs and by the production of autoantibodies directed against intracellular components. Several different autoepitopes in humans have been identified: double stranded DNA (dsDNA), nucleosomes, Ro (ribonucleoprotein complex), La (RNA-binding protein), phospholipids, C1q (subunit of the C1 complement) and alpha-actinin (cytoskeleton component) [186] [185]. Anti-dsDNA antibodies are highly specific for lupus, and, even if they are probably not the main source of kidney damage, they have been associated with lupus nephritis. Two different theories have been proposed to explain their role in the development of tissue damage. The first one proposes that anti-dsDNA antibodies can bind to nucleosomes in the bloodstream and then deposit as complexes in the renal glomerular basement membrane where they activate the complement leading to glomerulonephritis [187]. The second model posits that anti-

dsDNA antibodies are characterized by high polyreactivity and have a pathogenic role in the kidney by reacting with renal proteins. Kidney pathology, however, has also been linked to the presence of autoantibodies against anti- α -actinin, a protein which cross-links actin and which is critical to maintain proper functionality of podocytes, components of the glomerular filtration barrier [185].

Different pathways have been shown to be affected in lupus, and altered functionality of both T and B lymphocytes has been described. In general, T lymphocytes provide excessive help to B cells and are characterized by impaired production of IL-2. Indeed, in T cells isolated from lupus patients stimulation of the TCR induces an early and enhanced signaling response characterized by increased calcium flux and cytosolic protein tyrosine phosphorylation caused by the decreased expression of CD3 ζ and its replacement by FcR γ [188]. This effect has been explained by decreased levels of Elf-1 in SLE T cells. The transcription factor Elf-1, indeed, can bind to the promoter regions of both CD3 ζ and FcR γ genes, enhancing the activity of the first promoter, and repressing the activity of the second [189]. Moreover, T cells from the lupus prone MRL/lpr mouse display aggregated lipid raft containing high concentrations of signaling molecules, which can enhance T cell activation, and the number of lipid raft-containing T cells increases with age and disease development [190]. As described in chapter 2.1.3.1, also the transcription factor NFAT is important in maintaining peripheral T cell tolerance. Indeed, upregulation of NFAT in T cells from lupus patients causes increased expression of the co-stimulatory molecule CD40L, but it fails to upregulate IL-2 because of decreased AP1 levels in SLE T cells [191]. Together with enhanced T cell activation, lupus patients display aberrant cytokine production. In particular, the defective IL-2 production is responsible for impaired T_{reg} cell function [192] and decreased AICD [188]. IL-17, which can amplify an inflammatory response by recruiting effector cells, is instead increased in sera of patients with lupus and its levels correlate with disease severity. IL-17 acts in synergy with BAFF to promote survival and proliferation of B cells, GC formation and differentiation towards Ig-secreting cells [193].

The B cell compartment of lupus patients shows evidence for violation of several B cell tolerance checkpoints. In general, SLE B cells are hyperactive, and BCR stimulation induces higher calcium flux and protein tyrosine phosphorylation [194]. As previously described, inhibitory co-receptors modulate the threshold of activation of B lymphocytes. Decreased expression of the inhibitory co-receptor Fc γ RIIb on memory B cells of lupus patients [195] or decreased Lyn levels [196], a protein tyrosine kinase which mediates Fc γ RIIb signaling, might account for increased BCR signaling.

In mice, overexpression of the CD19 co-receptor has also been associated with increased autoantibodies production and breakdown of peripheral tolerance by increasing BCR signaling [197]. Together with altered B cell activation threshold, the second common defect within the SLE B cell compartment is represented by an increased cell survival. In mice many defects have been shown to increase B cell longevity. Enforced Bcl-2 expression [198] leads to survival of autoreactive B cell clones which are usually deleted by negative selection and to development of a lupus-like syndrome in mice. In humans, the Bcl-2 family member Bfl-1 has been shown to be upregulated in SLE B cells [199]. B cell extrinsic signals can also allow autoreactive B cells to escape negative selection. As seen in chapter 2.2.2.1, BAFF is a potent costimulator of B cell survival when coupled with BCR ligation in the periphery. Indeed, transgenic mice overexpressing BAFF were shown to develop autoimmune disorders [200] and elevated serum levels of BAFF have been reported for lupus patients [201]. Moreover, constitutive activation of the canonical NF- κ B pathway can replace BAFF-R signaling in B cells and increase survival of potentially autoreactive transitional B cells in mice [126].

4.2 The etiology of Systemic Lupus Erythematosus

The etiology of SLE is mostly unknown, but probably both genetic and environmental factors play an important role in the development of the disease.

Environmental factors which have been shown to favor development of SLE include drugs such as procainamide, hydralazine and quinidine (drug-induced lupus) or viral infections. In particular, Epstein Barr Virus (EBV) infection has been linked to SLE through serological and DNA studies. Infection with EBV leads to production of antibodies against the viral protein EBNA-1, which, through a process of molecular mimicry, cross-reacts with lupus-associated self antigens [202]. Moreover, through the process of epitope spreading, the cross-reactive autoantibodies can target additional, non-cross-reactive autoepitopes, leading to production of different, pathogenic autoantibodies.

In both humans and mice several genetic loci have been linked to SLE. Genetic contribution is an important factor in development of SLE. However, genetic factors might not be sufficient to cause the disease. Indeed, it has been shown that monozygotic twins have a concordance rate for lupus of ~ 25%, while it decreases at ~ 2% among dizygotic twins [185]. One of the most important and best well studied ones is present at the cytogenetic location 1q23. Within this locus the Fc γ receptors cluster together. They function to clear IgG antibodies and immune complexes from

the circulation and, since renal disease in SLE patients is often caused by immune complex deposition, they have been considered target genes since long time [203]. The HLA (human leukocyte antigen) region has also been described as susceptibility region for SLE when specific haplotypes spanning the MHC class II region are present [204]. Loss of one allele of three different components of the early classical complement pathway, C1q, C2 and C4 can also predispose to development of lupus [205]. Deficiency of complement components might lead to less efficient removal of apoptotic debris by phagocytes increasing the source of autoantigens which are usually confined inside the cells [206]. Recently, polymorphisms within the *TNFAIP3* genomic locus, encoding for the NF- κ B inhibitory protein A20, have been associated with autoimmune disorders, including SLE. Most of the disease associated polymorphisms have been mapped outside of the *A20* gene or in intronic sequences, except 2 non-synonymous SNPs in exon 3, both of which map into the DUB domain of the protein and result in decreased inhibitory activity of A20 and NF- κ B hyperactivation [207].

Finally, it has been recently shown that a subset of SLE human patients display a cellular phenotype which is consistent with defects identified in sanroque mice. In sanroque mice abundance of T_{FH} cells in the GCs can be monitored as proportional increase in circulating T_{FH} cells. Circulating T_{FH} , defined as ICOS^{hi}CXCR5⁺CD4⁺ cells, have been used as marker for GC pathway in patients with SLE and healthy controls. In a subset of SLE patients (5 out of 29) the absolute number of circulating T_{FH} cells was increased and it has been shown to correlate with particular clinical manifestations as glomerulonephritis on kidney biopsy, thrombocytopenia and high titers of autoantibodies [208]. These results further confirm the importance of the GC tolerance pathway in preventing development of lupus in human patients.

Aim of the thesis

Roquin is an RNA-binding protein which has been proposed to regulate a critical tolerance checkpoint during germinal center reactions in mice. Expansion of the follicular helper T cell compartment in sanroque mice, a systemic lupus erythematosus mouse model, was thought to be due to ectopic expression of the inducible costimulator ICOS, which expression is regulated by Roquin.

The aim of this project was to investigate the precise function of Roquin in different compartments of the immune system, in particular B and T lymphocytes. In order to assess these functions *in vivo*, and to analyze the contribution of different Roquin knockout lymphocytes subsets to autoimmunity development, we generated and analyzed a conditional Roquin knockout model.

Secondly, we wanted to assess the B cell intrinsic function of A20, a critical negative regulator of NF- κ B signaling. Polymorphisms and mutations in the *Tnfrsf3* gene, encoding for A20, have been found in various human autoimmune disorders, including systemic lupus erythematosus. To investigate its B cell specific functions and its connection with autoimmune disorders, we analyzed a conditional A20 knockout mouse model.

Brief summaries of the publications

Paper I: *B cells lacking the tumor suppressor TNFAIP3/A20 display impaired differentiation and hyperactivation and cause inflammation and autoimmunity in aged mice*

The aim of this work was to clarify B cell intrinsic functions of the ubiquitin-editing enzyme A20, a critical negative regulator of NF- κ B signaling, and to investigate a possible function of A20 knockout B cells in the pathogenesis of autoimmune disorders.

By using a mouse model for conditional ablation of A20 specifically in B cells, we found that loss of A20 leads to severe defects in late B-cell development and differentiation. Firstly, the marginal zone B cell compartment mislocalized inside the follicles and marginal zone B cell precursors were expanded. However, an *in vitro* differentiation assay clearly indicated defects in the functionality of A20 knockout marginal zone B cells. Moreover, the numbers of B1a cells, which, together with marginal zone B cells, mediate innate functions of the B lineage, were reduced in B cell-specific A20 knockout mice. Secondly, A20 ablation caused increased germinal center formation in the gut-associated lymphoid tissues, where B cells are constantly triggered by bacterial antigens.

A20 loss in B cells results in immune deregulation which is partially caused by B cell extrinsic mechanisms. Indeed, we described expansion of regulatory T, activated CD4 and CD8 and myeloid cells in A20 knockout mice which might be caused by increased production of the pro-inflammatory cytokine IL-6 by A20-deficient B cells. Furthermore, A20-deficiency in B cells amplified B cell responses *in vitro*, in agreement with stronger activation of the canonical NF- κ B pathway induced by B cell receptor cross-linking, T cell costimulation and microbial components.

Finally, we investigated the role of A20-deficient B cells in the pathogenesis of autoimmune disorders. The chronic inflammatory condition detected in A20 knockout mice results in progressive loss of tolerance which in old mice leads to autoimmune manifestations as formation of inflammatory infiltrates and immune complex deposition in kidneys and accumulation of class-switched autoantibodies in serum.

In conclusion, loss of A20 in B cells, which results in increased NF- κ B activity, impairs late B cell development and exacerbates B cell responses. Moreover, A20 knockout B cells induce a condition of chronic inflammation which culminates in old mice in an autoimmune disorder.

Paper II: *Loss of Roquin induces early death and immune deregulation but not autoimmunity*

A point mutation in *Rc3h1*, the gene encoding for the RNA-binding protein Roquin, induces a systemic lupus erythematosus-like syndrome in sanroque mice. Roquin-mediated repression of the T cell inducible co-stimulator ICOS in follicular helper T cells was proposed to be instrumental to maintain tolerance within germinal centers preventing autoimmunity.

To understand the function of Roquin in different populations of the immune system, and to elucidate whether aberrant Roquin function outside the T cell compartment might account for the autoimmune phenotype of sanroque mice, we generated and analyzed a conditional Roquin knockout mouse model. Surprisingly, loss of Roquin in the T cell compartment or in the entire hematopoietic system was not sufficient to break tolerance to self and to induce autoimmunity. Moreover, T cell development and T cell central tolerance checkpoints function normally in Roquin knockout thymic epithelial cells. To finally conclude that loss of Roquin alone is not sufficient to trigger autoimmunity in mice, we generated a conventional Roquin knockout mouse strain. Homozygous Roquin knockout mice were born at Mendelian ratios, but on the C57BL/6 background they died within 6h after birth. To analyze the effect of loss of Roquin in adult mice we backcrossed the C57BL/6 strain on a CD1 outbred background. Complete loss of Roquin in the CD1 outbred mouse strain was however still not sufficient to cause an autoimmune syndrome, indicating that the effects caused by the sanroque mutation are not recapitulated by absence of Roquin.

In immune cells Roquin has several different functions. Loss of Roquin in the hematopoietic system causes immune deregulation, which is partially driven by Roquin knockout B cells. Indeed, ablation of Roquin in the B cell compartment leads to expansion of B lymphocytes, regulatory and effector T cells and eosinophils. In the T cell compartment, instead, Roquin prevents spontaneous differentiation of CD8 T lymphocytes towards short-lived effector cells and expansion of eosinophil and macrophage/monocyte populations.

In summary, we demonstrated in this study that Roquin is a critical regulator of immune homeostasis, but its absence is not sufficient to recapitulate the sanroque phenotype and to induce autoimmunity.

Acknowledgement

It would have not been possible to write this doctoral thesis without the help of the many people around me.

In particular I would like to express my deep gratitude to my supervisor, Dr. Marc Schmidt-Supprian, for choosing me first as PhD student and for teaching and guiding me during the following years. Thanks for your mentoring, your patience and your support.

I sincerely thank Prof. Dr. Reinhard Faessler for being my Doctor Father, for hosting and supporting Schmidt-Supprian lab and for his fruitful comments and advices.

I would like to thank the members of the thesis committee for reviewing my work: Prof. Dr. Reinhard Faessler as first referee, Prof. Dr. Ludger Klein as second referee, Prof. Dr. Klaus Foerstemann, Prof. Dr. Christian Wahl-Schott, Prof. Dr. Martin Biel and Prof. Dr. Angelika Vollmar.

Special thanks to our collaborating scientists Dr. Vigo Heissmeyer, Prof. Dr. Ludger Klein, Dr. Elke Glasmacher and Dr. Martin Aichinger for their help in the lab, discussions and ideas.

Furthermore, I want to thank all the present and former members of Schmidt-Supprian's group, Yuanyuan, David, Maïke, Dilip, Valeria, Paola, Barbara, Julia, Nathalie and Basma, and of the department for creating a nice working atmosphere. In particular I thank Aurelia for her help and support at the beginning of my PhD and Vaibhao and Federico for their friendship. Big thanks go also to Paola and Julia, for their help in the lab. And I want to say a special thank to Christoph and Klaus for their help and our discussions, but also for sharing with me good and bad moments of everyday life inside and outside the lab and for being good friends.

Furthermore I would like to thank also the animal caretakers for their help in the mouse house, in particular Bianca, Jens, Florian and Miriam, Sylvia Zehner, Carmen Schmitz and Ines Lach-Kusevic for administrative help and Dr. Walter Goehring and Dr. Armin Lambacher for technical support.

But above all I want to thank my family, my mother Rossanna and my father Sergio, for their constant support, and in particular Federico, for his daily patience, understanding, encouragement and for having been by my side through all these years.

Curriculum Vitae

PERSONAL INFORMATIONS

Name Arianna Bertossi

Nationality Italian

PUBLICATIONS

Chu et al. B cells lacking the tumor suppressor TNFAIP3/A20 display impaired differentiation and hyperactivation and cause inflammation and autoimmunity in aged mice. *Blood* (2011) vol. 117 (7) pp. 2227-36

Bertossi et al. Loss of Roquin induces early death and immune deregulation but not autoimmunity. *Journal of Experimental Medicine* (2011) pp. 1-15

References

1. Hogquist, K.A., T.A. Baldwin, and S.C. Jameson, *Central tolerance: learning self-control in the thymus*. Nat Rev Immunol, 2005. **5**(10): p. 772-82.
2. Kalia, V., et al., *Differentiation of memory B and T cells*. Curr Opin Immunol, 2006. **18**(3): p. 255-64.
3. Cambier, J.C., et al., *B-cell anergy: from transgenic models to naturally occurring anergic B cells?* Nat Rev Immunol, 2007. **7**(8): p. 633-43.
4. Garneau, N.L., J. Wilusz, and C.J. Wilusz, *The highways and byways of mRNA decay*. Nat Rev Mol Cell Biol, 2007. **8**(2): p. 113-26.
5. Vinuesa, C.G., et al., *A RING-type ubiquitin ligase family member required to repress follicular helper T cells and autoimmunity*. Nature, 2005. **435**(7041): p. 452-8.
6. Yu, D., et al., *Roquin represses autoimmunity by limiting inducible T-cell co-stimulator messenger RNA*. Nature, 2007. **450**(7167): p. 299-303.
7. Athanasopoulos, V., et al., *The ROQUIN family of proteins localizes to stress granules via the ROQ domain and binds target mRNAs*. FEBS J, 2010. **277**(9): p. 2109-27.
8. Glasmacher, E., et al., *Roquin binds inducible costimulator mRNA and effectors of mRNA decay to induce microRNA-independent post-transcriptional repression*. Nat Immunol, 2010. **11**(8): p. 725-33.
9. Linterman, M.A., et al., *Follicular helper T cells are required for systemic autoimmunity*. Journal of Experimental Medicine, 2009. **206**(3): p. 561-576.
10. Siess, D.C., et al., *A human gene coding for a membrane-associated nucleic acid-binding protein*. J Biol Chem, 2000. **275**(43): p. 33655-62.
11. Sheth, U. and R. Parker, *Decapping and decay of messenger RNA occur in cytoplasmic processing bodies*. Science, 2003. **300**(5620): p. 805-8.
12. Coller, J. and R. Parker, *General translational repression by activators of mRNA decapping*. Cell, 2005. **122**(6): p. 875-86.
13. Kedersha, N.L., et al., *RNA-binding proteins TIA-1 and TIAR link the phosphorylation of eIF-2 alpha to the assembly of mammalian stress granules*. The Journal of Cell Biology, 1999. **147**(7): p. 1431-42.
14. Reijns, M.A.M., et al., *A role for Q/N-rich aggregation-prone regions in P-body localization*. J Cell Sci, 2008. **121**(Pt 15): p. 2463-72.
15. Li, W., et al., *RLE-1, an E3 ubiquitin ligase, regulates C. elegans aging by catalyzing DAF-16 polyubiquitination*. Dev Cell, 2007. **12**(2): p. 235-46.
16. Athanasopoulos, V., et al., *The ROQUIN family of proteins localizes to stress granules via the ROQ domain and binds target mRNAs*. FEBS Journal, 2010: p. 1-19.
17. Rudd, C.E. and H. Schneider, *Unifying concepts in CD28, ICOS and CTLA4 co-receptor signalling*. Nat Rev Immunol, 2003. **3**(7): p. 544-556.
18. Linterman, M.A., et al., *Roquin differentiates the specialized functions of duplicated T cell costimulatory receptor genes CD28 and ICOS*. Immunity, 2009. **30**(2): p. 228-41.
19. Lee, Y., et al., *The nuclear RNase III Drosha initiates microRNA processing*. Nature, 2003. **425**(6956): p. 415-9.
20. Meyer, S., C. Temme, and E. Wahle, *Messenger RNA turnover in eukaryotes: pathways and enzymes*. Critical Reviews in Biochemistry and Molecular Biology, 2004. **39**(4): p. 197-216.
21. Yamashita, A., et al., *Concerted action of poly(A) nucleases and decapping enzyme in mammalian mRNA turnover*. Nat Struct Mol Biol, 2005. **12**(12): p. 1054-63.

22. Mitchell, P., et al., *The exosome: a conserved eukaryotic RNA processing complex containing multiple 3'→5' exoribonucleases*. Cell, 1997. **91**(4): p. 457-66.
23. Tharun, S. and R. Parker, *Targeting an mRNA for decapping: displacement of translation factors and association of the Lsm1p-7p complex on deadenylated yeast mRNAs*. Mol Cell, 2001. **8**(5): p. 1075-83.
24. Houseley, J. and D. Tollervey, *The many pathways of RNA degradation*. Cell, 2009. **136**(4): p. 763-76.
25. Badis, G., et al., *Targeted mRNA degradation by deadenylation-independent decapping*. Mol Cell, 2004. **15**(1): p. 5-15.
26. Binder, R., et al., *Evidence that the pathway of transferrin receptor mRNA degradation involves an endonucleolytic cleavage within the 3' UTR and does not involve poly(A) tail shortening*. EMBO J, 1994. **13**(8): p. 1969-80.
27. Lemm, I. and J. Ross, *Regulation of c-myc mRNA decay by translational pausing in a coding region instability determinant*. Mol Cell Biol, 2002. **22**(12): p. 3959-69.
28. Hentze, M.W., et al., *A cis-acting element is necessary and sufficient for translational regulation of human ferritin expression in response to iron*. Proc Natl Acad Sci USA, 1987. **84**(19): p. 6730-4.
29. Shaw, G. and R. Kamen, *A conserved AU sequence from the 3' untranslated region of GM-CSF mRNA mediates selective mRNA degradation*. Cell, 1986. **46**(5): p. 659-67.
30. Schott, J. and G. Stoecklin, *Networks controlling mRNA decay in the immune system*. WIREs RNA, 2010. **1**(3): p. 432-456.
31. Chen, C.Y., et al., *AU binding proteins recruit the exosome to degrade ARE-containing mRNAs*. Cell, 2001. **107**(4): p. 451-64.
32. Stoecklin, G., T. Mayo, and P. Anderson, *ARE-mRNA degradation requires the 5' -3' decay pathway*. EMBO Rep, 2006. **7**(1): p. 72-77.
33. Grosset, C., et al., *In vivo studies of translational repression mediated by the granulocyte-macrophage colony-stimulating factor AU-rich element*. J Biol Chem, 2004. **279**(14): p. 13354-62.
34. Frasca, D., et al., *Tristetraprolin, a negative regulator of mRNA stability, is increased in old B cells and is involved in the degradation of E47 mRNA*. J Immunol, 2007. **179**(2): p. 918-27.
35. Shen, Z.-J., S. Esnault, and J.S. Malter, *The peptidyl-prolyl isomerase Pin1 regulates the stability of granulocyte-macrophage colony-stimulating factor mRNA in activated eosinophils*. Nat Immunol, 2005. **6**(12): p. 1280-7.
36. Doller, A., et al., *Posttranslational modification of the AU-rich element binding protein HuR by protein kinase Cdelta elicits angiotensin II-induced stabilization and nuclear export of cyclooxygenase 2 mRNA*. Mol Cell Biol, 2008. **28**(8): p. 2608-25.
37. Lee, Y., et al., *MicroRNA genes are transcribed by RNA polymerase II*. EMBO J, 2004. **23**(20): p. 4051-60.
38. Rand, T.A., et al., *Argonaute2 cleaves the anti-guide strand of siRNA during RISC activation*. Cell, 2005. **123**(4): p. 621-9.
39. Meister, G., et al., *Human Argonaute2 mediates RNA cleavage targeted by miRNAs and siRNAs*. Mol Cell, 2004. **15**(2): p. 185-97.
40. Lewis, B.P., C.B. Burge, and D.P. Bartel, *Conserved seed pairing, often flanked by adenosines, indicates that thousands of human genes are microRNA targets*. Cell, 2005. **120**(1): p. 15-20.
41. Lund, E., et al., *Nuclear export of microRNA precursors*. Science, 2004. **303**(5654): p. 95-8.
42. Knight, S.W. and B.L. Bass, *A role for the RNase III enzyme DCR-1 in RNA interference and germ line development in Caenorhabditis elegans*. Science, 2001. **293**(5538): p. 2269-71.

43. Sen, G.L. and H.M. Blau, *Argonaute 2/RISC resides in sites of mammalian mRNA decay known as cytoplasmic bodies*. Nat Cell Biol, 2005. **7**(6): p. 633-6.
44. Kedersha, N., et al., *Stress granules and processing bodies are dynamically linked sites of mRNP remodeling*. The Journal of Cell Biology, 2005. **169**(6): p. 871-84.
45. Wells, S.E., et al., *Circularization of mRNA by eukaryotic translation initiation factors*. Mol Cell, 1998. **2**(1): p. 135-40.
46. Zekri, L., et al., *The silencing domain of GW182 interacts with PABPC1 to promote translational repression and degradation of microRNA targets and is required for target release*. Mol Cell Biol, 2009. **29**(23): p. 6220-31.
47. Carballo, E., W.S. Lai, and P.J. Blakeshear, *Feedback inhibition of macrophage tumor necrosis factor-alpha production by tristetraprolin*. Science, 1998. **281**(5379): p. 1001-5.
48. Stoecklin, G., et al., *Genome-wide analysis identifies interleukin-10 mRNA as target of tristetraprolin*. J Biol Chem, 2008. **283**(17): p. 11689-99.
49. Ming, X.F., et al., *Parallel and independent regulation of interleukin-3 mRNA turnover by phosphatidylinositol 3-kinase and p38 mitogen-activated protein kinase*. Mol Cell Biol, 2001. **21**(17): p. 5778-89.
50. Thai, T.-H., et al., *Regulation of the germinal center response by microRNA-155*. Science, 2007. **316**(5824): p. 604-8.
51. Vigorito, E., et al., *microRNA-155 regulates the generation of immunoglobulin class-switched plasma cells*. Immunity, 2007. **27**(6): p. 847-59.
52. Rodriguez, A., et al., *Requirement of bic/microRNA-155 for normal immune function*. Science, 2007. **316**(5824): p. 608-11.
53. Matsushita, K., et al., *Zc3h12a is an RNase essential for controlling immune responses by regulating mRNA decay*. Nature, 2009.
54. Paschoud, S., et al., *Destabilization of interleukin-6 mRNA requires a putative RNA stem-loop structure, an AU-rich element, and the RNA-binding protein AUF1*. Mol Cell Biol, 2006. **26**(22): p. 8228-41.
55. Jones, M.R., et al., *Zcchc11-dependent uridylation of microRNA directs cytokine expression*. Nat Cell Biol, 2009. **11**(9): p. 1157-63.
56. Grogan, J.L., et al., *Early transcription and silencing of cytokine genes underlie polarization of T helper cell subsets*. Immunity, 2001. **14**(3): p. 205-15.
57. Scheu, S., et al., *Activation of the integrated stress response during T helper cell differentiation*. Nat Immunol, 2006. **7**(6): p. 644-51.
58. Benz, C. and C.C. Bleul, *A multipotent precursor in the thymus maps to the branching point of the T versus B lineage decision*. J Exp Med, 2005. **202**(1): p. 21-31.
59. Palmer, E., *Negative selection--clearing out the bad apples from the T-cell repertoire*. Nat Rev Immunol, 2003. **3**(5): p. 383-91.
60. Pui, J.C., et al., *Notch1 expression in early lymphopoiesis influences B versus T lineage determination*. Immunity, 1999. **11**(3): p. 299-308.
61. Michie, A.M., et al., *Clonal characterization of a bipotent T cell and NK cell progenitor in the mouse fetal thymus*. J Immunol, 2000. **164**(4): p. 1730-3.
62. Godfrey, D.I., et al., *A developmental pathway involving four phenotypically and functionally distinct subsets of CD3-CD4-CD8- triple-negative adult mouse thymocytes defined by CD44 and CD25 expression*. J Immunol, 1993. **150**(10): p. 4244-52.
63. Fehling, H.J., et al., *Crucial role of the pre-T-cell receptor alpha gene in development of alpha beta but not gamma delta T cells*. Nature, 1995. **375**(6534): p. 795-8.

64. Dudley, E.C., et al., *T cell receptor beta chain gene rearrangement and selection during thymocyte development in adult mice*. *Immunity*, 1994. **1**(2): p. 83-93.
65. von Boehmer, H., et al., *Pleiotropic changes controlled by the pre-T-cell receptor*. *Curr Opin Immunol*, 1999. **11**(2): p. 135-42.
66. Michie, A.M. and J.C. Zúñiga-Pflücker, *Regulation of thymocyte differentiation: pre-TCR signals and beta-selection*. *Semin Immunol*, 2002. **14**(5): p. 311-23.
67. Khor, B. and B.P. Sleckman, *Allelic exclusion at the TCRbeta locus*. *Curr Opin Immunol*, 2002. **14**(2): p. 230-4.
68. Borgulya, P., et al., *Exclusion and inclusion of alpha and beta T cell receptor alleles*. *Cell*, 1992. **69**(3): p. 529-37.
69. Kyewski, B. and L. Klein, *A central role for central tolerance*. *Annu. Rev. Immunol.*, 2006. **24**: p. 571-606.
70. Wilkinson, R.W., et al., *Positive selection of thymocytes involves sustained interactions with the thymic microenvironment*. *J Immunol*, 1995. **155**(11): p. 5234-40.
71. Kotzin, B.L., S.K. Babcock, and L.R. Herron, *Deletion of potentially self-reactive T cell receptor specificities in L3T4-, Lyt-2- T cells of lpr mice*. *J Exp Med*, 1988. **168**(6): p. 2221-9.
72. Hara, H., et al., *The apoptotic protease-activating factor 1-mediated pathway of apoptosis is dispensable for negative selection of thymocytes*. *J Immunol*, 2002. **168**(5): p. 2288-95.
73. Bouillet, P., et al., *BH3-only Bcl-2 family member Bim is required for apoptosis of autoreactive thymocytes*. *Nature*, 2002. **415**(6874): p. 922-6.
74. Brocker, T., *The role of dendritic cells in T cell selection and survival*. *Journal of Leukocyte Biology*, 1999. **66**(2): p. 331-5.
75. Gallegos, A.M. and M.J. Bevan, *Central tolerance to tissue-specific antigens mediated by direct and indirect antigen presentation*. *J Exp Med*, 2004. **200**(8): p. 1039-49.
76. Derbinski, J., et al., *Promiscuous gene expression in medullary thymic epithelial cells mirrors the peripheral self*. *Nat Immunol*, 2001. **2**(11): p. 1032-9.
77. Consortium, F.-G.A., *An autoimmune disease, APECED, caused by mutations in a novel gene featuring two PHD-type zinc-finger domains*. *Nat Genet*, 1997. **17**(4): p. 399-403.
78. Anderson, M.S., et al., *Projection of an immunological self shadow within the thymus by the aire protein*. *Science*, 2002. **298**(5597): p. 1395-401.
79. McGargill, M.A., J.M. Derbinski, and K.A. Hogquist, *Receptor editing in developing T cells*. *Nat Immunol*, 2000. **1**(4): p. 336-41.
80. McCaughy, T.M., et al., *Clonal deletion of thymocytes can occur in the cortex with no involvement of the medulla*. *J Exp Med*, 2008. **205**(11): p. 2575-84.
81. Schönrich, G., et al., *Anergy induced by thymic medullary epithelium*. *Eur J Immunol*, 1992. **22**(7): p. 1687-91.
82. Walker, L.S.K. and A.K. Abbas, *The enemy within: keeping self-reactive T cells at bay in the periphery*. *Nat Rev Immunol*, 2002. **2**(1): p. 11-9.
83. Ohashi, P.S., et al., *Ablation of "tolerance" and induction of diabetes by virus infection in viral antigen transgenic mice*. *Cell*, 1991. **65**(2): p. 305-17.
84. Kurts, C., et al., *Major histocompatibility complex class I-restricted cross-presentation is biased towards high dose antigens and those released during cellular destruction*. *J Exp Med*, 1998. **188**(2): p. 409-14.
85. Jenkins, M.K. and R.H. Schwartz, *Antigen presentation by chemically modified splenocytes induces antigen-specific T cell unresponsiveness in vitro and in vivo*. *J Exp Med*, 1987. **165**(2): p. 302-19.

86. Perez, V.L., et al., *Induction of peripheral T cell tolerance in vivo requires CTLA-4 engagement*. *Immunity*, 1997. **6**(4): p. 411-7.
87. Nishimura, H., et al., *Development of lupus-like autoimmune diseases by disruption of the PD-1 gene encoding an ITIM motif-carrying immunoreceptor*. *Immunity*, 1999. **11**(2): p. 141-51.
88. DeSilva, D.R., et al., *Anergic T cells are defective in both jun NH2-terminal kinase and mitogen-activated protein kinase signaling pathways*. *J Exp Med*, 1996. **183**(5): p. 2017-23.
89. Schneider, H., et al., *T cell antigen CD28 binds to the GRB-2/SOS complex, regulators of p21ras*. *Eur J Immunol*, 1995. **25**(4): p. 1044-50.
90. Fathman, C.G. and N.B. Lineberry, *Molecular mechanisms of CD4+ T-cell anergy*. *Nat Rev Immunol*, 2007. **7**(8): p. 599-609.
91. Rao, N., I. Dodge, and H. Band, *The Cbl family of ubiquitin ligases: critical negative regulators of tyrosine kinase signaling in the immune system*. *Journal of Leukocyte Biology*, 2002. **71**(5): p. 753-63.
92. Bachmaier, K., et al., *Negative regulation of lymphocyte activation and autoimmunity by the molecular adaptor Cbl-b*. *Nature*, 2000. **403**(6766): p. 211-6.
93. Walker, L.S., et al., *Compromised OX40 function in CD28-deficient mice is linked with failure to develop CXC chemokine receptor 5-positive CD4 cells and germinal centers*. *J Exp Med*, 1999. **190**(8): p. 1115-22.
94. Fisher, G.H., et al., *Dominant interfering Fas gene mutations impair apoptosis in a human autoimmune lymphoproliferative syndrome*. *Cell*, 1995. **81**(6): p. 935-46.
95. Watanabe-Fukunaga, R., et al., *Lymphoproliferation disorder in mice explained by defects in Fas antigen that mediates apoptosis*. *Nature*, 1992. **356**(6367): p. 314-7.
96. Janeway, C.A., *The immune system evolved to discriminate infectious nonself from noninfectious self*. *Immunol Today*, 1992. **13**(1): p. 11-6.
97. Medzhitov, R., P. Preston-Hurlburt, and C.A. Janeway, *A human homologue of the Drosophila Toll protein signals activation of adaptive immunity*. *Nature*, 1997. **388**(6640): p. 394-7.
98. Matzinger, P., *Tolerance, danger, and the extended family*. *Annu. Rev. Immunol.*, 1994. **12**: p. 991-1045.
99. Thornton, A.M. and E.M. Shevach, *Suppressor effector function of CD4+CD25+ immunoregulatory T cells is antigen nonspecific*. *J Immunol*, 2000. **164**(1): p. 183-90.
100. Itoh, M., et al., *Thymus and autoimmunity: production of CD25+CD4+ naturally anergic and suppressive T cells as a key function of the thymus in maintaining immunologic self-tolerance*. *J Immunol*, 1999. **162**(9): p. 5317-26.
101. Fehérvári, Z. and S. Sakaguchi, *Development and function of CD25+CD4+ regulatory T cells*. *Curr Opin Immunol*, 2004. **16**(2): p. 203-8.
102. Wirnsberger, G., M. Hinterberger, and L. Klein, *Regulatory T-cell differentiation versus clonal deletion of autoreactive thymocytes*. *Immunol Cell Biol*, 2011. **89**(1): p. 45-53.
103. Hori, S., T. Nomura, and S. Sakaguchi, *Control of regulatory T cell development by the transcription factor Foxp3*. *Science*, 2003. **299**(5609): p. 1057-61.
104. Bennett, C.L., et al., *The immune dysregulation, polyendocrinopathy, enteropathy, X-linked syndrome (IPEX) is caused by mutations of FOXP3*. *Nat Genet*, 2001. **27**(1): p. 20-1.
105. Rosenbauer, F. and D.G. Tenen, *Transcription factors in myeloid development: balancing differentiation with transformation*. *Nat Rev Immunol*, 2007. **7**(2): p. 105-17.

106. Nutt, S.L., et al., *Commitment to the B-lymphoid lineage depends on the transcription factor Pax5*. Nature, 1999. **401**(6753): p. 556-62.
107. Alt, F.W., et al., *VDJ recombination*. Immunol Today, 1992. **13**(8): p. 306-14.
108. Karasuyama, H., A. Kudo, and F. Melchers, *The proteins encoded by the VpreB and lambda 5 pre-B cell-specific genes can associate with each other and with mu heavy chain*. J Exp Med, 1990. **172**(3): p. 969-72.
109. Nagata, K., et al., *The Ig alpha/Igbeta heterodimer on mu-negative proB cells is competent for transducing signals to induce early B cell differentiation*. Immunity, 1997. **7**(4): p. 559-70.
110. Karasuyama, H., A. Rolink, and F. Melchers, *Surrogate light chain in B cell development*. Adv Immunol, 1996. **63**: p. 1-41.
111. Neuberger, M.S., *Antigen receptor signaling gives lymphocytes a long life*. Cell, 1997. **90**(6): p. 971-3.
112. Keenan, R.A., et al., *Censoring of autoreactive B cell development by the pre-B cell receptor*. Science, 2008. **321**(5889): p. 696-9.
113. Alt, F.W., et al., *Activity of multiple light chain genes in murine myeloma cells producing a single, functional light chain*. Cell, 1980. **21**(1): p. 1-12.
114. Nemazee, D.A. and K. Bürki, *Clonal deletion of B lymphocytes in a transgenic mouse bearing anti-MHC class I antibody genes*. Nature, 1989. **337**(6207): p. 562-6.
115. Goodnow, C.C., et al., *Altered immunoglobulin expression and functional silencing of self-reactive B lymphocytes in transgenic mice*. Nature, 1988. **334**(6184): p. 676-82.
116. Sandel, P.C. and J.G. Monroe, *Negative selection of immature B cells by receptor editing or deletion is determined by site of antigen encounter*. Immunity, 1999. **10**(3): p. 289-99.
117. Tiegs, S.L., D.M. Russell, and D. Nemazee, *Receptor editing in self-reactive bone marrow B cells*. J Exp Med, 1993. **177**(4): p. 1009-20.
118. Halverson, R., R.M. Torres, and R. Pelanda, *Receptor editing is the main mechanism of B cell tolerance toward membrane antigens*. Nat Immunol, 2004. **5**(6): p. 645-50.
119. Wen, L., et al., *Evidence of marginal-zone B cell-positive selection in spleen*. Immunity, 2005. **23**(3): p. 297-308.
120. Hayakawa, K., et al., *Positive selection of natural autoreactive B cells*. Science, 1999. **285**(5424): p. 113-6.
121. Schiemann, B., et al., *An essential role for BAFF in the normal development of B cells through a BCMA-independent pathway*. Science, 2001. **293**(5537): p. 2111-4.
122. Siebenlist, U., K. Brown, and E. Claudio, *Control of lymphocyte development by nuclear factor-kappaB*. Nat Rev Immunol, 2005. **5**(6): p. 435-45.
123. Jun, J.E., et al., *Identifying the MAGUK protein Carma-1 as a central regulator of humoral immune responses and atopy by genome-wide mouse mutagenesis*. Immunity, 2003. **18**(6): p. 751-62.
124. Ruland, J., et al., *Bcl10 is a positive regulator of antigen receptor-induced activation of NF-kappaB and neural tube closure*. Cell, 2001. **104**(1): p. 33-42.
125. Ruland, J., et al., *Differential requirement for Malt1 in T and B cell antigen receptor signaling*. Immunity, 2003. **19**(5): p. 749-58.
126. Sasaki, Y., et al., *Canonical NF-kappaB activity, dispensable for B cell development, replaces BAFF-receptor signals and promotes B cell proliferation upon activation*. Immunity, 2006. **24**(6): p. 729-39.
127. Kaisho, T., et al., *IkappaB kinase alpha is essential for mature B cell development and function*. J Exp Med, 2001. **193**(4): p. 417-26.
128. Allman, D.M., et al., *Peripheral B cell maturation. II. Heat-stable antigen(hi) splenic B cells are an immature developmental intermediate in the production of long-lived marrow-derived B cells*. J Immunol, 1993. **151**(9): p. 4431-44.

129. Norvell, A., L. Mandik, and J.G. Monroe, *Engagement of the antigen-receptor on immature murine B lymphocytes results in death by apoptosis*. J Immunol, 1995. **154**(9): p. 4404-13.
130. Sproul, T.W., et al., *Cutting edge: B cell antigen receptor signaling occurs outside lipid rafts in immature B cells*. J Immunol, 2000. **165**(11): p. 6020-3.
131. Karnell, F.G., et al., *Membrane cholesterol content accounts for developmental differences in surface B cell receptor compartmentalization and signaling*. J Biol Chem, 2005. **280**(27): p. 25621-8.
132. Tarasenko, T., J.A. Dean, and S. Bolland, *FcγRIIB as a modulator of autoimmune disease susceptibility*. Autoimmunity, 2007. **40**(6): p. 409-17.
133. Xiu, Y., et al., *Transcriptional regulation of Fcγr2b gene by polymorphic promoter region and its contribution to humoral immune responses*. J Immunol, 2002. **169**(8): p. 4340-6.
134. Pugh-Bernard, A.E., et al., *Regulation of inherently autoreactive VH4-34 B cells in the maintenance of human B cell tolerance*. J Clin Invest, 2001. **108**(7): p. 1061-70.
135. Ruprecht, C.R. and A. Lanzavecchia, *Toll-like receptor stimulation as a third signal required for activation of human naive B cells*. Eur J Immunol, 2006. **36**(4): p. 810-6.
136. Jacob, J. and G. Kelsoe, *In situ studies of the primary immune response to (4-hydroxy-3-nitrophenyl)acetyl. II. A common clonal origin for periarteriolar lymphoid sheath-associated foci and germinal centers*. J Exp Med, 1992. **176**(3): p. 679-87.
137. Wykes, M., et al., *Dendritic cells interact directly with naive B lymphocytes to transfer antigen and initiate class switching in a primary T-dependent response*. J Immunol, 1998. **161**(3): p. 1313-9.
138. Reif, K., et al., *Balanced responsiveness to chemoattractants from adjacent zones determines B-cell position*. Nature, 2002. **416**(6876): p. 94-9.
139. Shaffer, A.L., et al., *Blimp-1 orchestrates plasma cell differentiation by extinguishing the mature B cell gene expression program*. Immunity, 2002. **17**(1): p. 51-62.
140. Smith, K.G., et al., *The phenotype and fate of the antibody-forming cells of the splenic foci*. Eur J Immunol, 1996. **26**(2): p. 444-8.
141. Sze, D.M., et al., *Intrinsic constraint on plasmablast growth and extrinsic limits of plasma cell survival*. J Exp Med, 2000. **192**(6): p. 813-21.
142. Paus, D., et al., *Antigen recognition strength regulates the choice between extrafollicular plasma cell and germinal center B cell differentiation*. J Exp Med, 2006. **203**(4): p. 1081-91.
143. Toyama, H., et al., *Memory B cells without somatic hypermutation are generated from Bcl6-deficient B cells*. Immunity, 2002. **17**(3): p. 329-39.
144. Wang, D., et al., *Reaction of germinal centers in the T-cell-independent response to the bacterial polysaccharide alpha(1-->6)dextran*. Proc Natl Acad Sci USA, 1994. **91**(7): p. 2502-6.
145. Sverremark, E. and C. Fernandez, *Germinal center formation following immunization with the polysaccharide dextran B512 is substantially increased by cholera toxin*. Int Immunol, 1998. **10**(7): p. 851-9.
146. MacLennan, I.C., *Germinal centers*. Annu. Rev. Immunol., 1994. **12**: p. 117-39.
147. Muramatsu, M., et al., *Class switch recombination and hypermutation require activation-induced cytidine deaminase (AID), a potential RNA editing enzyme*. Cell, 2000. **102**(5): p. 553-63.
148. Goossens, T., U. Klein, and R. Küppers, *Frequent occurrence of deletions and duplications during somatic hypermutation: implications for oncogene translocations and heavy chain disease*. Proc Natl Acad Sci USA, 1998. **95**(5): p. 2463-8.

149. Allen, C.D.C., et al., *Germinal center dark and light zone organization is mediated by CXCR4 and CXCR5*. *Nat Immunol*, 2004. **5**(9): p. 943-52.
150. Fazilleau, N., et al., *Follicular helper T cells: lineage and location*. *Immunity*, 2009. **30**(3): p. 324-35.
151. Martinez-Valdez, H., et al., *Human germinal center B cells express the apoptosis-inducing genes Fas, c-myc, P53, and Bax but not the survival gene bcl-2*. *J Exp Med*, 1996. **183**(3): p. 971-7.
152. Fazilleau, N., et al., *The function of follicular helper T cells is regulated by the strength of T cell antigen receptor binding*. *Nat Immunol*, 2009. **10**(4): p. 375-84.
153. Ansel, K.M., et al., *In vivo-activated CD4 T cells upregulate CXC chemokine receptor 5 and reprogram their response to lymphoid chemokines*. *J Exp Med*, 1999. **190**(8): p. 1123-34.
154. Breitfeld, D., et al., *Follicular B helper T cells express CXC chemokine receptor 5, localize to B cell follicles, and support immunoglobulin production*. *J Exp Med*, 2000. **192**(11): p. 1545-52.
155. Oxenius, A., et al., *CD40-CD40 ligand interactions are critical in T-B cooperation but not for other anti-viral CD4+ T cell functions*. *J Exp Med*, 1996. **183**(5): p. 2209-18.
156. van Kooten, C. and J. Banchereau, *CD40-CD40 ligand*. *Journal of Leukocyte Biology*, 2000. **67**(1): p. 2-17.
157. Hutloff, A., et al., *ICOS is an inducible T-cell co-stimulator structurally and functionally related to CD28*. *Nature*, 1999. **397**(6716): p. 263-6.
158. McAdam, A.J., et al., *Mouse inducible costimulatory molecule (ICOS) expression is enhanced by CD28 costimulation and regulates differentiation of CD4+ T cells*. *J Immunol*, 2000. **165**(9): p. 5035-40.
159. Nurieva, R.I., et al., *Generation of T follicular helper cells is mediated by interleukin-21 but independent of T helper 1, 2, or 17 cell lineages*. *Immunity*, 2008. **29**(1): p. 138-49.
160. Ozaki, K., et al., *Regulation of B cell differentiation and plasma cell generation by IL-21, a novel inducer of Blimp-1 and Bcl-6*. *J Immunol*, 2004. **173**(9): p. 5361-71.
161. Zotos, D., et al., *IL-21 regulates germinal center B cell differentiation and proliferation through a B cell-intrinsic mechanism*. *J Exp Med*, 2010. **207**(2): p. 365-78.
162. King, I.L. and M. Mohrs, *IL-4-producing CD4+ T cells in reactive lymph nodes during helminth infection are T follicular helper cells*. *J Exp Med*, 2009. **206**(5): p. 1001-7.
163. Phan, T.G., et al., *High affinity germinal center B cells are actively selected into the plasma cell compartment*. *J Exp Med*, 2006. **203**(11): p. 2419-24.
164. Kallies, A., et al., *Initiation of plasma-cell differentiation is independent of the transcription factor Blimp-1*. *Immunity*, 2007. **26**(5): p. 555-66.
165. Shaffer, A.L., et al., *BCL-6 represses genes that function in lymphocyte differentiation, inflammation, and cell cycle control*. *Immunity*, 2000. **13**(2): p. 199-212.
166. Marinova, E., S. Han, and B. Zheng, *Human germinal center T cells are unique Th cells with high propensity for apoptosis induction*. *Int Immunol*, 2006. **18**(8): p. 1337-45.
167. Lim, H.W., P. Hillsamer, and C.H. Kim, *Regulatory T cells can migrate to follicles upon T cell activation and suppress GC-Th cells and GC-Th cell-driven B cell responses*. *J Clin Invest*, 2004. **114**(11): p. 1640-9.
168. Curtsinger, J.M., et al., *Inflammatory cytokines provide a third signal for activation of naive CD4+ and CD8+ T cells*. *J Immunol*, 1999. **162**(6): p. 3256-62.

169. Jacob, J. and D. Baltimore, *Modelling T-cell memory by genetic marking of memory T cells in vivo*. Nature, 1999. **399**(6736): p. 593-7.
170. Kaech, S.M., et al., *Selective expression of the interleukin 7 receptor identifies effector CD8 T cells that give rise to long-lived memory cells*. Nat Immunol, 2003. **4**(12): p. 1191-8.
171. Curtsinger, J.M., C.M. Johnson, and M.F. Mescher, *CD8 T cell clonal expansion and development of effector function require prolonged exposure to antigen, costimulation, and signal 3 cytokine*. J Immunol, 2003. **171**(10): p. 5165-71.
172. Kolumam, G.A., et al., *Type I interferons act directly on CD8 T cells to allow clonal expansion and memory formation in response to viral infection*. J Exp Med, 2005. **202**(5): p. 637-50.
173. Zeng, R., et al., *Synergy of IL-21 and IL-15 in regulating CD8+ T cell expansion and function*. J Exp Med, 2005. **201**(1): p. 139-48.
174. Badovinac, V.P., B.B. Porter, and J.T. Harty, *CD8+ T cell contraction is controlled by early inflammation*. Nat Immunol, 2004. **5**(8): p. 809-17.
175. Ahmed, R. and D. Gray, *Immunological memory and protective immunity: understanding their relation*. Science, 1996. **272**(5258): p. 54-60.
176. Joshi, N.S., et al., *Inflammation directs memory precursor and short-lived effector CD8(+) T cell fates via the graded expression of T-bet transcription factor*. Immunity, 2007. **27**(2): p. 281-95.
177. Weninger, W., et al., *Migratory properties of naive, effector, and memory CD8(+) T cells*. J Exp Med, 2001. **194**(7): p. 953-66.
178. Sallusto, F., et al., *Two subsets of memory T lymphocytes with distinct homing potentials and effector functions*. Nature, 1999. **401**(6754): p. 708-12.
179. Henkart, P.A. and M.V. Sitkovsky, *Cytotoxic lymphocytes. Two ways to kill target cells*. Curr Biol, 1994. **4**(10): p. 923-5.
180. Heusel, J.W., et al., *Cytotoxic lymphocytes require granzyme B for the rapid induction of DNA fragmentation and apoptosis in allogeneic target cells*. Cell, 1994. **76**(6): p. 977-87.
181. Rouvier, E., M.F. Luciani, and P. Golstein, *Fas involvement in Ca(2+)-independent T cell-mediated cytotoxicity*. J Exp Med, 1993. **177**(1): p. 195-200.
182. Samsom, J.N., et al., *Tumour necrosis factor, but not interferon-gamma, is essential for acquired resistance to Listeria monocytogenes during a secondary infection in mice*. Immunology, 1995. **86**(2): p. 256-62.
183. Teixeira, L.K., et al., *IFN-gamma production by CD8+ T cells depends on NFAT1 transcription factor and regulates Th differentiation*. J Immunol, 2005. **175**(9): p. 5931-9.
184. Johnson, A.E., et al., *The prevalence and incidence of systemic lupus erythematosus in Birmingham, England. Relationship to ethnicity and country of birth*. Arthritis Rheum, 1995. **38**(4): p. 551-8.
185. Rahman, A. and D.A. Isenberg, *Systemic lupus erythematosus*. N Engl J Med, 2008. **358**(9): p. 929-39.
186. Mannik, M., et al., *Multiple autoantibodies form the glomerular immune deposits in patients with systemic lupus erythematosus*. J Rheumatol, 2003. **30**(7): p. 1495-504.
187. van Bruggen, M.C., et al., *Antigen specificity of anti-nuclear antibodies complexed to nucleosomes determines glomerular basement membrane binding in vivo*. Eur J Immunol, 1997. **27**(6): p. 1564-9.
188. Crispin, J.C., et al., *How signaling and gene transcription aberrations dictate the systemic lupus erythematosus T cell phenotype*. Trends in Immunology, 2008. **29**(3): p. 110-5.

189. Juang, Y.-T., et al., *Defective production of functional 98-kDa form of Elf-1 is responsible for the decreased expression of TCR zeta-chain in patients with systemic lupus erythematosus*. J Immunol, 2002. **169**(10): p. 6048-55.
190. Deng, G.-M. and G.C. Tsokos, *Cholera toxin B accelerates disease progression in lupus-prone mice by promoting lipid raft aggregation*. J Immunol, 2008. **181**(6): p. 4019-26.
191. Kytтарыs, V.C., et al., *Increased levels of NF-ATc2 differentially regulate CD154 and IL-2 genes in T cells from patients with systemic lupus erythematosus*. J Immunol, 2007. **178**(3): p. 1960-6.
192. Yu, A. and T.R. Malek, *Selective availability of IL-2 is a major determinant controlling the production of CD4+CD25+Foxp3+ T regulatory cells*. J Immunol, 2006. **177**(8): p. 5115-21.
193. Doreau, A., et al., *Interleukin 17 acts in synergy with B cell-activating factor to influence B cell biology and the pathophysiology of systemic lupus erythematosus*. Nat Immunol, 2009. **10**(7): p. 778-85.
194. Liossis, S.N., et al., *B cells from patients with systemic lupus erythematosus display abnormal antigen receptor-mediated early signal transduction events*. J Clin Invest, 1996. **98**(11): p. 2549-57.
195. Su, K., et al., *Expression profile of FcgammaRIIb on leukocytes and its dysregulation in systemic lupus erythematosus*. J Immunol, 2007. **178**(5): p. 3272-80.
196. Crispin, J.C., et al., *Pathogenesis of human systemic lupus erythematosus: recent advances*. Trends Mol Med, 2010. **16**(2): p. 47-57.
197. Inaoki, M., et al., *CD19-regulated signaling thresholds control peripheral tolerance and autoantibody production in B lymphocytes*. J Exp Med, 1997. **186**(11): p. 1923-31.
198. Strasser, A., et al., *Enforced BCL2 expression in B-lymphoid cells prolongs antibody responses and elicits autoimmune disease*. Proc Natl Acad Sci USA, 1991. **88**(19): p. 8661-5.
199. Andre, J.-M., et al., *Overexpression of the antiapoptotic gene Bfl-1 in B cells from patients with familial systemic lupus erythematosus*. Lupus, 2007. **16**(2): p. 95-100.
200. Mackay, F., et al., *Mice transgenic for BAFF develop lymphocytic disorders along with autoimmune manifestations*. J Exp Med, 1999. **190**(11): p. 1697-710.
201. Zhang, J., et al., *Cutting edge: a role for B lymphocyte stimulator in systemic lupus erythematosus*. J Immunol, 2001. **166**(1): p. 6-10.
202. Poole, B.D., et al., *Epstein-Barr virus and molecular mimicry in systemic lupus erythematosus*. Autoimmunity, 2006. **39**(1): p. 63-70.
203. Tsao, B.P., et al., *Evidence for linkage of a candidate chromosome 1 region to human systemic lupus erythematosus*. J Clin Invest, 1997. **99**(4): p. 725-31.
204. Wakeland, E.K., et al., *Delineating the genetic basis of systemic lupus erythematosus*. Immunity, 2001. **15**(3): p. 397-408.
205. Carroll, M.C., *The role of complement and complement receptors in induction and regulation of immunity*. Annu. Rev. Immunol., 1998. **16**: p. 545-68.
206. Munoz, L.E., et al., *SLE--a disease of clearance deficiency?* Rheumatology (Oxford), 2005. **44**(9): p. 1101-7.
207. Musone, S.L., et al., *Multiple polymorphisms in the TNFAIP3 region are independently associated with systemic lupus erythematosus*. Nat Genet, 2008. **40**(9): p. 1062-4.
208. Simpson, N., et al., *Expansion of circulating T cells resembling follicular helper T cells is a fixed phenotype that identifies a subset of severe systemic lupus erythematosus*. Arthritis Rheum, 2010. **62**(1): p. 234-44.

Supplements

In the following, papers I and II are reprinted.

Paper I

blood

2011 117: 2227-2236
Prepublished online Nov 18, 2010;
doi:10.1182/blood-2010-09-306019

B cells lacking the tumor suppressor TNFAIP3/A20 display impaired differentiation and hyperactivation and cause inflammation and autoimmunity in aged mice

Yuanyuan Chu, J. Christoph Vahl, Dilip Kumar, Klaus Heger, Arianna Bertossi, Edyta Wójtowicz, Valeria Soberon, Dominik Schenten, Brigitte Mack, Miriam Reutelshöfer, Rudi Beyaert, Kerstin Amann, Geert van Loo and Marc Schmidt-Suppran

Updated information and services can be found at:
<http://bloodjournal.hematologylibrary.org/cgi/content/full/117/7/2227>

Articles on similar topics may be found in the following *Blood* collections:
[Immunobiology](#) (4369 articles)

Information about reproducing this article in parts or in its entirety may be found online at:
http://bloodjournal.hematologylibrary.org/misc/rights.dtl#repub_requests

Information about ordering reprints may be found online at:
<http://bloodjournal.hematologylibrary.org/misc/rights.dtl#reprints>

Information about subscriptions and ASH membership may be found online at:
<http://bloodjournal.hematologylibrary.org/subscriptions/index.dtl>

Blood (print ISSN 0006-4971, online ISSN 1528-0020), is published weekly by the American Society of Hematology, 2021 L St, NW, Suite 900, Washington DC 20036.
[Copyright 2011 by The American Society of Hematology; all rights reserved.](#)



B cells lacking the tumor suppressor TNFAIP3/A20 display impaired differentiation and hyperactivation and cause inflammation and autoimmunity in aged mice

Yuanyuan Chu,¹ J. Christoph Vahl,¹ Dilip Kumar,¹ Klaus Heger,¹ Arianna Bertossi,¹ Edyta Wójtowicz,¹ Valeria Soberon,¹ Dominik Schenten,² Brigitte Mack,³ Miriam Reutelshöfer,⁴ Rudi Beyaert,⁵ Kerstin Amann,⁴ Geert van Loo,⁵ and Marc Schmidt-Supprian¹

¹Max Planck Institute of Biochemistry, Martinsried, Germany; ²Yale University School of Medicine, New Haven, CT; ³Department of Otorhinolaryngology, Head and Neck Surgery, Grosshadern Medical Center, Ludwig-Maximilians-University of Munich, Munich, Germany; ⁴Universitätsklinikum Erlangen, Pathologisches Institut, Abt Nephropathologie, Erlangen, Germany; and ⁵Department for Molecular Biomedical Research, VIB and Department of Biomedical Molecular Biology, Ghent University, Ghent, Belgium

The ubiquitin-editing enzyme A20/TNFAIP3 is essential for controlling signals inducing the activation of nuclear factor- κ B transcription factors. Polymorphisms and mutations in the TNFAIP3 gene are linked to various human autoimmune conditions, and inactivation of A20 is a frequent event in human B-cell lymphomas characterized by constitutive nuclear factor- κ B activity. Through B cell-

specific ablation in the mouse, we show here that A20 is required for the normal differentiation of the marginal zone B and B1 cell subsets. However, loss of A20 in B cells lowers their activation threshold and enhances proliferation and survival in a gene-dose-dependent fashion. Through the expression of proinflammatory cytokines, most notably interleukin-6, A20-deficient B cells trigger a pro-

gressive inflammatory reaction in naive mice characterized by the expansion of myeloid cells, effector-type T cells, and regulatory T cells. This culminates in old mice in an autoimmune syndrome characterized by splenomegaly, plasma cell hyperplasia, and the presence of class-switched, tissue-specific autoantibodies. (Blood. 2011;117(7):2227-2236)

Introduction

B cells play essential roles during protective immune responses to invading pathogens. On encounter of foreign antigen and with cognate T-cell help, B lymphocytes proliferate and form distinct histologic structures, termed germinal center (GC). In the GC, they undergo somatic hypermutation and class-switch recombination. During somatic hypermutation, they introduce random mutations into their immunoglobulin variable regions while they exchange the heavy chain constant region during class-switch recombination to allow for different effector functions. After a selection process by antigen, B cells differentiate into memory B cells and plasma cells (PCs), which secrete antibodies.¹ The deregulation of this process is heavily implicated in human disease. Production of class-switched antibodies against self-antigens causes or contributes to various autoimmune syndromes and unrestrained B-cell proliferation and survival can result in lymphomas.^{1,2} It is thought that the majority of human lymphomas derive from the GC, probably because the DNA damage inherent to the GC reaction facilitates mutations and chromosomal translocations.^{1,3}

Recently, the ubiquitin-editing enzyme A20, encoded by the tumor necrosis factor- α -inducible gene 3 (*TNFAIP3*), has been associated with both autoimmunity and lymphomagenesis. Polymorphisms and mutations in or near the *TNFAIP3* genomic locus have been linked with various human autoimmune syndromes with a strong humoral component, such as systemic lupus erythematosus (SLE),^{4,5} rheumatoid arthritis,^{6,7} and celiac disease.⁸ Loss of A20

function through mutations, chromosomal deletions, and/or promoter methylation is a frequent event in several human lymphomas,⁹⁻¹² all of which are characterized by constitutive activation of nuclear factor- κ B (NF- κ B).¹³ These factors regulate a plethora of genes encoding for proinflammatory mediators, antiapoptotic proteins, cell adhesion molecules and, for negative feedback control, inhibitory proteins, such as p100, I κ B α , and A20.^{14,15}

During the transmission of NF- κ B activating signals from cell-surface receptors such as the B-cell receptor (BCR), CD40, or Toll-like receptors (TLRs), signal transduction occurs via the attachment of polyubiquitin chains to key proteins, including MALT1 or TRAF6. Polyubiquitin chains, linked via K63 or linear assembly, serve to recruit different kinase complexes. In the case of canonical NF- κ B, induced proximity allows the upstream kinase TAK1 to phosphorylate its target IKK2, which then effects NF- κ B activation. A20, whose transcription is induced by NF- κ B, dampens signaling through 2 main activities. First, as deubiquitinase A20 removes K63-linked polyubiquitin chains from essential signaling intermediates, such as TRAF6. Second, A20 induces, in concert with other proteins, degradation of some of its molecular targets, through addition of K48-linked ubiquitin chains.^{14,16} Degradation of RIP1 limits TNF-induced signaling,¹⁴ whereas degradation of the K63-chain-specific E2 ligases Ubc13/UbcH5c generally affects the assembly of K63-linked polyubiquitin chains.¹⁷

Submitted September 8, 2010; accepted October 28, 2010. Prepublished online as *Blood* First Edition paper, November 18, 2010; DOI 10.1182/blood-2010-09-306019.

An Inside *Blood* analysis of this article appears at the front of this issue.

The online version of this article contains a data supplement.

The publication costs of this article were defrayed in part by page charge payment. Therefore, and solely to indicate this fact, this article is hereby marked "advertisement" in accordance with 18 USC section 1734.

© 2011 by The American Society of Hematology

To date, the main molecular action of A20 is to prevent prolonged NF- κ B activation in response to stimulation of TNF-R, TLR-, or NOD-like receptors and the TCR.^{14,16} Signal containment by A20 is crucial for immune homeostasis because A20-deficient mice die early on due to an uncontrolled inflammatory disease. The inflammation is triggered via MyD88-dependent TLRs by the commensal intestinal flora.¹⁸ To study the cell-type-specific and cell-intrinsic roles of A20 in the mouse, we recently generated a conditional *Tnfrif3* allele (A20^F).¹⁹ Given the implication of A20/TNFAIP3 in B-cell lymphomas and autoimmune diseases, we used B lineage-specific ablation of A20 to study its role in B-cell development, function, and disease.

Methods

Genetically modified mice

All mice described in this study are published and were originally generated using C57BL/6 ES cells, or backcrossed to C57BL/6 at least 6 times. Mice were housed in the specific pathogen-free animal facility of the Max Planck Institute. All animal procedures were approved by the Regierung of Oberbayern.

Flow cytometry

Single-cell suspensions were prepared²⁰ and stained with monoclonal antibodies: AA4.1(AA4.1), B220(RA3-6B2), CD1d(1B1), CD19(eBio1D3), CD22(2D6), CD23(B3B4), CD25(PC61.5), CD3(17A2), CD38(90), CD4(RM4-5), CD44(IM7), CD5(53-7.3), CD62L(MEL-14), CD69(H1.2F3), CD8(53-6.7), FoxP3(FJK-16s), GR-1(RB6-8C5), IgD(11-26), IgM(II/41), IL-10(JES5-16E3), IL-17A(eBio17B7), IL-4(11B11), IL-6(MP5-20F3), INF- γ (XMG1.2), Mac-1(M1/70), TCR- β (H57-597), TNF- α (MP6-XT22), CD95(15A7), CD21(7G6), CD86(GL-1), CD80(16-10A1), c-kit(2B8) (eBioscience), Ly-6G(1A8), Siglec-F(E50-2440), CD138(281-2) (BD Biosciences), and PNA (Vector Laboratories).

For intranuclear FoxP3 stainings (eBioscience) according to the manufacturer's instructions, dead cells were excluded with ethidium monoazide bromide. Samples were acquired on FACSCalibur and FACSCantoII (BD Biosciences) machines and analyzed with FlowJo software (TreeStar). For intracellular cytokine stainings, cells were stimulated for 5 hours at 37°C with 10nM phorbol myristate acetate (Calbiochem), 10nM ionomycin (Calbiochem), and 10nM brefeldin-A (Applichem). Cells were treated with Fc-block (eBioscience), and washed and surface-stained before fixation with 2% paraformaldehyde and permeabilization with 0.5% saponin. For in vitro culture, cells were purified by MACS (Miltenyi Biotec; > 85%-90% pure). Final concentrations of the activating stimuli: 2.5 μ g/mL α CD40 (HM40-3, eBioscience), 10 μ g/mL α IgM (Jackson ImmunoResearch Laboratories), 0.1 μ M CpG (InvivoGen), 20 μ g/mL lipopolysaccharide (LPS; Sigma-Aldrich), and 4 ng/mL IL-4 (R&D Systems). Enzyme-linked immunosorbent assays were conducted using antibody pairs to IL-6 (BD Biosciences) and TNF (BD Biosciences). Cell-cycle analyses by propidium iodide (PI) and carboxyfluorescein diacetate succinimidyl ester (CFDASE) were conducted as described.²⁰

Real-time PCR

RNA was isolated (QIAGEN RNeasy Mini Kit) and reverse transcribed (Promega) for quantitative real-time polymerase chain reaction (PCR) using probes and primers from the Universal Probe Library (Roche Diagnostics) according to the manufacturer's instructions.

Biochemistry

B-cell whole-cell, cytoplasmic, and nuclear lysates were essentially prepared as published.²⁰ PVDF membranes were blotted with the following antibodies: p-Ik β , p-ERK, ERK, p-JNK, JNK, p-Akt, Akt, p-p38, p38, p100/p52 (Cell Signaling); Ik β , PLC γ 2, RelB, RelA, c-Rel, Lamin B (Santa Cruz Biotechnology); tubulin (Upstate Biotechnology); p105/50 (Abcam); and A20.¹⁹

Immunofluorescence and immunohistochemistry

For immunofluorescence stainings, frozen 10- μ m sections were thawed, air-dried, methanol-fixed, and stained for 1 hour at room temperature in a humidified chamber with B220-fluorescein isothiocyanate (eBioscience), biotinylated rat anti-CD3 (BD Biosciences), biotinylated rat anti-CD138 (BD Biosciences), and rabbit anti-laminin (gift from Michael Sixt) followed by Cy3-streptavidin and Cy5-conjugated anti-rabbit antibodies (Jackson ImmunoResearch). Immunohistochemically, MZB cells were identified by anti-CD1d (eBioscience) and metallophilic macrophages by anti-MOMA1 (Serotec). Detection of IgG immune complexes in paraformaldehyde-fixed kidney sections was performed using peroxidase-labeled anti-mouse IgG antibodies and 3-amino-9-ethylcarbazole staining (Vector Laboratories). For the detection of tissue-specific autoantibodies, frozen sections from organs of *Rag2*^{-/-} mice were incubated with sera of aged and control mice and an anti-mouse IgG-Cy3 conjugate (Jackson ImmunoResearch Laboratories).

Images were acquired on a Zeiss Axiophot microscope (10 \times /0.3 or 20 \times /0.75 objectives; Carl Zeiss) using a Zeiss AxioCamMRm camera (Carl Zeiss) for monochromatic pictures and a Zeiss AxioCamMRC5 for RGB pictures. The following software programs were employed: Axiovision release 4.8 (Carl Zeiss), Photoshop CS4 and Illustrator CS4 (Adobe Systems).

Immunizations, ELISA

Mice were immunized intraperitoneally with 10 μ g NP-Ficoll (Biosearch Technologies) and bled by the tail vein. Serum immunoglobulin concentrations and NP-specific antibodies were determined by ELISA.²¹ The detection of antinuclear and anticardiolipin autoantibodies was performed using ELISA kits (Varelisa). Rheumatoid factor: ELISA plates were coated with rabbit IgG (Jackson ImmunoResearch Laboratories).

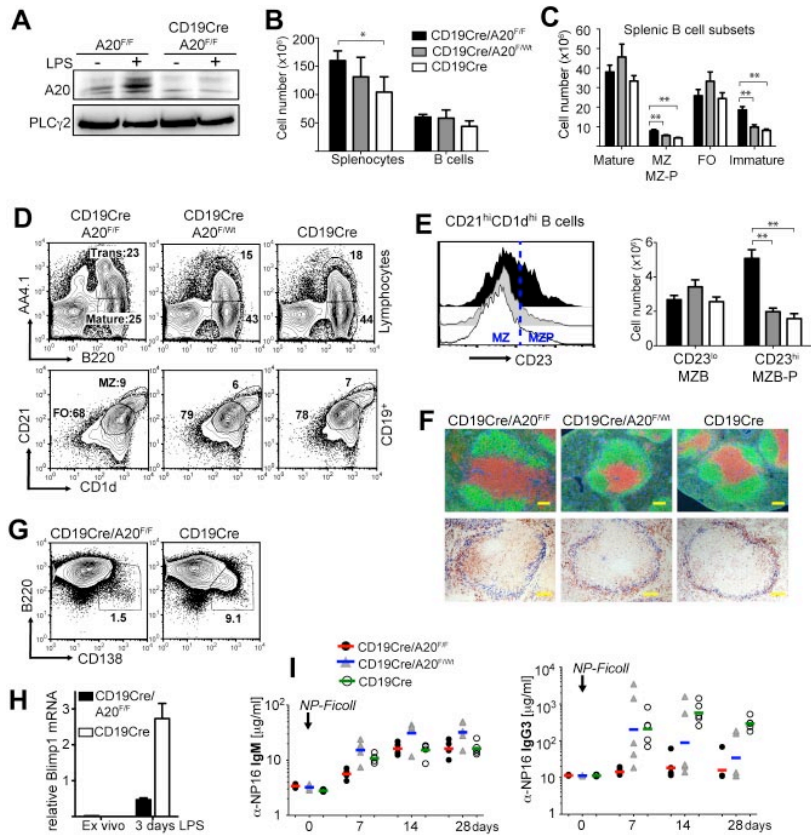
Results

Loss of A20 leads to defects in the generation and/or localization of mature B-cell subsets

To inactivate A20 specifically in B lineage cells at different developmental time points and to distinguish the specific effects of A20 ablation from potential artifacts inherent to individual cre-transgenic strains,²² we initially investigated the consequences of CD19cre- and Mb1cre-mediated ablation of A20 in parallel (supplemental Figure 1A, available on the *Blood* Web site; see the Supplemental Materials link at the top of the online article). Because we did not observe any significant differences between CD19cre/A20^{F/F} and Mb1cre/A20^{F/F} mice in our experiments, we refer to them collectively as B^{A20-/-} mice (B^{A20+/-} for heterozygous deletion). Most of the experiments presented here were conducted using CD19cre. Efficient loss of the NF- κ B-inducible A20 protein in B cells of these mice was confirmed by Western blot in both resting conditions and after treatment with LPS (Figure 1A).

Loss of A20 does not affect early B-cell development in the bone marrow, except for a minor increase in immature B cells. In contrast, the number of mature recirculating B cells is significantly reduced (supplemental Figure 1C-E). B^{A20-/-} mice have enlarged spleens, coinciding with a minor increase in total B-cell numbers (supplemental Figure 1B; Figure 1B), suggesting that other cell types are also expanded. Mature follicular B-cell numbers are unaffected by A20 deficiency, but immature transitional B cells accumulate (Figure 1C-D) without any apparent block within the transitional compartment (supplemental Figure 2A). The numbers of marginal zone B (MZB) cells, defined by CD1d and CD21 expression (Figure 1C), are elevated because of an expansion of CD23⁺ MZB precursor cells (Figure 1E; supplemental Figure 2B).

Figure 1. Conditional knockout of A20 in B cells induces severe defects in B-cell development and differentiation. (A) A20 protein expression in CD43-depleted B cells after 4-hour culture with or without 10 μ g/mL LPS. (B-E) Absolute cell numbers were calculated from 5 to 7 age-matched mice per genotype. Data are mean \pm SD. (B) Absolute splenocyte and B-cell numbers of the indicated genotypes. (C) Absolute cell numbers of splenic mature (B220⁺AA4.1⁻), marginal zone/marginal zone precursor (MZ; MZ-P: B220⁺CD1d^{high}CD21^{high}), follicular (B220⁺AA4.1⁻CD1d⁻CD23⁺), and transitional (B220⁺AA4.1⁺) B cells. (D) Representative proportions of transitional (Trans: B220⁺AA4.1⁺) and mature (B220⁺AA4.1⁻) B cells of total lymphocytes (top panels) and of follicular (FO: CD1d^{int}CD21^{int}) and marginal zone/marginal zone precursor (MZ: CD1d^{high}CD21^{high}) B cells of CD19⁺ B cells (bottom panels) in the spleen. (E) CD23 expression on B220⁺CD1d^{high}CD21^{hi} B cells (left panel). Absolute cell numbers of marginal zone (B220⁺CD1d^{high}CD21^{hi}CD23^{lo}) and marginal zone precursor (B220⁺CD1d^{high}CD21^{hi}CD23^{hi}) B cells (right panel). (F) Top panels: Immunofluorescence of spleen sections: green represents α B220, B cells; red, α CD3, T cells; and blue, laminin. Bottom panels: Immunohistochemistry of spleen sections: blue represents MOMA-1, metallophilic macrophages; and brown, CD1d-expressing cells. Bar represents 100 μ m. (G) Proportions of B220⁺CD138^{hi} plasma blasts in splenic B cells 3 days after LPS treatment. (H) Blimp1 mRNA expression relative to porphobilinogen deaminase was determined by real-time PCR in splenic B cells 3 days after LPS treatment. (I) Antigen-specific IgM and IgG3 serum titers in response to T-independent immunizations with 10 μ g NP-FicolI determined by ELISA. Lines represent geometric means for 5 mice per experimental group. * P < .05 (1-way analysis of variance). ** P < .001 (1-way analysis of variance).



Inspection of the splenic follicular organization by immunofluorescence revealed normal B- and T-cell compartments in B^{A20-/-} spleens (Figure 1F). However, in B^{A20-/-} spleen sections, CD1d-expressing MZB cells are mostly located inside the follicle, whose border is defined by MOMA-1-expressing metallophilic macrophages located adjacent to the marginal sinus. In contrast, on B^{A20+/-} and control spleen sections, CD1d-expressing cells are properly located in the marginal zone (Figure 1F). Immunofluorescent detection of laminin and B cells indicates that the B^{A20-/-} splenic marginal zone is essentially devoid of B cells (supplemental Figure 2B), further demonstrating that A20-deficient MZB cells are not at their proper location. To test MZB cell function, we treated splenocyte cultures with LPS for 3 days and monitored the differentiation of short-lived plasma cells. At early times after activation of splenic B cells by LPS MZB cells, and to much lesser extent follicular B cells, differentiate into short-lived plasma cells.²³ As opposed to control B cells, A20-deficient splenic B cells show a profound defect in their ability to differentiate into Blimp1-expressing plasmablasts after LPS stimulation in vitro (Figure 1G-H), indicating the absence or paucity of functional MZB cells. Further underscoring this notion, B^{A20-/-} mice display a significant reduction in the production of class-switched, antigen-specific IgG3 after immunizations with the TI-II antigen NP-FicolI (Figure 1I), a response exquisitely dependent on the presence of MZB cells.²⁴ These results are in line with a significant reduction of total IgG3 serum levels in naive B^{A20-/-} mice. IgG1 levels are also lower in these mice, whereas IgG2c and IgG2b levels are unchanged and IgM and IgA serum levels are strongly elevated (Figure 2A; supplemental Table 1). Supporting a role for A20 in B-cell differentiation and/or proper localization, peritoneal B1, especially B1a

cells, are reduced in B^{A20-/-} mice (Figure 2B; supplemental Figure 2E). In addition, thymic B cells are reduced in B^{A20-/-} mice, although they appear elevated in B^{A20+/-} mice (supplemental Figure 2D). Together, our results uncover several surprising deficiencies in the generation, differentiation, and/or maintenance of mature B-cell subsets in absence of A20. The affected subsets include MZB and B1 cells, which are thought to mediate the innate functions of the B lineage.²⁵

A20-deficiency enhances GC B-cell formation in gut-associated lymphoid tissues

Given A20's role as negative regulator of NF- κ B signaling, we expected A20-deficient B cells to be hyper-reactive to stimulation. We did not observe significant spontaneous GC formation in the spleens of the mice analyzed, indicating that spontaneous B-cell activation, if present in these mice, is not strong enough to induce GCs. In naive mice, gut-associated lymphoid tissue (GALT) is the place where B cells are constantly triggered by bacterial antigens to enter the GC.²⁶ The percentages and, to a lesser extent, absolute cell numbers of GC B cells in mesenteric lymph nodes and Peyer patches are increased in B^{A20-/-} and B^{A20+/-} mice (Figure 2C; and data not shown). This shows that, during B-cell activation by bacterial antigens in the GALT, strong hemizygous effects of A20 deficiency become apparent.

B cell-specific lack of A20 induces the spontaneous expansion of regulatory T, effector-type T, and myeloid cells

The increase in transitional and MZB precursor cell numbers is not sufficient to explain the higher splenocyte numbers in young B^{A20-/-} mice (Figure 1B). Further detailed analyses showed that

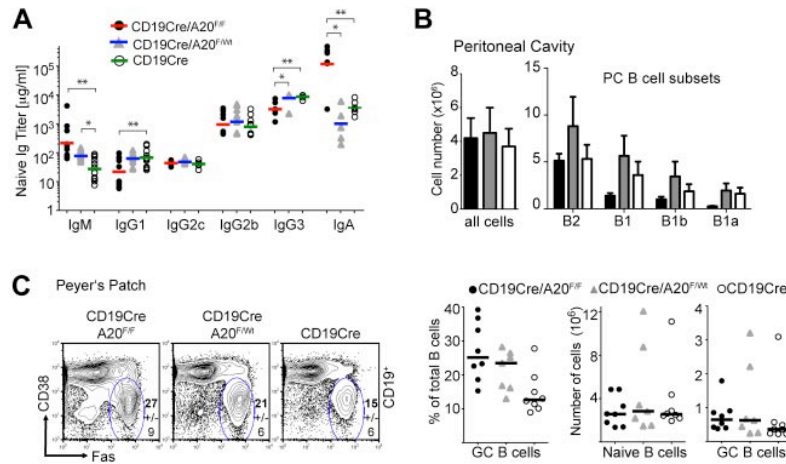


Figure 2. A20-deficiency impairs B1 cell generation but enhances GC formation in the GALT. (A) Titers of immunoglobulin isotypes were determined by ELISA; n = 6 to 12 per genotype. (B) Absolute cell numbers of B-cell subsets in the peritoneal cavity: B2 (CD19⁺ B220⁺), B1 (CD19^{high} B220^{low}), B1a (CD19^{high} B220^{low} CD5⁺), and B1b (CD19^{high} B220^{low} CD5⁻) cell numbers were calculated from 5 to 7 age-matched mice per genotype. Data are mean ± SD. (C) Left panel: Proportions of GC (CD19⁺ PNA^{hi} Fas^{hi} CD38^{lo}) of total B cells in Peyer patches. Data are mean ± SD of 8 mice per genotype. Right panel: Proportions of GC B cells depicted as individual data points (left chart), absolute cell numbers for naive B cells (mantle zone B cells: CD19⁺ PNA⁻ Fas⁻ CD38^{hi}; middle chart), and GC B cells (right chart). Bars represent medians of 8 mice per group (same as in the left panel). *P < .05 (1-way analysis of variance). **P < .001 (1-way analysis of variance).

homozygous and heterozygous ablation of A20 in B cells induces elevated numbers of T and myeloid cells. The sizes of many splenic T-cell compartments are increased in B^{A20-/-} mice, especially the regulatory (Figure 3A-B), memory-type and effector-type CD4 (Figure 3B), and effector-type CD8 T cells (Figure 3C). Similar effects on T cells were observed in the lymph nodes (data not shown). The analysis of ex vivo T-cell cytokine production by intracellular staining revealed comparable proportions of IL-17-, interferon-γ- and TNF-producing cells between B^{A20-/-} and control mice (Figure 3E). We were unable to detect any IL-4-producing cells (not shown). These analyses suggest the absence of detectable T-cell differentiation into specific T-helper lineages. The cell numbers of all splenic myeloid subsets analyzed were higher in B^{A20-/-} compared with control mice, with significant increases in dendritic cells and eosinophils (Figure 3D). Importantly, heterozygous loss of A20 in B cells induces an intermediate phenotype (Figures 3A-D) in most aspects of this immune deregulation. B^{A20+/-}

mice contain even higher proportions of splenic regulatory and effector T cells than B^{A20-/-} mice (Figure 3A). However, the higher absolute cell numbers of total CD4 T cells in B^{A20-/-} mice leads to the greatest absolute cell numbers also in these subsets (Figure 3B). B^{A20-/-} and B^{A20+/-} mice contain elevated proportions of IL-10-producing B cells (supplemental Figure 2C), excluding the possibility that absence of this immunoregulatory B-cell subset²⁷ causes the perturbation in immune homeostasis. To validate that CD19cre mediates inactivation of A20 alleles only in B cells, we performed PCR on DNA purified from splenic cell subsets of B^{A20-/-} mice. The purified T cells, dendritic cells, macrophages, and granulocytes contain less than 0.2% A20-knockout cells, which could be contaminating B cells (supplemental Figure 3). Our findings therefore indicate that the absence or gene-dose reduction of A20, specifically in B cells, induces an immune deregulation reminiscent of sterile inflammation, possibly held in check by regulatory lymphocyte subsets.

Figure 3. Ablation of A20 in the B-lineage has B cell-extrinsic effects on immune homeostasis.

(A) Dot-plots showing percentages of CD4⁺ Foxp3⁺ regulatory T cells and CD4⁺ CD25⁻ T cells (naïve indicates CD44^{hi} CD62L^{hi}; memory, CD44^{hi} CD62L^{hi}; and effector, CD44^{hi} CD62L^{lo}) in the spleen. Numbers indicate the mean of 4 to 6 mice for each genotype. (B-D) Absolute cell numbers of CD4 T (B), CD8 T (C), and myeloid cell (D) subsets in B^{A20-/-}, B^{A20+/-}, and CD19cre mice (n = 6 per group; 8-12 weeks old). Data are mean ± SD. Treg indicates Foxp3⁺; naive, CD44^{hi} CD62L^{hi}; memory, CD44^{hi} CD62L^{hi}; effector/memory, CD44^{hi} CD62L^{lo}; DC, dendritic cell (CD11c⁺); Eos, eosinophils (Gr1^{hi} SiglecF⁺); Mac, macrophages (Mac1⁺ Gr1^{lo}); and Neu, neutrophils (Gr1^{hi} Ly6G⁺). (E) Intracellular cytokine staining of ex vivo isolated splenocytes (gated on T cells). Numbers represent mean plus or minus SD of 3 mice per genotype. *P < .05 (1-way analysis of variance). **P < .001 (1-way analysis of variance).

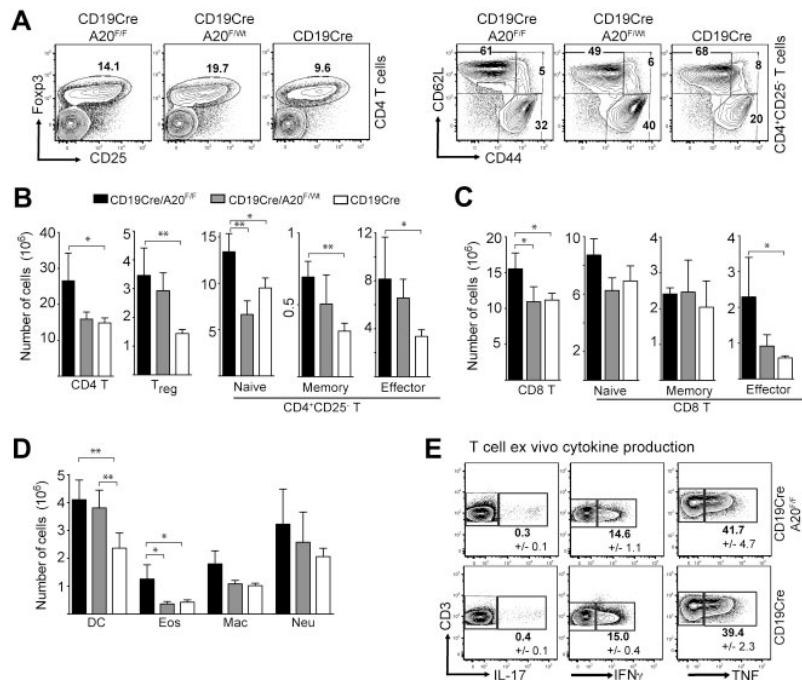
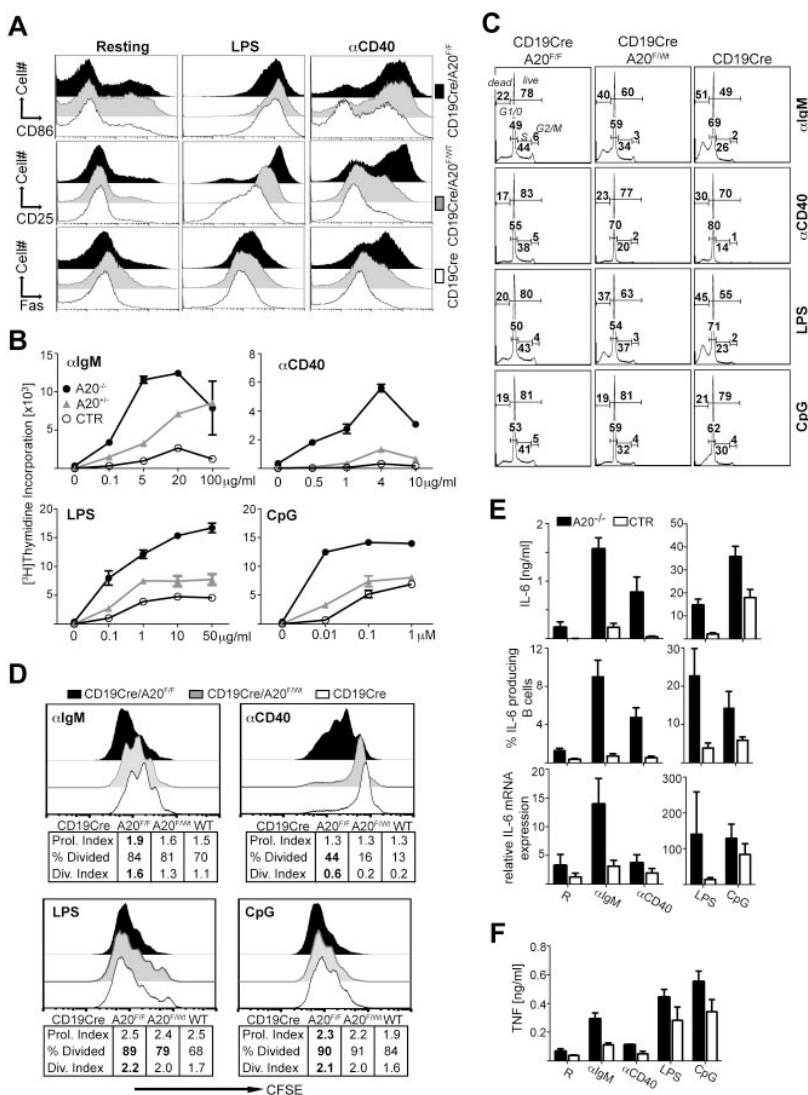


Figure 4. A20-deficiency amplifies B-cell responses.

(A) Expression levels of the respective B-cell activation marker after overnight stimulation with LPS or α CD40. The dot-plots are representative of 3 to 6 independent experiments. (B) [³H]Thymidine incorporation during a 10-hour pulse 48 hours after stimulation of B-cell cultures with α IgM, α CD40, LPS, or CpG. Data are mean \pm SD of triplicate measurements. The experiment was repeated with similar results. (C) Cell cycle profile analysis by propidium iodide staining of B cells 2 days after stimulation with the indicated mitogens. Percentages of dead (sub G₀) and live cells are indicated at the top of each histogram. The distribution within the cell cycle was calculated with the FlowJo software Version 8.7.3 using the Watson model (values do not add up to 100%). Data are means of 2 independent experiments. (D) Assessment of proliferation by the carboxyfluorescein succinimidyl ester dilution assay: histograms represent carboxyfluorescein succinimidyl ester intensities 3 days after stimulation. The tables under each histogram show the proliferation index (Prol. Index: average number of divisions of the proliferating cells), the percentage of dividing cells (% Divided: the proportion of cells that initially started to divide), and the division index (Div. Index: average number of divisions of all cells); values were calculated with the FlowJo software. Data represent the means of 5 independent experiments, and bold values are significantly different (*P* < .05) from wild-type according to 1-way analysis of variance analysis. (E) Evaluation of IL-6 production in overnight activated B cells by ELISA (top panels), intracellular FACS (middle panels), and real-time PCR (bottom panels). For intracellular FACS, B cells were stimulated for 3 days. cDNA was quantified relative to porphobilinogen deaminase. Data are mean \pm SD of 3 independent experiments. (F) Quantification of TNF production by overnight-stimulated B cells via ELISA. Data are mean \pm SD of 3 independent experiments.



A20 regulates B-cell responses in vitro in a gene-dose-dependent fashion

Our observations of enhanced GC B-cell formation in the GALT in B^{A20-/-} and B^{A20+/-} mice suggested the possibility that their B cells are more easily activated in this context. To analyze this in more detail, we first quantified the relative A20 mRNA expression at different time points after activation with α IgM, α CD40, LPS, CpG DNA, and TNF. All these stimuli induced a strong increase in A20 mRNA, peaking at approximately 1 hour (supplemental Figure 4A), prompting us to test the in vitro responses of purified A20-deficient and A20^{+/-} B cells to these mitogens. B cells up-regulate certain cell surface molecules (activation markers) upon activation, among them B7.1/CD80, B7.2/CD86, MHC II, CD25, and Fas. The expression of these markers was already slightly higher in unstimulated B cells purified from B^{A20-/-} and B^{A20+/-} mice compared with control B cells (Figure 4A; supplemental 4B). This is probably because of the latent immune activation we observed in these mice. Upon activation with the indicated mitogens, A20-deficient B cells produced higher surface levels of many activation markers (Figure 4A; supplemental Figure 3B). B cells carrying one functional A20 allele showed an intermediate

phenotype regarding expression of these activation markers (Figure 4A). We then monitored α IgM-, α CD40-, LPS-, and CpG DNA-induced proliferation by 3 assays: Both [³H]thymidine incorporation (Figure 4B) and cell cycle analysis (Figure 4C) showed increased proliferative activity in the A20-deficient B-cell cultures in response to all stimuli, and quantification of live cells revealed increased survival after all stimuli, except for CpG DNA (Figure 4C). By CFSE dilution assay (Figure 4D), we determined that the absence of A20 increased the proportion of B cells that initially start to divide (% divided) in response to α CD40 and LPS. Only CpG DNA and BCR crosslinking enhanced the proliferation of dividing A20-deficient B cells (Proliferation Index; Figure 4D). Combination of stimuli, such as LPS and α IgM, or the addition of IL-4, did not yield additive effects (supplemental Figure 4C). In all stimulations, the magnitude of the A20^{+/-} B-cell response was in between A20^{-/-} and control B cells (Figure 4B-D). Taken together, our studies show that reduction of A20 function magnifies B-cell responses through 3 mechanisms, depending on the activating stimulus: lowering the threshold for initial activation (α CD40, LPS), protecting activated B cells against apoptosis (α IgM, α CD40, LPS), and enhancing the proliferation of cells that were activated to divide (α IgM, CpG).

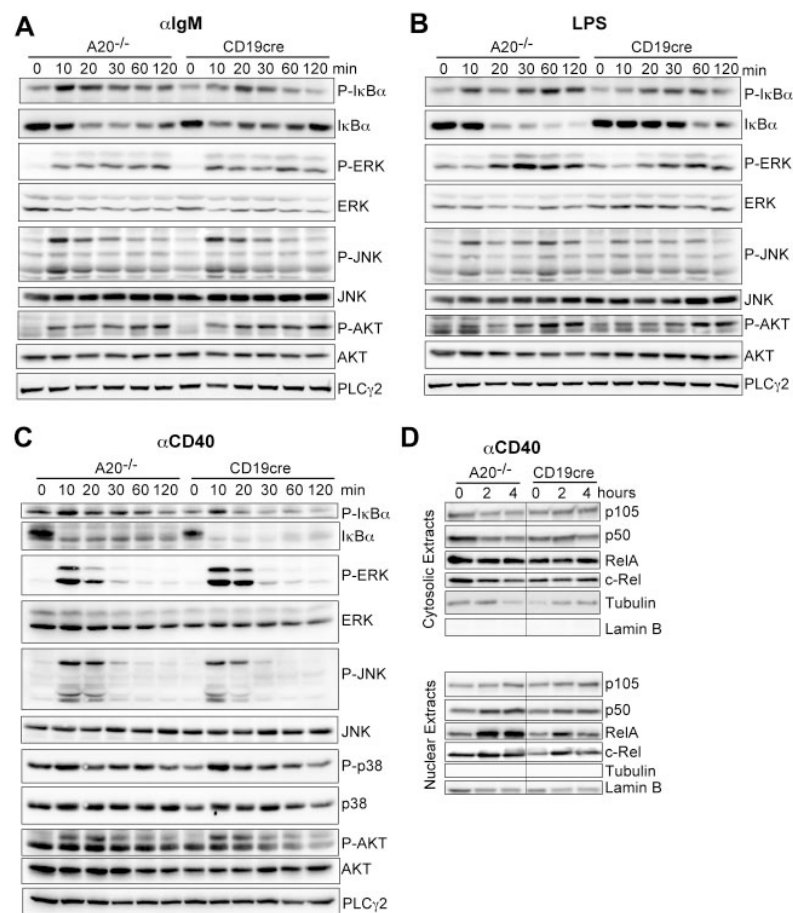


Figure 5. A20 controls canonical NF- κ B activation in response to B-cell mitogens. (A-C) Western blot of whole cell lysates stimulated for the indicated time points with (A) 10 μ g/mL α IgM, (B) 20 μ g/mL LPS, and (C) 10 μ g/mL α CD40. (D) Western blots on cytoplasmic and nuclear extracts after stimulation with α CD40. Results are representative of 2 or 3 independent experiments.

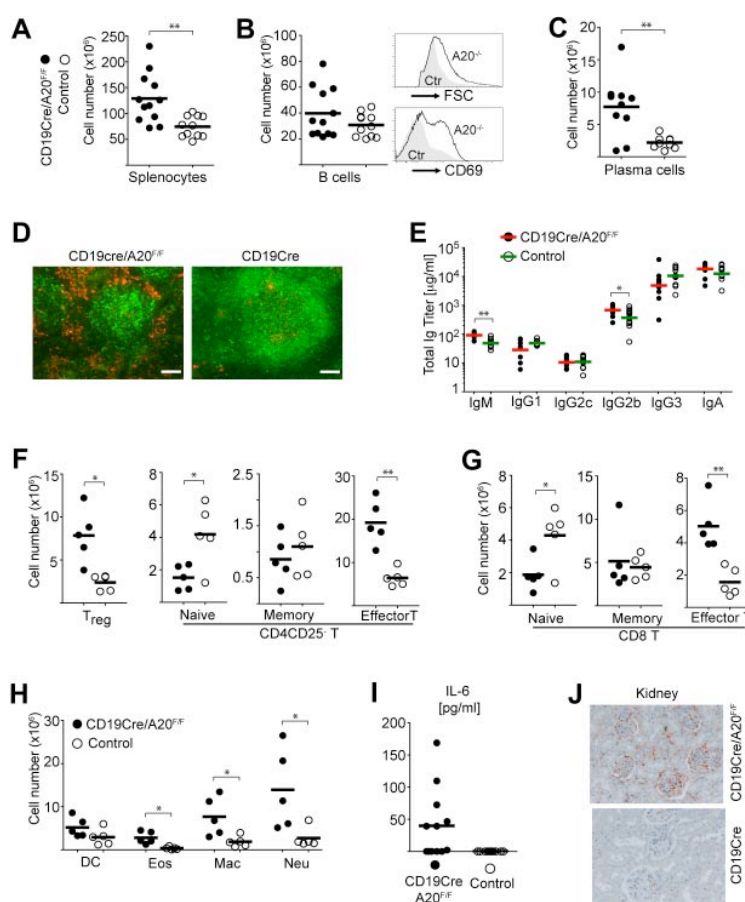
A20-deficient B cells exhibit spontaneous IL-6 secretion and highly elevated IL-6 secretion on activation

In light of the T effector and myeloid cell expansion, we wondered whether the higher excitability of A20-deficient B cells leads to secretion of proinflammatory cytokines, which in turn affect the differentiation and expansion of immune cells. IL-6 is a pleiotropic cytokine with inflammatory activity, and its levels are up-regulated in various autoimmune diseases, such as rheumatoid arthritis and SLE.²⁸ Activated A20-deficient B cells produced dramatically more IL-6 mRNA and protein than control B cells in response to all mitogens (Figure 4E). We could again detect an intermediate phenotype in A20^{+/-} B cells (supplemental Figure 4D). Indeed, A20-deficient B cells spontaneously produced and released IL-6 into the cell culture medium in the absence of stimulation in comparable amounts to the IL-6 secretion in α IgM-stimulated control B cells (Figure 4E). A20-deficient B cells also produced slightly more TNF in response to all stimuli (Figure 4F). In accord with these findings, we detected more IL-6 and TNF-producing cells in ex vivo isolated A20-deficient compared with control B cells (supplemental Figure 4E). The evaluation of IL-6 production in immune cell subsets of 3- to 4-month-old B^{A20-/-} mice by intracellular flow cytometry and real-time PCR revealed that, in addition to B cells, dendritic cells and, to a lesser extent, macrophages also produce IL-6 (supplemental Figure 5). This suggests that secondary activation of myeloid cells by A20-deficient B cells exacerbates the immune deregulation in B^{A20-/-} mice.

A20 negatively regulates canonical NF- κ B, but not MAPK or AKT activation, in response to engagement of the BCR, CD40, and TLRs

We established that A20 is a gene-dose-dependent negative regulator of B-cell activation in response to triggering of the BCR, CD40, and TLRs. A20 was reported to limit the activation of canonical NF- κ B in response to various stimuli in other cell types.^{14,16} Therefore, we wanted to confirm that the hyper-reactivity of A20-deficient B cells also correlates with enhanced canonical NF- κ B activity in response to the stimuli used in our study. Indeed, the absence of A20 selectively enhances the activation of the canonical NF- κ B pathway, evidenced by prolonged increased I κ B α phosphorylation and degradation (Figure 5A-C). The activation of MAPK pathways or AKT phosphorylation was unaltered in response to α IgM, LPS, and α CD40 (Figure 5A-C). The increased I κ B α phosphorylation correlated well with an increase in nuclear translocation of p50 and RelA 2 and 4 hours after activation with α CD40 (Figure 5D). We detected elevated expression of p100 and RelB, substrates of the alternative NF- κ B pathway and transcriptional targets of canonical NF- κ B in whole cell extracts of A20-deficient B cells (data not shown) in accord with the higher canonical NF- κ B activity in these cells. Taken together, although we do not rule out that A20 has additional functions, we demonstrate that deficiency for A20 in B cells strongly enhances activation of the canonical NF- κ B pathway in response to BCR cross-linking (antigen), T-cell costimulation (α CD40), and microbial components (TLRs).

Figure 6. Splenomegaly and plasma cell hyperplasia in old B^{A20-/-} mice. Cohort description: age range, 60 to 85 weeks; mean age of experimental group, 68 weeks; mean age of control group, 66 weeks. (A) Absolute cell numbers of splenocytes (n(B^{A20-/-}) = 10, n(control) = 9). (B) Left panel: Absolute cell numbers of B cells (CD19⁺; n(B^{A20-/-}) = 12, n(control) = 11). Right panel: Representative size and CD69 expression of splenic B220⁺ B cells. (C) Absolute cell numbers of splenic plasma cells (B220⁺CD138^{hi}; n(B^{A20-/-}) = 10, n(control) = 9). (D) Representative immunofluorescence analysis of plasma cells in the spleen, plasma cells (red represents α CD138), B cells (green represents α B220). Bar represents 100 μ m. (E) Titers of immunoglobulin isotypes in aged mice were determined by ELISA; n(B^{A20-/-}) = 12, n(control) = 11. (F-H) Absolute splenic cell numbers for the following cellular subsets: CD4⁺ T cells. (F) Treg (CD4⁺CD25⁺); CD4⁺ naive (CD25⁻CD44^{int}CD62L^{hi}), memory-type (CD25⁻CD44^{hi}CD62L^{hi}), and effector T (CD4⁺CD44^{hi}CD62L^{lo}); CD8⁺ T cells. (G) Naive (CD44^{int}CD62L^{hi}), memory-type (CD44^{hi}CD62L^{hi}), and effector T (CD44^{hi}CD62L^{lo}); myeloid cells (H): DC indicates dendritic cell (CD11c⁺); Eos, eosinophils (Gr1^{int}SiglecF⁺); Mac, macrophages (Mac1⁺Gr1^{lo}); and Neu, neutrophils (Gr1^{hi}Ly6G⁺). n(B^{A20-/-}) = 5, n(control) = 5. (I) Serum IL-6 (pg/mL) in aged mice was measured by ELISA; n(B^{A20-/-}) = 12, n(control) = 11. (J) Representative stainings of IgG immune complexes in kidneys of B^{A20-/-} and control mice. Original magnification \times 20. **P* < .05 (1-way analysis of variance). ***P* < .001 (1-way analysis of variance).



Loss of A20 in B cells leads to autoimmune pathology in old mice

To assess the impact of the chronic proinflammatory state induced by B cell-specific loss of A20 in old age, we aged a cohort of B^{A20-/-} and control mice. Histologic analysis of organs from 20-week-old B^{A20-/-} mice did not yield any signs of inflammation (not shown). B^{A20-/-} mice, more than one year old, on the contrary, were characterized by splenomegaly (Figure 6A; supplemental Figure 6A-B). Although total B-cell numbers were not significantly elevated in old B^{A20-/-} compared with control mice, all A20^{-/-} B cells appeared activated, as judged by the larger cell size and elevated levels of the activation marker CD69 (Figure 6B). In addition, we observed a marked expansion of PCs in the spleen (Figure 6C; supplemental Figure 6C), but not in the bone marrow (data not shown). Immunofluorescence analysis of the enlarged spleens revealed a diffuse pattern of PCs surrounding altered and disrupted B-cell follicles (Figure 6D). Analysis of the serum isotype titers in aged B^{A20-/-} mice revealed higher IgM titers compared with controls, as seen in young mice. However, in contrast to the latter, in old B^{A20-/-} mice the levels of the pathogenic IgG2b isotype²⁹ are elevated (Figure 6E; supplemental Table 2). The increase of effector and regulatory T cells, already apparent in young B^{A20-/-} mice, has further expanded in old mice, at the expense of the respective naive compartments (Figure 6F-G). In addition, the expansion of myeloid cell subsets was much more pronounced (Figure 6H). The progressive nature of the inflammation in the B^{A20-/-} mice is also reflected in elevated levels of serum IL-6 in aged B^{A20-/-} mice (Figure 6I), which could not be detected

in the 20-week-old B^{A20-/-} mice (not shown). Histologic analysis of organs from aged mice revealed inflammatory infiltrates in the liver and kidney of most of the old B^{A20-/-} mice (supplemental Figure 6D). Examinations of the renal pathology revealed no extensive glomerular damage but clear IgG immune complex depositions in aged B^{A20-/-} mice (Figure 6J).

Given this finding, we tested the sera of all old B^{A20-/-} and control mice for indicators of self-recognition. Class-switched antibodies against nuclear self-antigens (ANAs) are the most common autoantibodies observed in autoimmune conditions in mice and humans.³⁰ Sera from B^{A20-/-} mice did not contain significantly higher ANA levels than sera from the controls, and we also did not detect enhanced reactivity to endogenous red blood cells (Figure 7A). In addition, we observed increased levels of rheumatoid factor of the IgM isotype in some B^{A20-/-} mice, but not of the IgG isotype (Figure 7A). However, we detected significantly elevated amounts of anticardiolipin IgG antibodies in aged B^{A20-/-} mice (Figure 7A), demonstrating systemic class-switched autoimmune reactivity. To evaluate whether antiphospholipid antibodies are already detectable in younger mice, we screened the sera of 3-month-old mice. We detected elevated anticardiolipin IgG antibodies in sera from B^{A20-/-} mice (and B^{A20+/-} mice) compared with control sera, but the differences were not statistically significant (Figure 7C).

To screen for further autoreactivity against potentially tissue-specific self-antigens, we incubated organ sections of Rag2^{-/-} mice with the sera of the aged mice. We detected autoreactive class-switched IgG antibodies in the sera of B^{A20-/-}, but not of

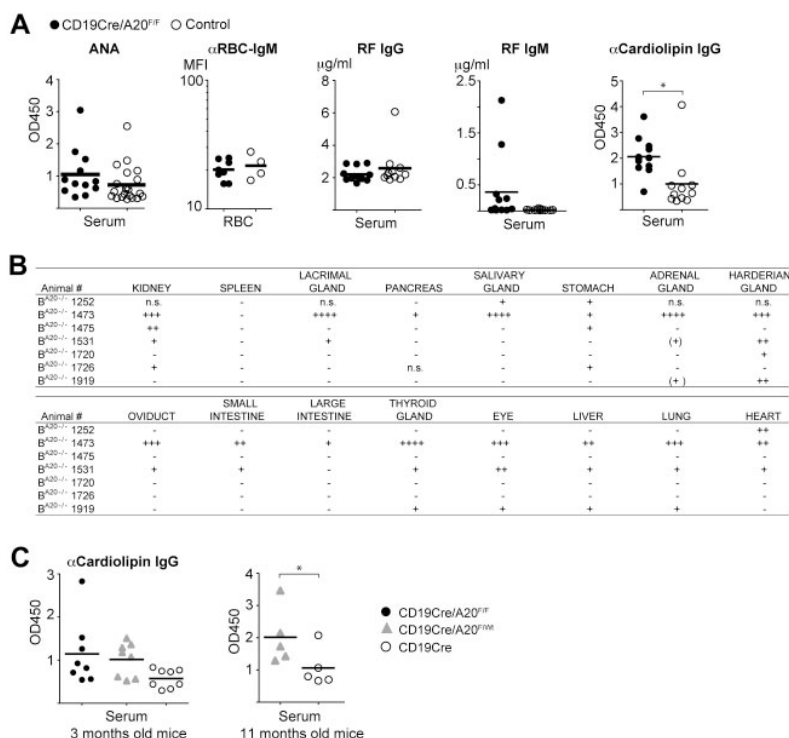


Figure 7. Autoimmune manifestations in old BA^{A20-/-} mice. (A) Analysis of autoantibodies in aged mice. ANA indicates that antinuclear IgG antibodies were detected by ELISA; n(BA^{A20-/-}) = 12, n(control) = 21; αRBC-IgM, antierythrocyte IgM was detected by FACS and represented as mean fluorescence intensity, n(BA^{A20-/-}) = 8, n(control) = 4. IgG and IgM rheumatoid factor (RF) was measured by ELISA; n(BA^{A20-/-}) = 12, n(control) = 11. α-Cardiolipin IgG antibodies were detected by ELISA; n(BA^{A20-/-}) = 12, n(control) = 11. *P < .05 (2-tailed unpaired Student t test). **P < .001 (2-tailed unpaired Student t test). (B) Table depicting the self-reactivity of sera from individual BA^{A20-/-} mice against the indicated organs from Rag2^{-/-} mice. +, ++, and +++ indicate the severity of autoreactivity; and n.s., not screened. (C) Levels of α-cardiolipin IgG autoantibodies in 3-month-old mice (left panel; n = 8 per genotype) and in 11-month-old mice (right panel; n = 5 per genotype) were detected by ELISA. *P < .05 (1-tailed unpaired Student t test).

control mice, directed predominantly against kidney, harderian gland, stomach, thyroid gland, eye, liver, and lung (Figure 7B; supplemental Figure 6E). Pancreas, salivary, lacrimal, and adrenal glands were also recognized by sera from few BA^{A20-/-} mice but with a lower penetrance compared with the organs mentioned earlier (Figure 7B). Notably, the kidney was recognized by autoantibodies in the sera of the majority of BA^{A20-/-} mice. Therefore, we conclude that A20-deficient B cells induce chronic progressive inflammation, which results in significant autoimmune manifestations and pathologic alterations in old mice.

Discussion

The prevalent inactivation of the ubiquitin-editing enzyme A20 in human B-cell lymphoma and the linkage of polymorphisms in the A20/TNFAIP3 gene to human autoimmune diseases raise the question of its function in the B-lineage, especially during B-cell activation.

The major molecular function of A20 uncovered to date is the negative regulation of canonical NF-κB activation.¹⁴ We confirm that, also in B cells, A20 limits activation of this signaling pathway by all relevant physiologic inducers. Constitutive activation of canonical NF-κB in B cells induces B-cell hyperplasia, especially pronounced in MZB cells.²⁰ In contrast, we uncovered that A20 activity is required for the correct localization of MZB cells and for MZB cell function. Therefore, we conclude that proper differentiation of A20-deficient MZB cells does not take place. In addition, A20 is needed for the generation or cellular maintenance of peritoneal B1, bone marrow recirculating and thymic B cells, either directly or by mediating their correct localization. Reduced cellular maintenance could be caused by lower sensitivity to survival signals available in naive mice, but also by increased terminal differentiation because of their hyperactivatable state. The

elevated IgA serum levels could be a consequence of the enhanced GC reactivity in the GALT of BA^{A20-/-} mice. Another possible explanation is that the lower levels of B1a cells could, at least in part, be caused by their enhanced differentiation to IgA-producing plasma cells in response to inducing signals, such as IL-15,³¹ a cytokine known to induce NF-κB activation. This phenomenon could also contribute to the elevated IgM levels. Because B1 cells are thought to be the main source of naturally occurring autoantibodies in naive mice,³² this could signify that also natural autoantibody IgM titers, which are not pathogenic but rather play a protective role, are enhanced in the BA^{A20-/-} mice. The accumulation of A20-deficient precursor populations (transitional B cells and MZB cell precursors) points to blocks in development, although we cannot exclude a role for impaired negative selection.

Taken together, our data on B-cell development and in vitro activation studies suggest the following: A20 activity is required to limit acute B-cell activation induced by stimuli connected to invasion by pathogens. Its absence reduces the activation threshold and enhances survival and proliferation in response to such stimuli. On the other side, the absence of A20 does not render B cells more responsive to maintenance signals required for mature resting cells.

Increased B cell-mediated IL-6 secretion resulting from sporadic local activation and, at least in the case of A20 deficiency, spontaneous production and release of IL-6 is a probable underlying cause of the effector T-cell differentiation and myeloid cell hyperplasia that we observed in BA^{A20-/-} and BA^{A20+/-} mice. Subsequent cytokine secretion by activated myeloid cells most probably amplifies this response. Indeed, Tsantikos et al recently showed that effector T-cell activation, myeloid cell expansion, and the development of autoimmune disease in Lyn-deficient mice, which strikingly resemble BA^{A20-/-} and BA^{A20+/-} mice in this regard, are entirely dependent on the secretion of IL-6.³³ Interestingly, the authors also observed expansion of CD4⁺CD25⁺ T cells but did not investigate whether they represent activated or regulatory

T cells.³³ The enhanced numbers of Tregs we observe in the B^{A20^{-/-}} and B^{A20^{+/-}} mice appear paradoxical in the context of elevated IL-6 levels.³⁴ We suggest that they expand and/or are induced in reaction to the IL-6-driven inflammation. However, the presence of IL-6 increases the resistance of effector T cells to suppression by regulatory T cells,³⁵ both systemically and locally. Expansion of Tregs has also been observed in the BWF1 mouse model for human SLE.³⁶ Whether, and to what extent, an expanded Treg population serves to keep the sterile inflammation in check is an intriguing question to be tested in future studies.

While this manuscript was in preparation, a study by Tavares et al on the same topic was published.³⁷ The authors also found a convincing gene-dose-dependent effect of A20 ablation on B-cell activation. They detected elevated levels of antibodies in the serum of CD19cre/A20^{Fl/Fl} mice that recognize self-antigens on a protein array. However, in their approach, anti-mouse Ig was used to detect autoantibodies, which also recognizes IgM. Indeed, both studies find highly elevated titers of IgM in naive B^{A20^{-/-}} mice (in our case, a 10-fold difference in the geometric mean). Naturally occurring autoantibodies are mostly of the IgM isotype.^{38,39} Therefore, the increased recognition of self observed by Tavares et al³⁷ could reflect, at least to some degree, this increase in natural autoantibodies. This possibility is substantiated by the fact that only IgM⁺ dsDNA-recognizing plasma cells were detected and that IgM immune complex deposits were revealed in naive 6-month-old mice, in the absence of any sign of pathology.³⁷ Given that the role of IgM autoantibodies is also discussed as being protective,^{38,39} it is unclear whether the autoreactivity observed in younger mice contributes to the development of, or helps to prevent, disease.

We observed significant autoreactivity of class-switched antibodies only in old mice, together with autoimmune pathology and inflammation. The chronic inflammation induced by the A20-deficient B cells perhaps contributes to a progressive break in B-cell tolerance resulting in the production of class-switched, autoreactive antibodies. The immune senescence of old age might also contribute to this break in tolerance.³² The inflammatory microenvironment in the spleen, and potentially in other affected organs, together with the elevated presence of the pleiotropic cytokine IL-6, may serve as a niche for the (autoreactive) plasma cells. However, we do not detect significant levels of IgG ANAs, the hallmark of SLE.³⁰ Instead, we observe general IgG autoreactivity to cardiolipin, a common autoantigen in autoimmune disease^{30,40} in old B^{A20^{-/-}} mice. The presence of tissue-specific class-switched autoantibodies strongly underscores the loss of tolerance. Some pathologic features of the old B^{A20^{-/-}} mice are reminiscent of human Castleman disease, namely, massive infiltrations of plasma cells and the elevated presence of IL-6.^{28,41} It is indeed possible that the disturbed B-cell development, including the elevated levels of naturally occurring auto-IgM, are preventing a more severe syndrome. Heterozygous B^{A20^{+/-}} mice display

inflammation and B-cell hyper-reactivity, but no developmental defects. Therefore, they might represent a good tool for modeling the reduced expression or function of A20 that should underlie the link between mutations and polymorphisms in A20/TNFAIP3 and human autoimmune disease. Indeed, initial analyses revealed elevated class-switched antibodies against cardiolipin in a cohort of 11-month-old B^{A20^{+/-}} mice (Figure 7C).

We demonstrate here that selective loss of A20 in B cells is sufficient to cause an inflammatory syndrome with autoimmune manifestations in old mice. This condition is characterized by a progressive chronic inflammation, elevated levels of IL-6, dramatic plasma cell expansion, and the presence of class-switched systemic and tissue-specific autoantibodies. The exquisite dose effects of monoallelic loss of A20 make it a prime target for deregulation by proinflammatory miRNAs and oncomirs in disease contexts. Our results demonstrate that B-cell hyper-reactivity caused by reduced A20 function can contribute to the observed link between inherited genetic mutations or polymorphisms in A20/TNFAIP3 and various human autoimmune diseases.

Acknowledgments

The authors thank Reinhard Fässler for support; Julia Knogler and Barbara Habermehl for technical assistance; Reinhard Voll and Michael Sixt for advice; Guru Krishnamoorthy for help with thymidine incorporation assays; Ludger Klein for tissues of Rag2^{-/-} mice; Claudia Uthoff-Hachenberg for ELISA reagents; and Michael Sixt, Charo Robles, Vigo Heissmeyer, Stefano Casola, Sergei Koralov, Manu Derudder, and Dinis Calado for critical reading of the manuscript.

This work was supported by the Deutsche Forschungsgemeinschaft (SFB684) and an Emmy Noether grant (M.S.-S.). J.C.V. and K.H. received PhD stipends from the Ernst Schering Foundation and the Boehringer Ingelheim Fonds, respectively. G.v.L. is a FWO postdoctoral researcher with an Odysseus Grant. K.A. was supported by the IZKF Erlangen (project A31) and D.S. by the Cancer Research Institute.

Authorship

Contribution: Y.C. and M.S.-S. designed and performed research, analyzed data, and wrote the paper; J.C.V., D.K., K.H., A.B., E.W., V.S., B.M., and M.R. performed research; D.S. and K.A. analyzed data; and R.B. and G.v.L. contributed new reagents.

Conflict-of-interest disclosure: The authors declare no competing financial interests.

Correspondence: Marc Schmidt-Supprian, Max Planck Institute of Biochemistry, Am Klopferspitz 18, D-82152 Martinsried, Germany; e-mail: supprian@biochem.mpg.de.

References

- Klein U, Dalla-Favera R. Germinal centres: role in B-cell physiology and malignancy. *Nat Rev Immunol*. 2008;8(1):22-33.
- Goodnow CC. Multistep pathogenesis of autoimmune disease. *Cell*. 2007;130(1):25-35.
- Kuppers R. Mechanisms of B-cell lymphoma pathogenesis. *Nat Rev Cancer*. 2005;5(4):251-262.
- Graham RR, Cotsapas C, Davies L, et al. Genetic variants near TNFAIP3 on 6q23 are associated with systemic lupus erythematosus. *Nat Genet*. 2008;40(9):1059-1061.
- Musone SL, Taylor KE, Lu TT, et al. Multiple polymorphisms in the TNFAIP3 region are independently associated with systemic lupus erythematosus. *Nat Genet*. 2008;40(9):1062-1064.
- Plenge RM, Cotsapas C, Davies L, et al. Two independent alleles at 6q23 associated with risk of rheumatoid arthritis. *Nat Genet*. 2007;39(12):1477-1482.
- Thomson W, Barton A, Ke X, et al. Rheumatoid arthritis association at 6q23. *Nat Genet*. 2007;39(12):1431-1433.
- Trynka G, Zhernakova A, Romanos J, et al. Coeliac disease-associated risk variants in TNFAIP3 and REL implicate altered NF-kappaB signalling. *Gut*. 2009;58(8):1078-1083.
- Schmitz R, Hansmann ML, Bohle V, et al. TNFAIP3 (A20) is a tumor suppressor gene in Hodgkin lymphoma and primary mediastinal B cell lymphoma. *J Exp Med*. 2009;206(5):981-989.
- Chanudet E, Huang Y, Ichimura K, et al. A20 is targeted by promoter methylation, deletion and inactivating mutation in MALT lymphoma. *Leukemia*. 2010;24(2):483-487.

11. Honma K, Tsuzuki S, Nakagawa M, et al. TNFAIP3 is the target gene of chromosome band 6q23.3-q24.1 loss in ocular adnexal marginal zone B cell lymphoma. *Genes Chromosomes Cancer*. 2008;47(1):1-7.
12. Novak U, Rinaldi A, Kwee I, et al. The NF- κ B negative regulator TNFAIP3 (A20) is inactivated by somatic mutations and genomic deletions in marginal zone lymphomas. *Blood*. 2009;113(20):4918-4921.
13. Packham G. The role of NF-kappaB in lymphoid malignancies. *Br J Haematol*. 2008;143(1):3-15.
14. Hymowitz SG, Wertz IE. A20: from ubiquitin editing to tumour suppression. *Nat Rev Cancer*. 2010;10(5):332-341.
15. Karin M, Cao Y, Greten FR, Li ZW. NF-kappaB in cancer: from innocent bystander to major culprit. *Nat Rev Cancer*. 2002;2(4):301-310.
16. Vereecke L, Beyaert R, van Loo G. The ubiquitin-editing enzyme A20 (TNFAIP3) is a central regulator of immunopathology. *Trends Immunol*. 2009;30(8):383-391.
17. Shembade N, Ma A, Harhaj EW. Inhibition of NF-kappaB signaling by A20 through disruption of ubiquitin enzyme complexes. *Science*. 2010;327(5969):1135-1139.
18. Turer EE, Tavares RM, Mortier E, et al. Homeostatic MyD88-dependent signals cause lethal inflammation in the absence of A20. *J Exp Med*. 2008;205(2):451-464.
19. Vereecke L, Sze M, Guire CM, et al. Enterocyte-specific A20 deficiency sensitizes to tumor necrosis factor-induced toxicity and experimental colitis. *J Exp Med*. 2010;207(7):1513-1523.
20. Sasaki Y, Derudder E, Hobeika E, et al. Canonical NF-kappaB activity, dispensable for B cell development, replaces BAFF-receptor signals and promotes B-cell proliferation upon activation. *Immunity*. 2006;24(6):729-739.
21. Schmidt-Supprian M, Tian J, Ji H, et al. I kappa B kinase 2 deficiency in T cells leads to defects in priming, B cell help, germinal center reactions, and homeostatic expansion. *J Immunol*. 2004;173(3):1612-1619.
22. Schmidt-Supprian M, Rajewsky K. Vagaries of conditional gene targeting. *Nat Immunol*. 2007;8(7):665-668.
23. Fairfax KA, Kallies A, Nutt SL, Tarlinton DM. Plasma cell development: from B-cell subsets to long-term survival niches. *Semin Immunol*. 2008;20(1):49-58.
24. Guinamard R, Okigaki M, Schlessinger J, Ravetch JV. Absence of marginal zone B cells in Pyk-2-deficient mice defines their role in the humoral response. *Nat Immunol*. 2000;1(1):31-36.
25. Allman D, Pillai S. Peripheral B-cell subsets. *Curr Opin Immunol*. 2008;20(2):149-157.
26. Casola S, Rajewsky K. B cell recruitment and selection in mouse GALT germinal centers. *Curr Top Microbiol Immunol*. 2006;308:155-171.
27. Bouaziz JD, Yanaba K, Tedder TF. Regulatory B cells as inhibitors of immune responses and inflammation. *Immunol Rev*. 2008;224:201-214.
28. Nishimoto N, Kishimoto T. Inhibition of IL-6 for the treatment of inflammatory diseases. *Curr Opin Pharmacol*. 2004;4(4):386-391.
29. Ehlers M, Fukuyama H, McGaha TL, Aderem A, Ravetch JV. TLR9/MyD88 signaling is required for class switching to pathogenic IgG2a and 2b autoantibodies in SLE. *J Exp Med*. 2006;203(3):553-561.
30. Vinuesa CG, Sanz I, Cook MC. Dysregulation of germinal centres in autoimmune disease. *Nat Rev Immunol*. 2009;9(12):845-857.
31. Hiroi T, Yanagita M, Ohta N, Sakaue G, Kiyono H. IL-15 and IL-15 receptor selectively regulate differentiation of common mucosal immune system-independent B-1 cells for IgA responses. *J Immunol*. 2000;165(8):4329-4337.
32. Cancro MP, Hao Y, Scholz JL, et al. B cells and aging: molecules and mechanisms. *Trends Immunol*. 2009;30(7):313-318.
33. Tsantikos E, Oracki SA, Quilici C, Anderson GP, Tarlinton DM, Hibbs ML. Autoimmune disease in Lyn-deficient mice is dependent on an inflammatory environment established by IL-6. *J Immunol*. 2010;184(3):1348-1360.
34. Kimura A, Kishimoto T. IL-6: regulator of Treg/Th17 balance. *Eur J Immunol*. 2010;40(7):1830-1835.
35. Pasare C, Medzhitov R. Toll pathway-dependent blockade of CD4+CD25+ T cell-mediated suppression by dendritic cells. *Science*. 2003;299(5609):1033-1036.
36. Abe J, Ueha S, Suzuki J, Tokano Y, Matsushima K, Ishikawa S. Increased Foxp3(+) CD4(+) regulatory T cells with intact suppressive activity but altered cellular localization in murine lupus. *Am J Pathol*. 2008;173(6):1682-1692.
37. Tavares RM, Turer EE, Liu CL, et al. The ubiquitin modifying enzyme A20 restricts B cell survival and prevents autoimmunity. *Immunity*. 2010;33(2):181-191.
38. Shoenfeld Y, Toubi E. Protective autoantibodies: role in homeostasis, clinical importance, and therapeutic potential. *Arthritis Rheum*. 2005;52(9):2599-2606.
39. Witte T. IgM antibodies against dsDNA in SLE. *Clin Rev Allergy Immunol*. 2008;34(3):345-347.
40. Font J, Cervera R, Lopez-Soto A, et al. Anticardiolipin antibodies in patients with autoimmune diseases: isotype distribution and clinical associations. *Clin Rheumatol*. 1989;8(4):475-483.
41. Kishimoto T. IL-6: from its discovery to clinical applications. *Int Immunol*. 2010;22(5):347-352.

Supplemental Materials Paper I

Cell purification and flow cytometry

The purification of lymphocyte and leukocyte subsets was achieved by a two step procedure. Splenic cell suspensions were first separated into CD43-expressing and CD43-negative fractions by MACS (Miltenyi). The CD43-negative fraction was stained with antibodies against B220 (eBioscience) and CD19 (eBioscience) and B220⁺CD19⁺ B cells were purified using a FACS Aria (BD). The CD43-positive fraction was stained with antibodies against B220, TCR β , CD11c, Gr-1 and Mac1 (all eBioscience). The following subsets were purified by FACS: T cells (B220⁻TCR β ⁺), dendritic cells (B220⁻TCR β ⁻CD11c⁺), granulocytes (B220⁻TCR β ⁻CD11c⁻Gr1⁺Mac1^{lo}) and macrophages (B220⁻TCR β ⁻CD11c⁻Gr1^{lo}Mac1^{hi}). All cell populations were over 99% pure.

For intracellular ex vivo IL-6 stainings of lymphocytes and leukocyte subsets, cells were stimulated for 5 h at 37°C with 10 nM brefeldin-A (Applichem).

PCR to identify A20 knock-out cells

PCR was performed using the primers a (CATTTAACCCCTTCTGAGTTTCCA), b (CCGGGCTTTAACCACTCTC), c (CCACCCCTATTACTACGTGACC) and the following touchdown program: (1) 95°C 3min, (2) 95°C 30s, (3) 65°C 45s, (4) 72°C 60s, while steps (2)–(4) are repeated 10 times, the annealing temperature is decreased by 1°C/cycle, until 55°C is reached; (5) 95°C 30s, (6) 55°C 45s, (7) 72°C 60s, (5)–(7) are repeated 20 times; (8) 72°C 5min, (9) 4°C 15min. The PCR was conducted with either all three primers or only two (b, c) to specifically amplify the A20-knockout allele. PCR was performed on DNA isolated from the purified cell subsets. To estimate the sensitivity of the PCR for the knockout allele, we diluted DNA from CD19^{cre}/A20^{F/F} B cells at different ratios in DNA from A20^{F/F} macrophages.

Immunohistochemistry

Spleen, kidney, liver were fixed in 4% PFA, processed, and embedded in paraffin. 2- μ m sections for PAS stainings were prepared according to routine protocols. For the detection of tissue-specific autoantibodies, frozen sections from organs of *Rag2*^{-/-} mice were incubated with sera of aged and control mice and an anti-mouse IgG–Cy3 conjugate (Jackson ImmunoResearch).

Table S1. Immunoglobulin titers in young mice

IgM		IgG1		IgG2c		IgG2b		IgG3		IgA					
KO	Het	KO	Het	KO	Het	KO	Het	KO	Het	KO	Het				
841	150	66	81	56	71	3493	1178	2959	10141	480439	1923				
131	70	33	72	32	47	1588	4593	1177	9541	285393	6048				
4220	121	97	82	42	41	2886	4480	5473	10099	124031	1923				
581	71	96	94	39	49	2815	3059	2389	9961	137648	327				
581	50	70	61	45	45	2123	4868	3235	2287	351497	753				
201	90	53	122	52	44	544	1874	7495	9829	3237	194				
63	75	6	66	31		482	479	467							
73	79	6	30	60		446	470	469							
172	63	10	63	25		483	478	449							
85	49	7	28	29		485	455	464							
70	52	10	49	54		455	485	414							
69	116	8	71	32		494	488	442							
216	77	22	63	44	49	41	49	41	41	3214	7762	8734	117737	1012	3655

Numbers represent individual values ($\mu\text{g/ml}$) as determined by ELISA. Geometric means are shown in bold and italics in the last row.
 KO = CD19cre/A20^{F/F}, Het = CD19cre/A20^{F/Wt}, WT = A \times CD19cre; B \times other.

Table S2. Immunoglobulin titers in old mice

KO	IgM		IgG1		IgG2c		IgG2b		IgG3		IgA	
	WT	KO	WT	KO	WT	KO	WT	KO	WT	KO	WT	KO
95	36	16	56	17	10	1085	346	7912	9512	26417	24875	
97	40	36	43	10	18	991	552	5752	23912	21417	8208	
116	37	64	73	14	17	956	239	38552	5192	4750	18625	
59	59	69	58	14	7	615	385	2952	16472	24750	16958	
80	28	50	56	9	7	249	506	5432	20952	23083	10708	
57	70	37	41	8	7	403	266	1752	2312	23917	10292	
124	38	48	41	19	19	828	737	312	4632	23917	19875	
122	60	6	46	11	17	920	917	7512	9832	18917	3208	
104	87	16	43	6	16	544	616	4232	19752	28917	26542	
107	53	33	42	6	11	781	196	10472	20232	23917	8208	
82	49	10	39	13	13	928	648	6552	10712	16417		
95		37		9	4	598	54	5192		8083		
92	48	28	48	10	11	689	371	4861	10568	18419	12573	

Numbers represent individual values ($\mu\text{g/ml}$) as determined by ELISA. Geometric means are shown in bold and italics in the last row.
 KO = CD19cre/A20^{F/F}, WT = A \times CD19cre; B \times other.

Figure S1. Loss of A20 B-lineage cells leads to decreased numbers of recirculating B cells in the bone marrow

(A) Scheme of B cell development and developmental time-frame (depicted as arrow), during which Mb1cre and CD19cre mouse strains express the cre recombinase. CD19cre induces partial recombination in preB and immature B cells: dotted line. (B) Representative spleen sizes of 8–12-week-old age-matched mice. (C) Representative dotplots showing proportions of pre/pro (B220⁺IgM⁻), immature (B220^{lo}IgM⁺) and mature/recirculating (B220^{hi}IgM⁺) B cells of lymphocytes (upper panels) and pro (proB: CD25⁻c-Kit⁺) and pre (preB: CD25⁺c-Kit⁻) B cells of B220⁺IgM⁻ cells (lower panels) in the bone marrow. (D) Absolute cell numbers of lymphocyte subsets in the bone marrow: total bone marrow cells, B cells (B220⁺), proB, preB, immature B and recirculating B cells (defined as in C). Values represent means and s.d. calculated from 5–6 mice per genotype. (E) Effects of Mb1cre-mediated ablation of A20 on B-lineage cells in the bone marrow: upper two sets of panels as in (C), lower panels: percentages of large (B220^{hi}IgM⁺CD25⁺c-Kit⁻FSC^{hi}) preB of total preB cells. * = p < 0.05; ** = p < 0.001; one-way anova

Figure S2. Loss of A20 B-lineage cells leads to an accumulation of transitional B cells in the spleen

(A) Representative dotplots showing proportions (left) and bar charts with absolute cell numbers (right) of B220⁺AA4.1⁺ transitional B cell subsets in the spleen: IgM^{hi}CD23⁻ T1, IgM^{hi}CD23⁺ T2 and IgM^{lo}CD23⁺ T3 (anergic). Values represent means and s.d. calculated from 5–6 mice per genotype. (B) Upper panels: representative dotplots showing proportions of CD19⁺CD21^{hi}CD1d^{hi} B cells in the spleen: CD23^{lo} MZ and CD23^{hi} MZ precursor B cells. Values represent means and s.d. calculated from 5–6 mice per genotype. Lower panels: immunofluorescence of spleen sections demonstrating the marginal sinus (depicted as dotted yellow line) as border between the marginal and follicular zone: green = αB220, B cells; red = αCD3, T cells; blue = laminin. Magnification: 20×. (C) Representative dotplots showing proportions of IL-10 producing B cells (B220⁺IL10⁺) after 5h stimulation with PMA/ionomycin/BFA/LPS. Values represent means and s.d. of 3 mice per genotype. (D) Representative dotplots showing proportions of B cells in the thymus (B220⁺TCRβ⁻). Values represent means and s.d. of 3 mice per genotype. (E) Representative dotplots showing proportions of B cell subsets in the peritoneal cavity (absolute cell numbers are shown in Fig. 2B): B220^{hi}CD19⁺ B2 and B220^{lo}CD19^{hi} B1 cells of total lymphocytes (upper panels) and CD43^{lo}CD5⁻ B1b and CD43⁺CD5⁺ B1a cells of B1 cells (lower panels). * = p < 0.05; ** = p < 0.001; one-way anova

Figure S3. Fidelity of CD19cre for specific recombination of conditional A20 alleles only in B cells

(A) Scheme of the conditional A20 allele before (upper panel) and after (lower panel) cre-mediated recombination. The location of the primers (a–c) employed for the genotyping PCR are shown and the length of the respective PCR amplification products. Squares indicate exons (E3–E7) and triangles loxP sites. (B) Upper panels: representative PCR results for two PCR reactions on DNA from purified splenic cell subsets: the three primer PCR (a, b, c) amplifies A20 loxP-flanked and knockout alleles,

whereas the two primer PCR (a, c) amplifies only DNA from A20-knockout alleles. Splenic cell subsets (T cells = B220⁻TCRβ⁺, dendritic cells/DC = B220⁻TCRβ⁻CD11c⁺, macrophages/Mac = B220⁻TCRβ⁻CD11c⁻Gr1^{lo}Mac1^{hi} and granulocytes/Gr = B220⁻TCRβ⁻CD11c⁻Gr1⁺Mac1^{lo}) were MACS purified followed by cell sorting and were over 99% pure. Identical results were obtained for all the cellular subsets sorted from three individual CD19cre/A20^{F/F} mice. Lower panels: evaluation of the sensitivity of the two PCRs. A20-knockout cells were diluted at different ratios with A20^{F/F} cells. The PCRs are able to amplify the knockout allele at a dilution of 1 to 500. The amplification product for the knockout allele that could be observed with the DNA from purified T cells, DCs, macrophages and granulocyte was weaker than the amplification product from the 1:500 A20-knockout to A20^{F/F} dilution in all cases. This band therefore represents most likely the presence of less than 0.2% contaminating B cells in the respective purified cell-type. However, this analysis does not allow us to rule out the presence of less than 0.2% A20-knockout cells within each cell-type.

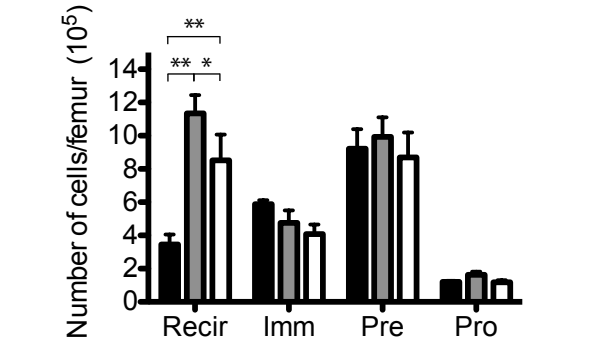
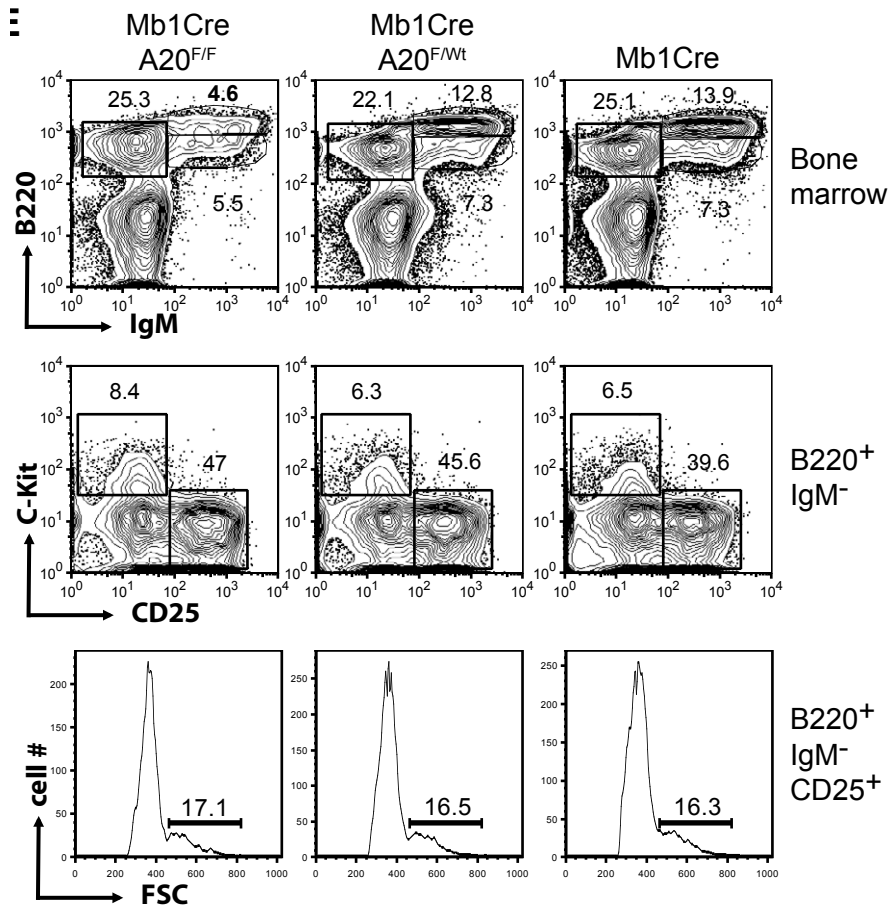
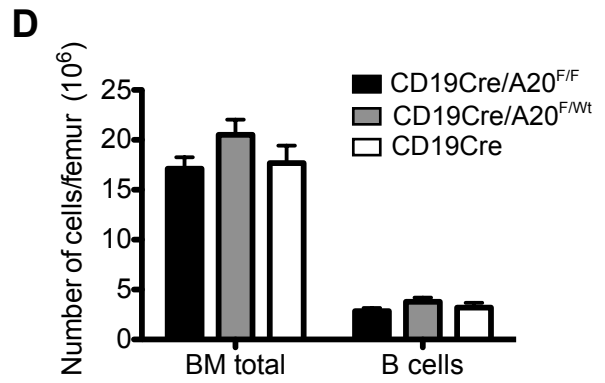
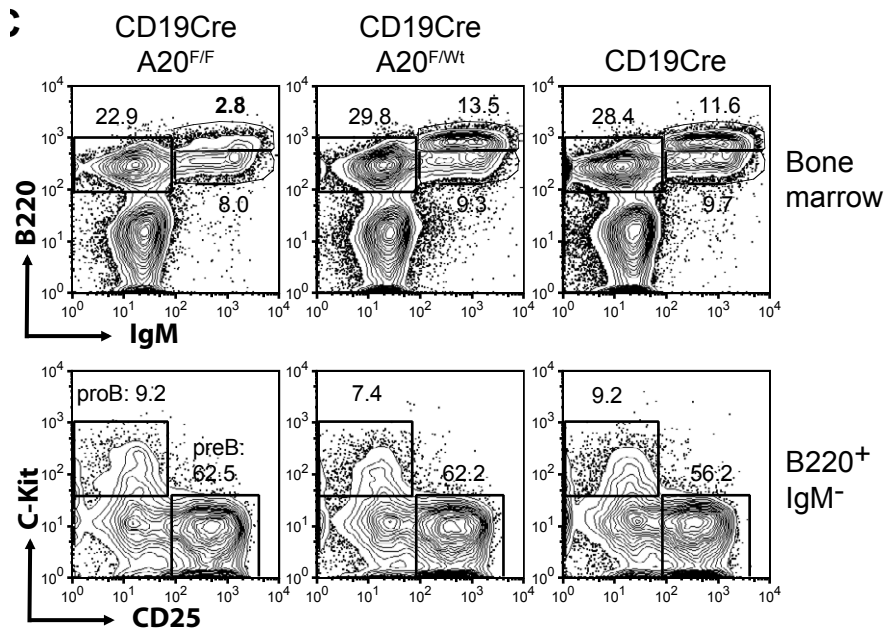
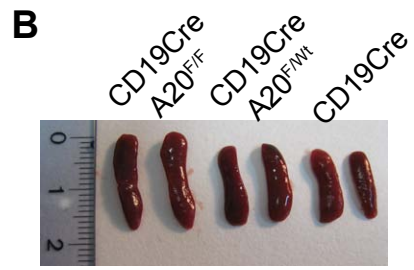
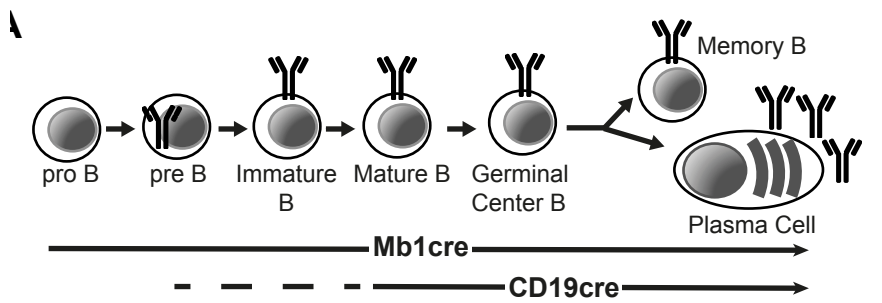
Figure S4. A20 regulates B cell activation in a dose-dependent fashion

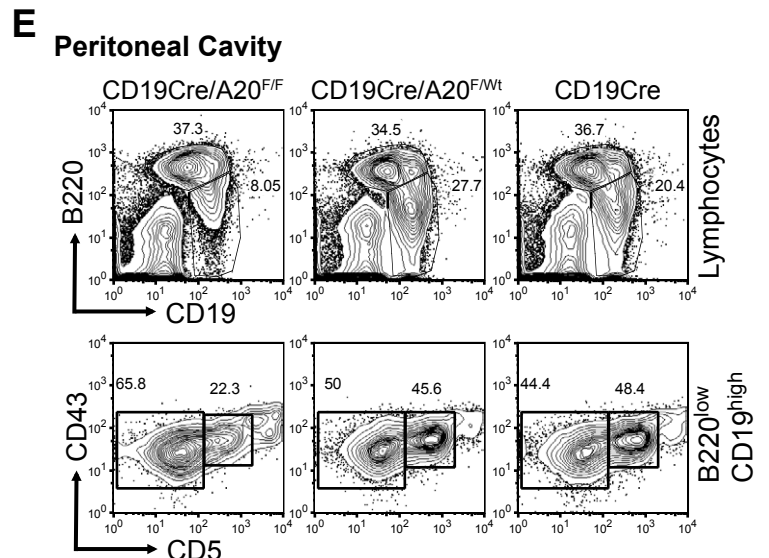
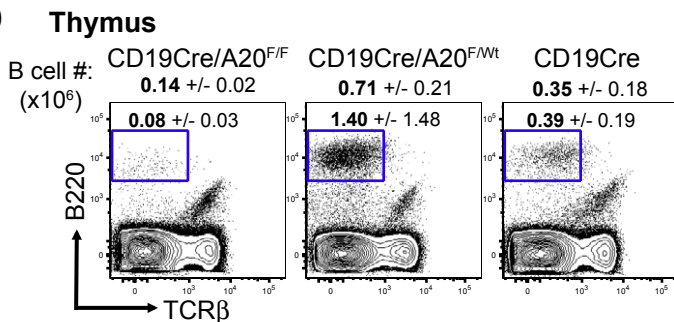
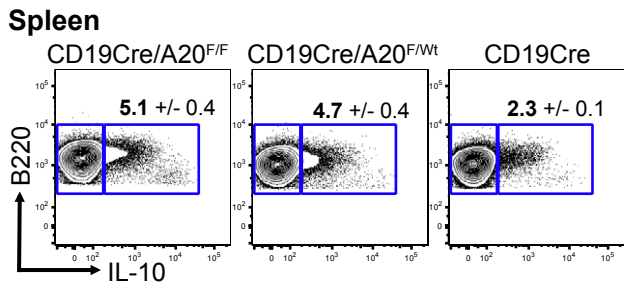
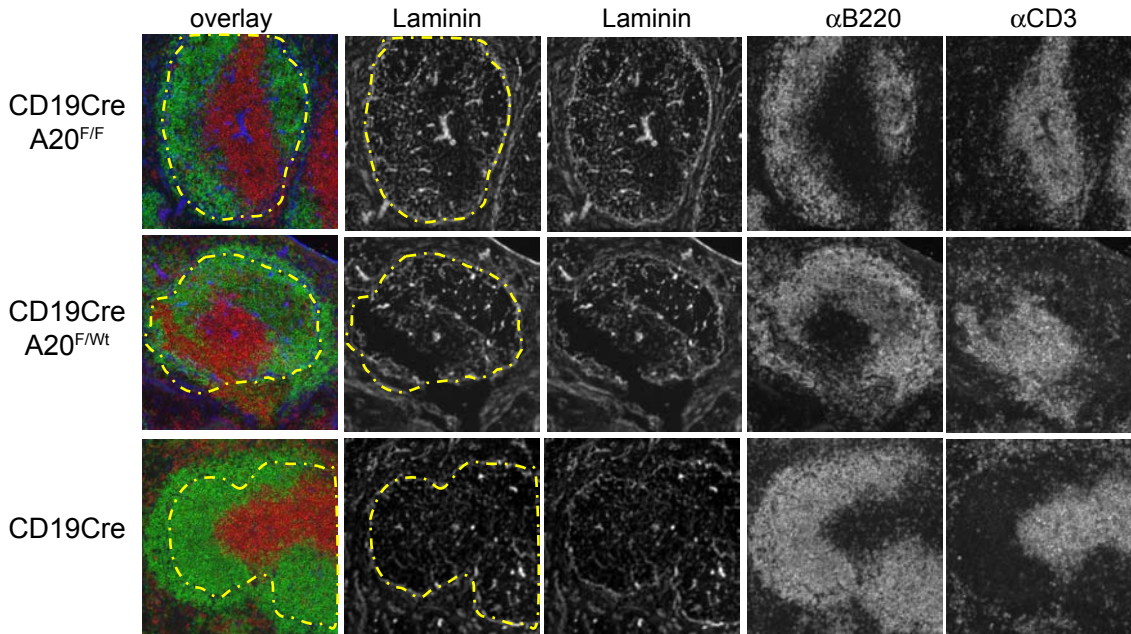
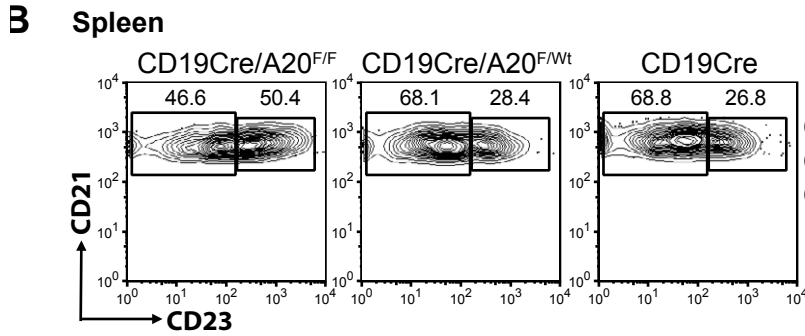
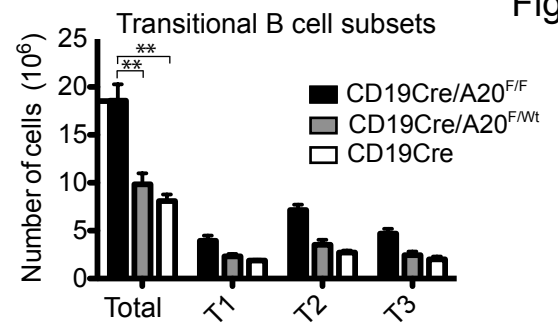
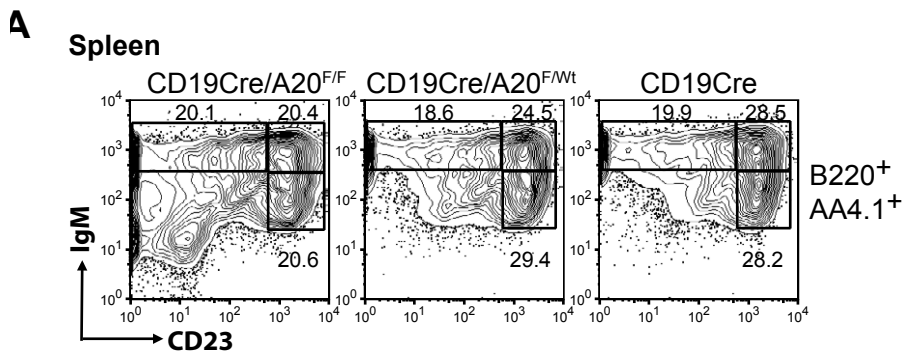
(A) Realtime PCR quantifying the amount of A20 mRNA relative to PBGD mRNA in wild-type B cells stimulated with the indicated mitogens for 1, 4 and 12 h. Means and s.d. of triplicate measurements are shown. (B) Expression levels of the B cell activation marker after o/n stimulation with αIgM, LPS, CpG or αCD40. The dotplots are representative of 3 independent experiments. (C) Assessment of proliferation by the CFSE dilution assay: histograms show CFSE intensities 3 days after stimulation with the indicated mitogens. The table depicts the proliferation index (Proliferation index: average number of divisions of the proliferating cells), the percentage of dividing cells (% Divided: the proportion of cells that initially started to divide) and the division index (Div. Index: average number of divisions of all cells). Numbers represent the means of 3 to 4 (αCD40/IL-4) independent experiments. (D) IL-6 levels were measured in the supernatant after o/n stimulation with αIgM, LPS, CpG or αCD40. (E) Representative dotplots showing proportions of TNFα- or IL-6-producing B cells (B220⁺ TNFα⁺ or B220⁺ IL-6⁺) after 5h stimulation with PMA/ionomycin/BFA. Values represent means and s.d. of 3 mice per genotype.

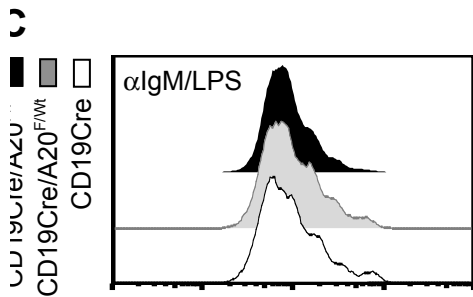
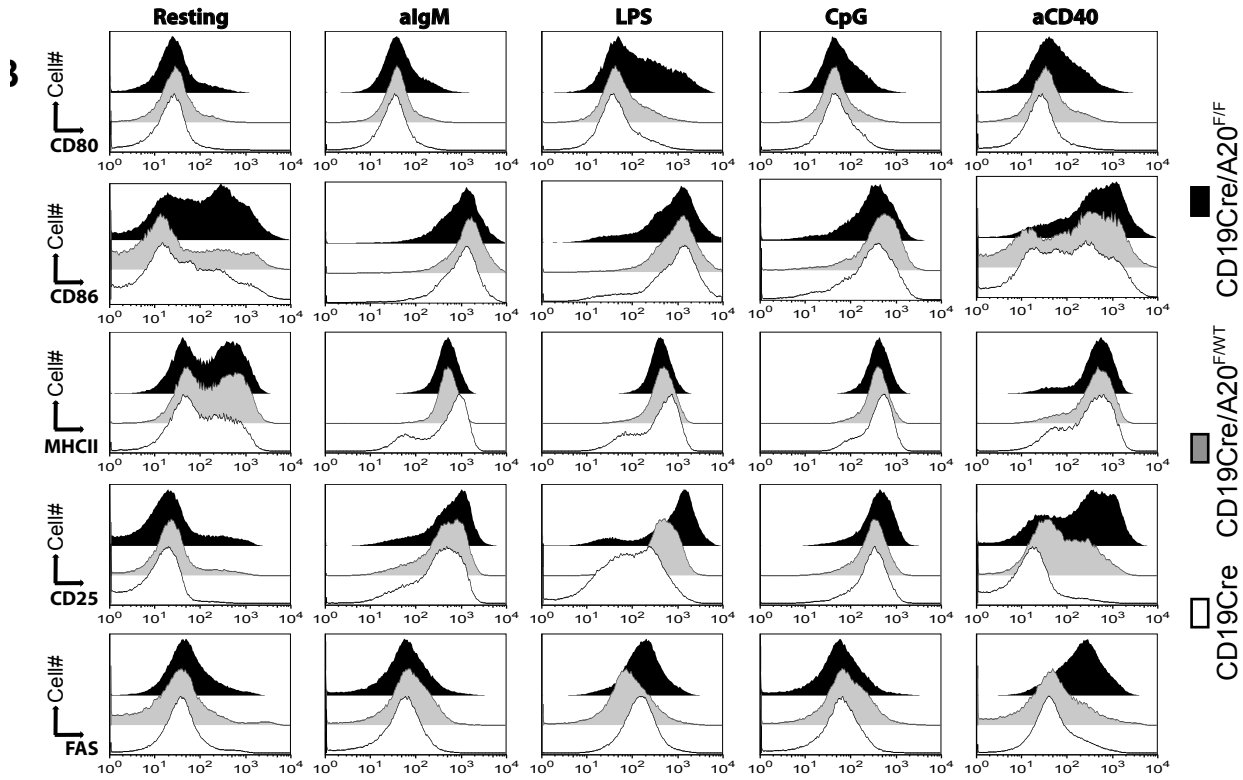
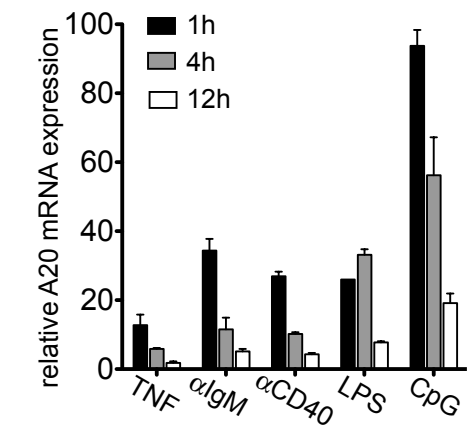
Figure S5. IL-6 producing cell-types in CD19cre/A20^{F/F} mice

(A) Realtime PCR analysis of IL-6 expression in FACS-purified splenic cell subsets of CD19cre/A20^{F/F} and CD19cre control mice. Splenic cell subsets (T cells = B220⁻TCRβ⁺, dendritic cells/DC = B220⁻TCRβ⁻CD11c⁺, macrophages/Mac = B220⁻TCRβ⁻CD11c⁻Gr1^{lo}Mac1^{hi} and granulocytes/Gr = B220⁻TCRβ⁻CD11c⁻Gr1⁺Mac1^{lo}) were MACS purified followed by cell sorting and were over 99% pure. IL6 cDNA was quantified relative to PBGD. Values represent means and s.d. of 3 independent experiments. (B) Proportions of IL-6 expressing cells of individual immune cell subsets in the spleen of CD19cre/A20^{F/F} and CD19cre control mice identified by intracellular FACS. Values represent means and s.d. of 3 independent experiments.

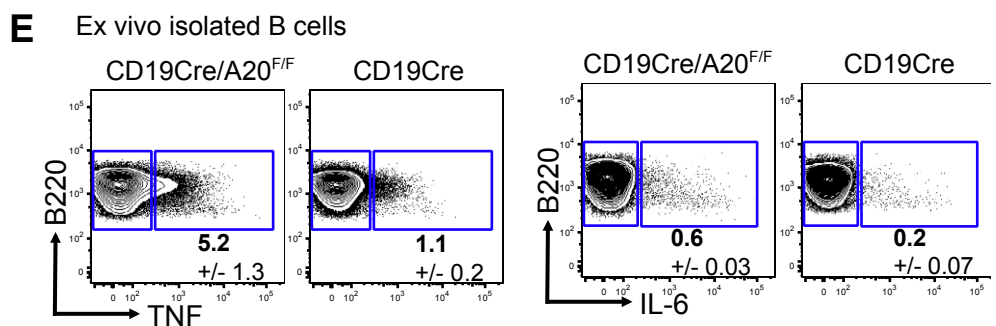
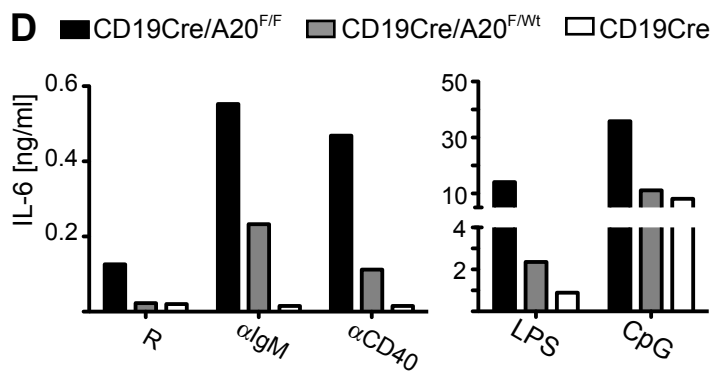
Figure S6. Chronic inflammation and autoreactivity in aged B^{A20-/-} mice
(A) Representative spleen size of old CD19cre/A20^{F/F} and age-matched CD19cre control mice. (B) Spleen weight (n(B^{A20-/-}) = 10, n(control) = 9). (C) Representative dotplot showing proportions of plasma cells (B220^{lo}CD138^{hi}), mean and s.d. for n = 9 mice per genotype are shown. (D) Representative PAS stainings of liver and kidney sections from aged mice. Magnification: 10×. (E) Representative immunofluorescence staining of tissue-specific IgG autoantibodies directed against kidney, harderian gland, stomach and lacrimal gland. Staining was performed by incubating sera from aged mice on sections of tissues isolated from Rag2^{-/-} mice. Magnification: 20×.

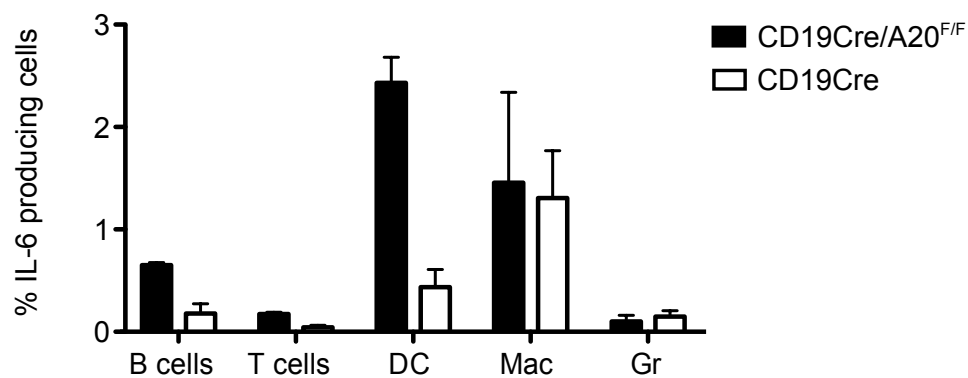
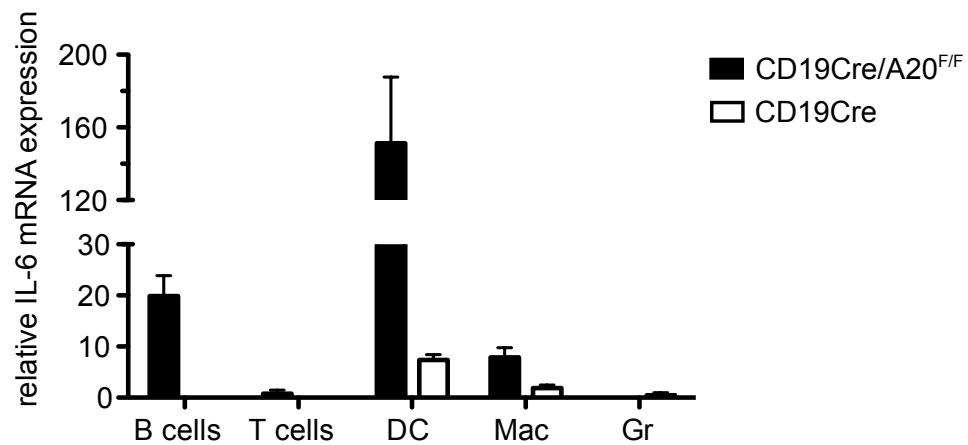


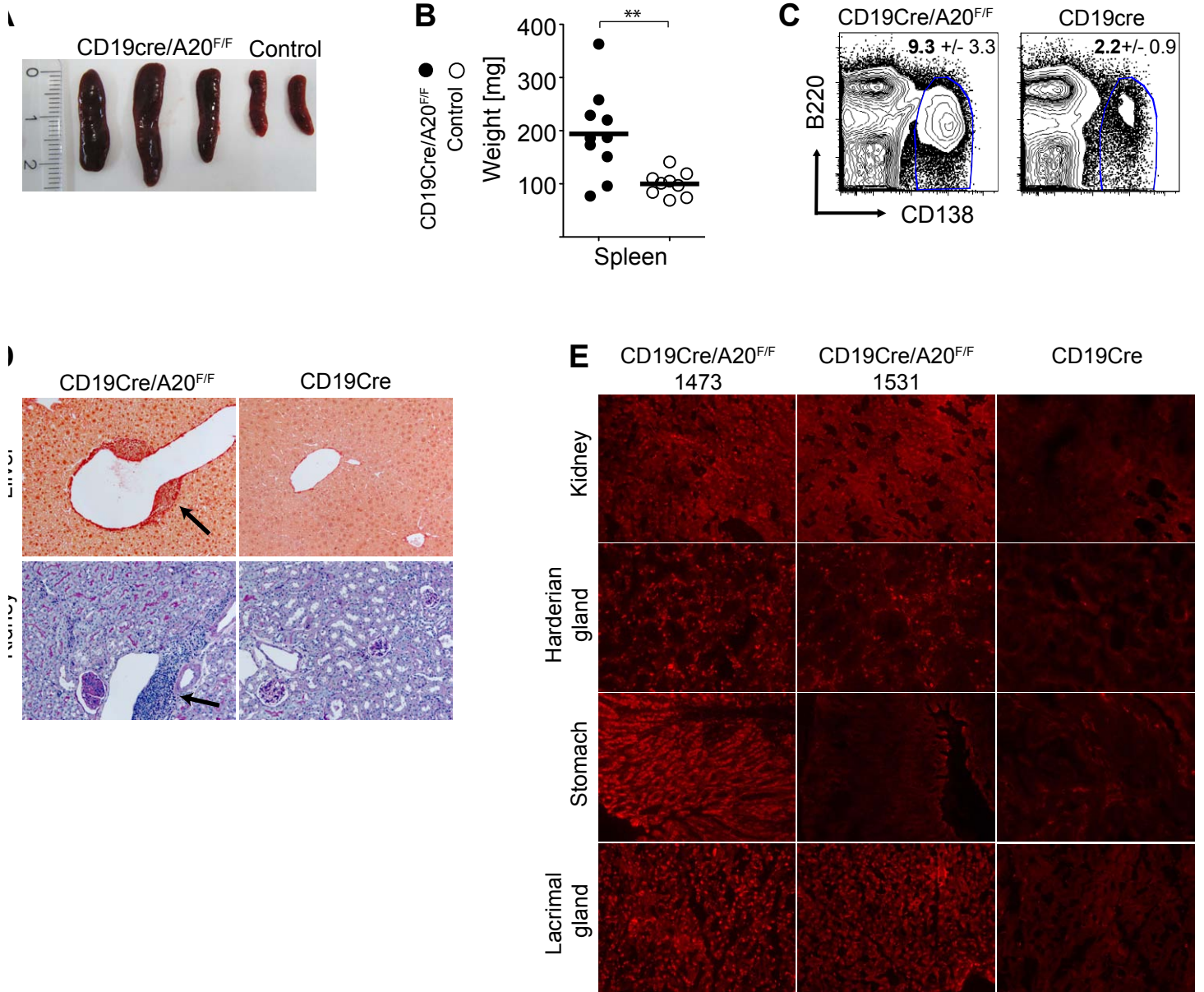




	CD19Cre	A20 ^{F/F}	A20 ^{F/WT}	WT
αIgM/IL-4	Prol. Index	1.9	1.6	1.5
	% Divided	90	94	92
	Div. Index	1.9	1.7	1.7
αCD40/IL-4	Prol. Index	1.4	1.2	1.2
	% Divided	66	24	34
	Div. Index	0.9	0.3	0.4
LPS/IL-4	Prol. Index	2.2	2.1	2.2
	% Divided	86	76	70
	Div. Index	1.9	1.6	1.5
IgM/LPS	Prol. Index	2.2	2.3	2.4
	% Divided	89	95	94
	Div. Index	2.0	2.2	2.2







Paper II

Loss of Roquin induces early death and immune deregulation but not autoimmunity

Arianna Bertossi,¹ Martin Aichinger,² Paola Sansonetti,¹ Maciej Lech,³ Frauke Neff,⁴ Martin Pal,^{5,6} F. Thomas Wunderlich,^{5,6} Hans-Joachim Anders,³ Ludger Klein,² and Marc Schmidt-Supprian¹

¹Max Planck Institute of Biochemistry, 82152 Martinsried, Germany

²Institute for Immunology, Ludwig-Maximilians University, 80336 Munich, Germany

³Nephrological Center, Medical Policlinic, University of Munich, 80336 Munich, Germany

⁴Helmholtz Center Munich, 85764 Neuherberg, Germany

⁵Institute for Genetics, University of Cologne, 50674 Cologne, Germany

⁶Max Planck Institute for Neurological Research, 50931 Cologne, Germany

The substitution of one amino acid in the Roquin protein by the *sanroque* mutation induces a dramatic autoimmune syndrome in mice. This is believed to occur through ectopic expression of inducible T cell co-stimulator (ICOS) and unrestrained differentiation of follicular T helper cells, which induce spontaneous germinal center reactions to self-antigens. In this study, we demonstrate that tissue-specific ablation of Roquin in T or B cells, in the entire hematopoietic system, or in epithelial cells of transplanted thymi did not cause autoimmunity. Loss of Roquin induced elevated expression of ICOS through T cell-intrinsic and -extrinsic mechanisms, which itself was not sufficient to break self-tolerance. Instead, ablation of Roquin in the hematopoietic system caused defined changes in immune homeostasis, including the expansion of macrophages, eosinophils, and T cell subsets, most dramatically CD8 effector-like T cells, through cell-autonomous and nonautonomous mechanisms. Germline Roquin deficiency led to perinatal lethality, which was partially rescued on the genetic background of an outbred strain. However, not even complete absence of Roquin resulted in overt self-reactivity, suggesting that the *sanroque* mutation induces autoimmunity through an as yet unknown mechanism.

Autoimmunity occurs when immune effector mechanisms, normally used to protect organisms against invading pathogens, are unleashed onto self-constituents. Most autoimmune diseases are complex, multifactorial processes, reflecting the number and the nature of checkpoints that have to be overcome (Goodnow, 2007).

Only a small number of critical proteins appear to play such central roles in the maintenance of immunological self-tolerance that alterations in their function strongly predispose to a rapid development of autoimmune syndromes. Vinuesa et al. (2005) identified the M199R amino acid substitution in the putative E3 ubiquitin ligase Roquin/Rc3h1 as the cause of the spontaneous lupus-like autoimmune disease characterizing the *sanroque* mouse strain. *san/san* mice display splenomegaly, lymphadenopathy, plasmacytosis, spontaneous germinal center formation, and glomerulonephritis with immune complex deposition. High affinity anti-DNA autoantibodies can be detected as early as 6 wk

after birth (Vinuesa et al., 2005). The dominant disease-preventing mechanism of Roquin is thought to be the inhibition of inappropriate inducible T cell co-stimulator (ICOS) expression on T cells (Linterman et al., 2009a; Yu and Vinuesa, 2010) through direct ICOS messenger RNA (mRNA) binding and targeting to P-bodies and components of the decapping machinery (Athanasopoulos et al., 2010; Glasmacher et al., 2010). The M199R *sanroque* mutation is located in a novel protein domain termed ROQ, which so far has been identified only in Roquin and its paralogue Mnab. The ROQ domain is critical for ICOS mRNA binding and repression. Because the M199R mutation does not affect binding to ICOS mRNA, it has been postulated that it interferes with Roquin's

CORRESPONDENCE

Marc Schmidt-Supprian:
supprian@biochem.mpg.de

Abbreviations used: ANOVA, analysis of variance; ES, embryonic stem; ICOS, inducible T cell co-stimulator; MFI, mean fluorescence intensity; mRNA, messenger RNA; PAS, periodic acid Schiff.

© 2011 Bertossi et al. This article is distributed under the terms of an Attribution-Noncommercial-Share Alike-No Mirror Sites license for the first six months after the publication date (see <http://www.rupress.org/terms>). After six months it is available under a Creative Commons License (Attribution-Noncommercial-Share Alike 3.0 Unported license, as described at <http://creativecommons.org/licenses/by-nc-sa/3.0/>).

ability to interact with as yet unknown critical effector proteins (Athanasopoulos et al., 2010).

ICOS is an essential co-stimulatory receptor for follicular T helper cell differentiation (King et al., 2008), and heterozygous ablation of ICOS (Yu et al., 2007) or depletion of follicular T helper cells each significantly reduces the autoimmune manifestations in *san/san* mice. Adoptive transfer of *san/san* follicular T helper cells induces spontaneous germinal center formation in recipient mice (Linterman et al., 2009b). Collectively, these data led to the current concept that the *sanroque* mutation induces accumulation and dysregulation of follicular helper T cells through T cell–intrinsic mechanisms, which in turn drive aberrant positive selection of autoreactive B cells in the germinal center with ensuing autoimmunity (Yu and Vinuesa, 2010). To study the tissue-specific function of Roquin in mouse physiology and autoimmune reactions, we generated a conditional Roquin knockout (*Rc3h1^f*) allele.

RESULTS AND DISCUSSION

Complete Roquin knockout causes perinatal lethality

To allow tissue-specific ablation of Roquin, we flanked exons 4–6 of the *Rc3h1* gene with loxP sites (Fig. S1 A). The genetic background of the gene-targeted embryonic stem (ES) cells and all Cre transgenic mice used for tissue-specific gene ablation of Roquin was C57BL/6. Western blotting using *Rc3h1^{EF/EF}* embryonic fibroblasts, in which exons 4–6 had been excised by cre protein transduction, demonstrated the generation of a true Roquin-null mutation (Fig. 1 A). A conventional Roquin knockout strain was produced through crosses with a germline cre-deleter strain. Roquin^{-/-} pups were born at Mendelian ratios (Fig. 1 B) but died within 6 h after birth. Roquin^{-/-} mice displayed a curly tail (Fig. 1 C) and malformations of the caudal spinal column (Fig. 1 D), which is often seen in mutant mice with delayed or abnormal neural tube closure (Harris and Juriloff, 2007). The death of the animals might be related to impaired lung function because the alveoli were not properly expanded in the lungs of Roquin-deficient pups (Fig. 1 E). Besides this, we could not detect obvious structural problems or indications of an acute respiratory distress syndrome in the lungs of Roquin^{-/-} mice.

Ablation of Roquin in the T lineage leads to elevated ICOS levels and expansion of effector CD8 T cells but not autoimmunity

The lupus-like symptoms in *san/san* mice have been ascribed to a T cell–intrinsic function of Roquin (Linterman et al., 2009a,b). To address whether ablation of Roquin specifically in T cells would recapitulate the effects of the *sanroque* mutation, we generated *CD4cre/Rc3h1^{EF/EF}* (*T^{ΔRc3h1}*) mice. As expected, Roquin deficiency led to a robust up-regulation of ICOS on all T cell subsets in thymus and secondary lymphoid organs (Fig. 2 A and Fig. S1 B). Loss of Roquin (Fig. S1 C) did not affect T cell development or subset composition in the thymus (Fig. S1 D). In peripheral lymphoid

organs, there was a significant increase in CD8 but not CD4 T cells that displayed an effector-like phenotype (CD44^{hi}CD62L^{lo}; Fig. 2, B and D; and Fig. S2 A). Further analysis of the CD44^{hi}CD62L^{lo} CD8 T cells revealed that most of them were CD127^{int}CD122^{hi}KLRG1^{hi}Tbet^{hi} (Fig. 2 C and Fig. S2 C) and therefore resembled short-lived effector cells. *T^{ΔRc3h1}* mice had normal-sized spleens with regular follicular organization (Fig. S2, B and D), although the numbers of eosinophils and monocytic/macrophage populations were doubled compared with control mice (Fig. 2 D). Most importantly, unlike what is seen in *san/san* mice (Vinuesa et al., 2005), we neither detected increased follicular T helper cell differentiation (Fig. S2 E) nor spontaneous germinal center formation (Fig. 2 E and Fig. S2 E). *T^{ΔRc3h1}* mice did not display any obvious autoimmune manifestations, including the production of autoantibodies (Fig. S2 F). We therefore conclude that the absence of Roquin specifically in T cells leads to the up-regulation of ICOS expression and expansion of CD8 effector phenotype T cells but not to aberrant follicular T helper cell differentiation or break of tolerance to self.

Roquin deficiency in hematopoietic cells causes immune deregulation

Because T cell–specific ablation of Roquin was not sufficient to recapitulate the dramatic breakdown of self-tolerance seen

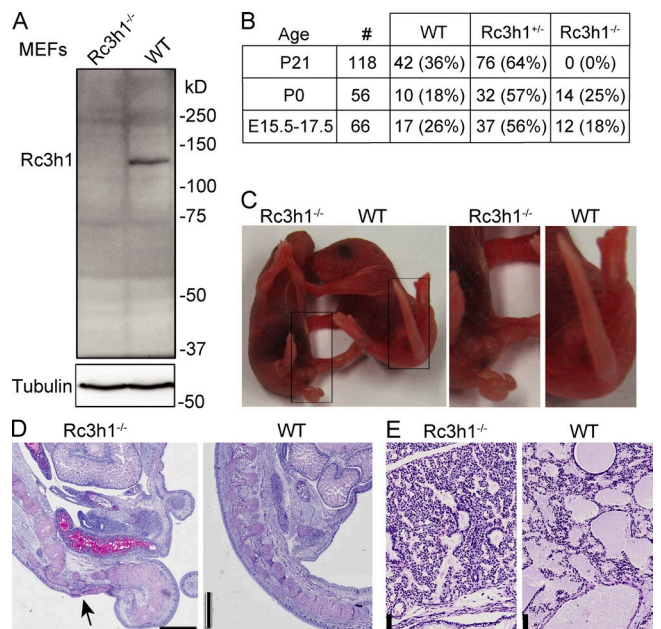


Figure 1. Loss of Roquin causes perinatal lethality. (A) Western blot of Roquin protein expression in wild-type and *Rc3h1^{-/-}* immortalized murine embryonic fibroblasts. (B) Genotype frequency of offspring from intercrosses of *Rc3h1^{+/-}* mice. (C) Newborn (P0) *Rc3h1^{-/-}* pups show a curly tail. (D) PAS stainings of sagittal sections of the sacral spinal column of *Rc3h1^{-/-}* and control newborn mice; the arrow indicates the skin, soft tissue, and bone defect. (E) PAS stainings of sagittal sections of lungs of *Rc3h1^{-/-}* and control newborn mice. Bars: (D) 1 mm; (E) 50 μm.

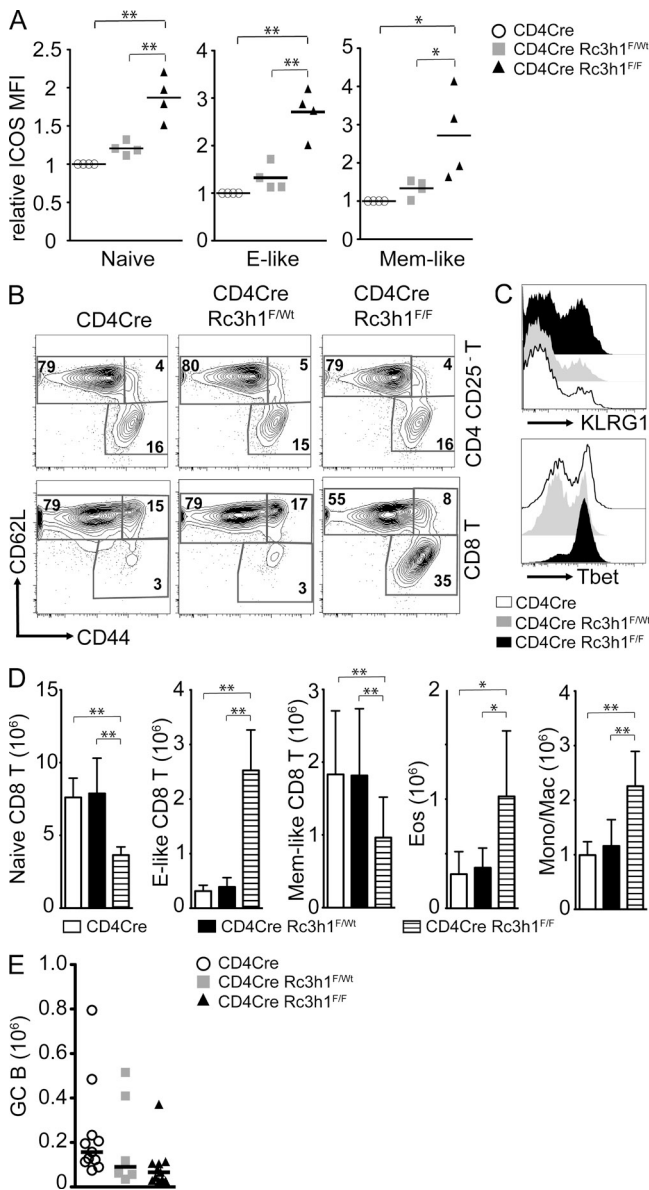


Figure 2. Roquin deficiency in T lymphocytes leads to CD8 effector-like T cell expansion. (A) Relative MFI of ICOS expression on CD4 T cell subsets in the spleens of mice of the indicated genotypes. Naive, CD25[−]CD44^{lo}CD62L^{hi}; effector (E)-like, CD25[−]CD44^{hi}CD62L^{lo}; memory (Mem)-like, CD25[−]CD44^{hi}CD62L^{hi}. Bars indicate medians of four mice per group, and ICOS levels on CD4Cre control T cell subsets are set to 1. (B) Representative contour plots of T cell (TCR-β⁺) subsets gated as indicated on the right. Numbers represent percentages of the gated populations of the indicated T cell subtype. (C) Histogram of KLRG1 and Tbet expression on CD44^{hi}CD62L^{lo}-gated effector-like CD8 T cells, representative of five experiments. (D) Bar charts of absolute numbers of indicated T cell (TCR-β⁺; subsets as in A) and myeloid cell subsets: Eos, eosinophils (Gr1^{int}SiglecF⁺); Mono/Mac, monocytes/macrophages (SiglecF-Gr1^{int}Mac1⁺). Columns and error bars indicate means ± SD calculated from six to nine mice per genotype. (E) Absolute numbers of splenic germinal center (GC; B220⁺PNA^{hi}Fas^{hi}CD38^{lo}) B cells of 11–6 mice per genotype. Bars indicate the median. *, P < 0.05; **, P < 0.001; one-way ANOVA.

in *san/san* mice, we hypothesized that loss of Roquin in other hematopoietic cells might synergize with its absence in T cells to induce autoimmunity. We therefore generated *VavCre/Roquin^{F/F}* (*Hem^{ΔRc3h1}*) mice to test the consequences of Roquin deficiency in the entire hematopoietic system (Fig. 3 A). *Hem^{ΔRc3h1}* mice displayed normal T cell development in the thymus (Fig. S3 A), whereas BM B cell development was affected through a reduction in immature and recirculating B cells (Fig. S3 B). Spleen size and cellular content were increased ~1.5-fold as the result of expansion of effector-like T cells, Foxp3⁺ regulatory T cells (T_{reg} cells), eosinophils, and monocytic/macrophage populations (Fig. 3, B–D; and Fig. S3, C and D). However, the increased splenic cellularity in *Hem^{ΔRc3h1}* mice did not reach the extent of splenomegaly observed in *san/san* mice, which occurs independently of the autoimmune syndrome (Linterman et al., 2009b). Analysis of splenic immune compartmentalization by immunofluorescence revealed both intact and somewhat disrupted (Fig. 3 E) follicles in *Hem^{ΔRc3h1}* mice. Moreover, we detected an increase in spontaneous germinal center formation in the spleens of *Hem^{ΔRc3h1}* mice (Fig. 3 G). Analysis of Ig serum levels by ELISA revealed a reduction in IgG1, IgG3, and IgA and an increase in IgG2b levels (Fig. S4 A). However, we did not detect elevated levels of autoantibodies in the serum of *Hem^{ΔRc3h1}* mice by ELISA for typical autoantigens (Fig. 3 H and Fig. S4 B) or by staining of kidney, harderian gland, and stomach sections of *Rag2^{-/-}* mice (not depicted). Importantly, there was no autoimmune tissue damage in kidney, liver, and lung of *Hem^{ΔRc3h1}* mice (not depicted).

Of note, the extent of ICOS up-regulation on CD4 and, to a lesser extent, CD8 T cells in *Hem^{ΔRc3h1}* mice exceeded the increase of ICOS levels in *T^{ΔRc3h1}* mice (compare Fig. 3 F and Fig. S4 C with Fig. 2 A and Fig. S1 B). This suggests that the loss of Roquin in immune cells other than T cells contributes to the elevated ICOS expression in *Hem^{ΔRc3h1}* mice. Along the same lines, no corresponding increase of regulatory or effector-like CD4 T cells had been observed upon T cell-specific ablation of Roquin, indicating that these alterations reflect a requirement for Roquin outside the T lineage.

Roquin-deficient B cells contribute to the general deregulation of immune homeostasis

To elucidate to which extent loss of Roquin function specifically in B cells contributes to the immune activation observed in *Hem^{ΔRc3h1}* mice, we generated *CD19cre/Rc3h1^{F/F}* (*B^{ΔRc3h1}*) mice. Ablation of Roquin specifically in B lymphocytes (Fig. S4 D) was sufficient to cause enlarged spleens (Fig. S4 E) resulting from the expansion of B cells, T_{reg} cells, CD4 and CD8 effector-like T cells, and eosinophils (Fig. 4 A and Fig. S4, F–I). There was a trend toward elevated spontaneous germinal center formation in the spleens of *B^{ΔRc3h1}* mice, but the observed differences were not statistically significant (Fig. 4 B). Therefore, our findings show that lack of Roquin in B cells contributed significantly to the disturbance of immune homeostasis in *Hem^{ΔRc3h1}* mice.

Roquin deficiency in thymic epithelial cells causes thymic atrophy but does not affect T cell selection

Loss of Roquin in hematopoietic cells does not cause a dramatic *sarcoque*-like autoimmune syndrome. We therefore hypothesized that Roquin-deficient nonhematopoietic cells might be crucial for the induction of autoimmunity. The thymic epithelium plays a critical role for immune tolerance, and perturbations of its development and/or function can lead to spontaneous autoimmunity (Kyewski and Klein, 2006). To assess the function of Roquin specifically in thymic epithelial cells during thymocyte development and selection, we transplanted immune cell-depleted Roquin-deficient and control embryonic thymi under the kidney capsule of athymic C57BL/6 nude mice. As a consequence, these chimeras contained a

Roquin-sufficient hematopoietic system, and T cells were selected on either Roquin-deficient ($Rc3h1^{-/-}$ → nude) or -sufficient ($Rc3h1^{+/+}$ → nude) thymic epithelium. Recipients of Roquin-deficient thymic epithelium gained weight normally after transplantation (Fig. 5 A) and did not show signs of disease by histological criteria (not depicted). Embryonic day (E) 16.5 $Rc3h1^{-/-}$ thymic lobes at the time of grafting appeared somewhat smaller than $Rc3h1^{+/+}$ controls, and the cellularity of $Rc3h1^{-/-}$ thymi 10 wk after transplantation was significantly reduced compared with controls (Fig. 5 B). Despite this thymic atrophy, which points to a thymic epithelium-intrinsic function of Roquin in epithelial homeostasis, thymocyte development was not affected (Fig. 5 C). T cell selection was also unaffected, as judged from the normal numbers of

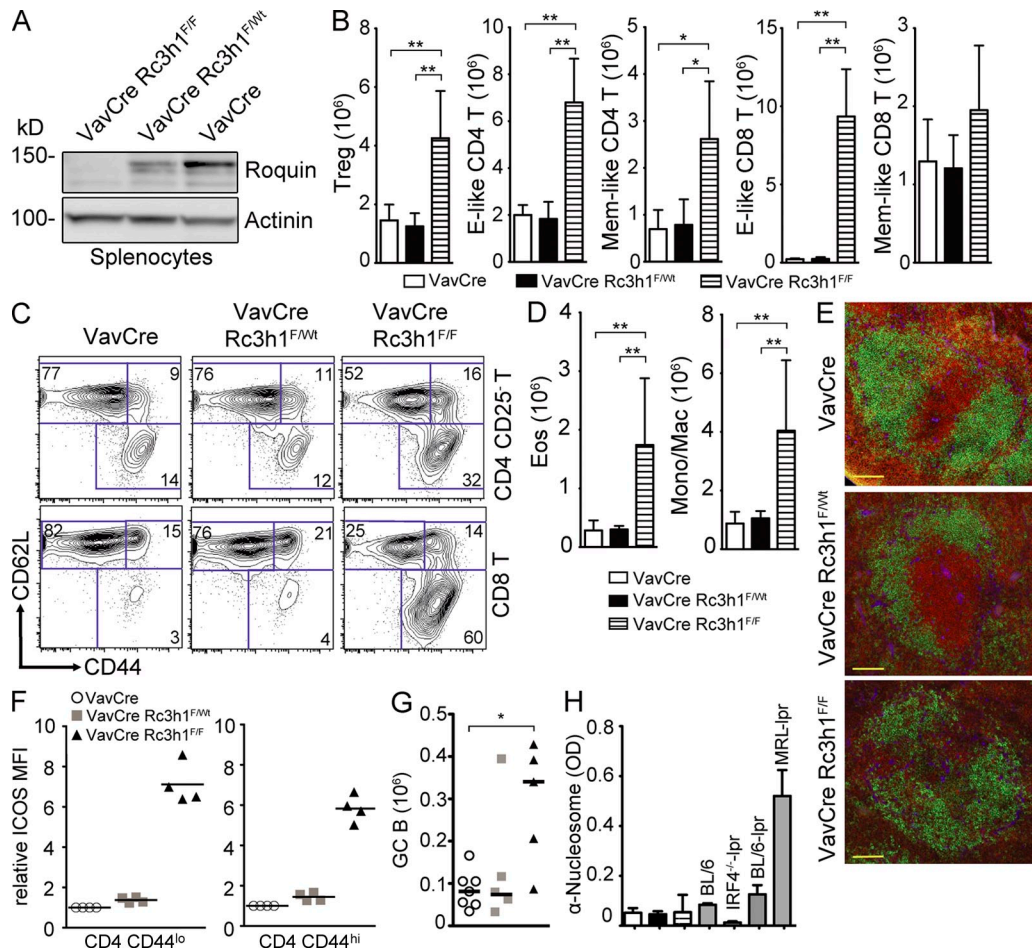


Figure 3. Deregulation of immune homeostasis in the absence of Roquin in the hematopoietic system. (A) Western blot analysis to evaluate Roquin protein expression in splenocytes. (B and C) Absolute cell numbers (B) and representative contour plots (C) of splenic T cell (TCR- β^+) subsets: effector (E)-like, CD44^{hi}CD62L^{lo}; and memory (Mem)-like, CD44^{hi}CD62L^{hi} ($n = 7-9$); T_{reg} cells, CD4⁺FoxP3⁺ ($n = 3-5$). Columns and error bars represent means \pm SD calculated from the number of mice indicated. (D) Columns and error bars represent means \pm SD of absolute cell numbers of eosinophils (Eos; Gr1^{int}SiglecF⁺) and monocytic/macrophages (Mono/Mac; SiglecF⁻Gr1^{int}Mac1⁺) calculated from four to six mice per group. (E) Immunofluorescence of spleen sections: green, α -B220; red, α -CD3; blue, α -laminin. Bars, 100 μ m. (F) Relative ICOS MFI of naive (CD44^{lo}) and memory/effector-like (CD44^{hi}) splenic CD4 T cells. Bars indicate medians. (G) Absolute cell numbers of germinal center (GC; B220⁺PNA^{hi}Fas^{hi}CD38^{lo}) B cells. Bars represent medians calculated from five to seven mice per genotype. (H) Titers of serum autoantibodies against nucleosomes measured by ELISA (2–7 mo old) from 8–10 mice of the indicated genotypes. Sera from BL/6, IRF4^{-/-}-lpr, BL/6-lpr, and MRL-lpr mice were used as positive or negative controls. Columns and error bars represent means \pm SD. *, $P < 0.05$; **, $P < 0.001$; one-way ANOVA.

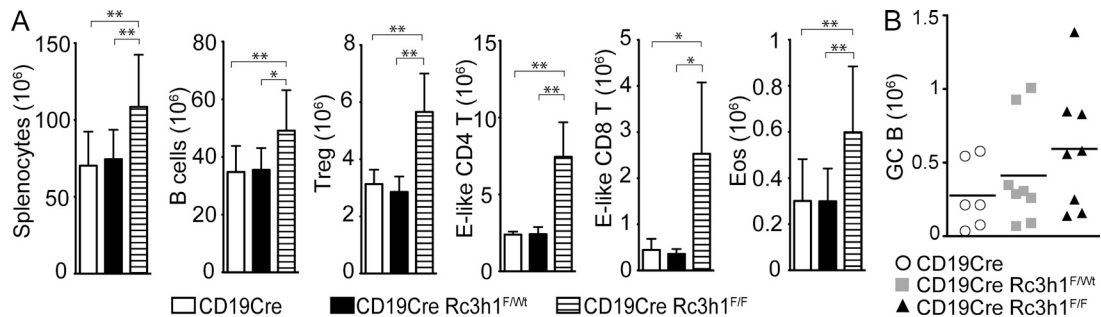


Figure 4. Roquin-deficient B cells cause effector-like T cell expansion. (A) Column and error bars represent means \pm SD of absolute cell numbers of splenocytes ($n = 8$), B cells (B220⁺; $n = 8$), T_{reg} cells (CD4⁺FoxP3⁺; $n = 4$), CD4 effector (E)-like T cells (CD25⁺CD44^{hi}CD62L^{lo}; $n = 4$), CD8 effector-like T cells (CD44^{hi}CD62L^{lo}; $n = 4$), and eosinophils (Eos; Gr1^{int}SiglecF⁺; $n = 8$). (B) Absolute cell numbers of germinal center (GC; B220⁺Fas^{hi}PNA^{hi}CD38^{lo}) B cells. Bars indicate medians calculated from six to eight mice per group. *, $P < 0.05$; **, $P < 0.001$; one-way ANOVA.

peripheral T cell subsets (Fig. S5 A) and normal proportions of TCRs bearing certain α and β chains (Fig. 5 D and Fig. S5 B). These data show that although absence of Roquin in the thymic epithelium reduced thymus size under these experimental conditions, it did not affect T cell selection or allow the escape of self-reactive T cells.

CD1 outbred Roquin^{-/-} mice survive at sub-Mendelian ratios and display growth retardation and relatively mild immune defects

To overcome the perinatal lethality that prevents the analysis of adult C57BL/6 Roquin-deficient mice, we crossed C57BL/6 Roquin^{+/-} mice onto a CD1 outbred background. 4% of CD1 Roquin^{-/-} mice survived to adulthood (Fig. 6 A) in heterozygous crosses, displaying growth retardation (Fig. 6 B) and the typical curly tail at birth, which was sometimes corrected later on (Fig. S6 A). In general, the immune phenotypes were somewhat milder in CD1 Roquin^{-/-} than in C57BL/6 Hem^{ΔRc3h1} mice, most likely because of the CD1 outbred background. CD1 Roquin^{-/-} mice displayed enlarged spleens (Fig. S6 B) with a trend toward increased

numbers of eosinophils and monocytic/macrophage populations (Fig. 6 C and Fig. S6 C). However, the most prominent effect was a dramatic and selective expansion of Roquin-deficient CD8 effector-like T cells (Fig. 6 C), showing that suppressing the generation of these cells is a dominant function of Roquin in naive mice. Splenic follicular organization was normal (Fig. 6 D), and the numbers of CD4 T cell subtypes and B cells (Fig. S6 D) were not significantly altered in CD1 Roquin^{-/-} mice. In addition, we did not detect spontaneous germinal center formation (Fig. 6 E), autoantibody production (Fig. 6 F and Fig. S6 E), or autoimmune tissue damage in CD1 Roquin^{-/-} mice (not depicted).

We show in this study that, unlike the *sanroque* mutation, systemic ablation of Roquin causes perinatal lethality, revealing a hitherto unappreciated critical role of Rc3h1 outside the immune system. In immune cells, loss of Roquin induces several defined perturbations. Deficiency in B cells leads to elevated numbers of B, regulatory and effector-like T cells, and eosinophils. Roquin deletion in T cells induces the expansion of eosinophils and macrophages and the dramatic spontaneous differentiation of effector-like CD8 T cells. Our findings

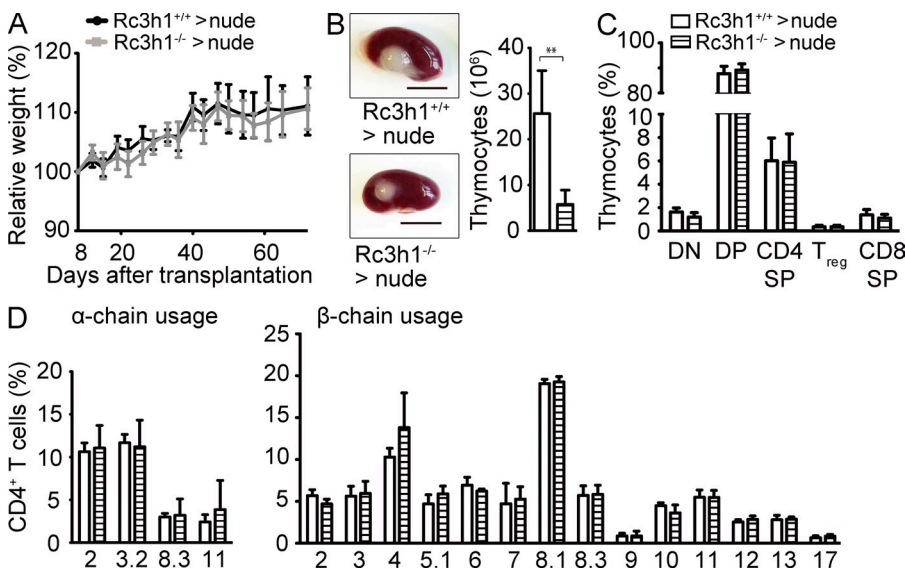


Figure 5. Effect of Roquin loss in thymic epithelial cells. (A) Growth curve of nude mice transplanted with fetal thymic epithelium as indicated. Means \pm SD for recipients of six wild-type and six Rc3h1^{-/-} thymi are shown. (B) Rc3h1^{+/-} and Rc3h1^{-/-} thymic epithelium-derived thymus lobes on kidneys of C57BL/6 nude mice 10 wk after transplantation. Bar chart shows absolute numbers of thymocytes. Bars, 500 μ m. (C) Proportions of thymocyte subsets. DN, (CD4/CD8) double negative; DP, double positive; SP, single positive; T_{reg} cells, CD4⁺FoxP3⁺. (D) Usage of individual V α (left) and V β (right) chains in the TCR on CD4⁺ T cells in mice of the indicated genotypes. (B–D) Columns and error bars represent means \pm SD of five to six mice per group. **, $P < 0.001$; Student's *t* test.

clearly demonstrate that ablation of Roquin, although it augments ICOS expression levels through T cell–autonomous and nonautonomous mechanisms, is not sufficient to cause autoimmunity. It remains possible that C57BL/6 complete Roquin knockout mice would develop a *sanroque*-like autoimmune syndrome if the perinatal lethality could be overcome

by some means. However, it seems more likely that the *sanroque* mutation causes to date unidentified perturbations, which are not recapitulated by the absence of Roquin. In this scenario, another protein such as the Roquin paralogue Mnab might compensate for the absence of Roquin, which it cannot do in the presence of Roquin_{M199R}. Therefore, the presence of Roquin_{M199R} in protein complexes might be more disruptive than the absence of the protein. This hypothesis is supported by the fact that heterozygous C57BL/6 *san*/WT (Vinuesa et al., 2005), but not C57BL/6 Roquin^{+/-} (Fig. S6 F) animals develop antinuclear autoantibodies. Be this as it may, our findings show that to bring about a spontaneous failure of immune tolerance, a complex and as yet ill-defined interplay of Roquin absence or malfunction in various cell types may be required.

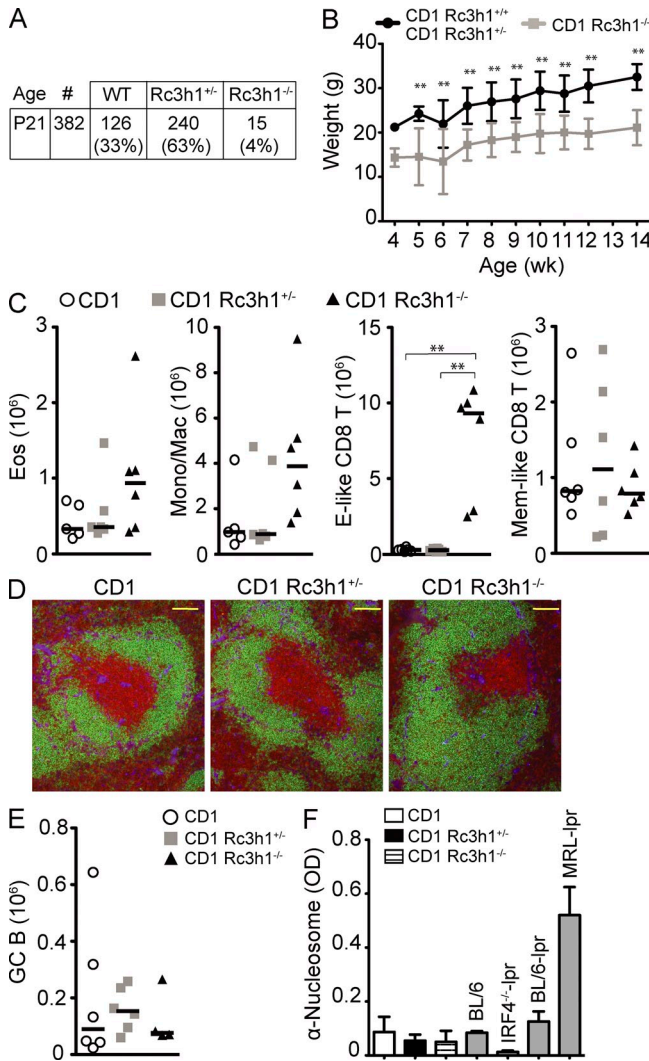


Figure 6. Roquin knockout mice can survive on a CD1 outbred genetic background. (A) Genotype frequency of offspring of heterozygous matings of CD1 Rc3h1^{+/-} mice. (B) Body weight curve of Rc3h1^{-/-} mice compared with control littermates (2–21 mice per group and time point). Error bars indicate SD. (C and E) Absolute cell numbers of eosinophils (Eos; Gr1^{int}Siglec-F⁺), monocytic/macrophages (Mono/Mac; Siglec-F⁻Gr1^{int}Mac1⁺), splenic CD8⁺ T cell subsets [Effector [E]-like, CD44^{hi}CD62L^{lo}; memory (Mem)-like, CD44^{hi}CD62L^{hi}]; (C) and germinal center (GC; B220⁺PNA^{hi}Fas^{hi}CD38^{lo}) B cells (E) calculated from six mice of the indicated genotypes. Bars represent medians. (D) Immunofluorescence of spleen sections: green, α-B220; red, α-CD3; blue, α-laminin. Bars, 100 μm. (F) Titers of autoantibodies against nucleosomes detected by ELISA in the serum of eight to nine 2.5–3.5-mo-old mice of the indicated genotypes. Columns and error bars indicate means ± SD. ** P < 0.001; one-way ANOVA.

MATERIALS AND METHODS

Genetically modified mice. To generate a conditional *rc3h1* allele, we cloned a targeting vector to flank exons 4–6 with loxP sites. An Frt site-flanked neo^R cassette was placed in the third intron of the *Rc3h1* gene. A 4.0-kb fragment was used as the 5' homology region, a 2-kb fragment was placed between the two loxP sites, and a 4.0-kb fragment was used as the 3' homology region. C57BL/6 ES cells were transfected, cultured, and selected essentially as previously described for Bruce 4 ES cells (Schmidt-Supprian et al., 2000). After blastocyst injection of correctly targeted clones and transmission of the conditional allele through the germline of resulting chimeras, the Frt-flanked neo^R cassette was removed by using an Flpe-deleter strain. *Rc3h1^f*, Nestin-cre (used as deleter mice; Betz et al., 1996), Flpe-deleter (Rodríguez et al., 2000), CD4cre (Lee et al., 2001), VavCre (de Boer et al., 2003), and CD19cre (Rickert et al., 1997) were kept on a C57BL/6 genetic background. All mice analyzed were 2–4 mo old, unless otherwise indicated. CD1 outbred mice were kept at the Max Planck Institute of Biochemistry (MpiCrIcr:CD-1). Mice were housed in the specific pathogen-free animal facility of the Max Planck Institute of Biochemistry. All animal procedures were approved by the Regierung of Oberbayern.

Flow cytometry. Single-cell suspensions were prepared and stained with monoclonal antibodies: PD-1 (J43), ICOS (7E.17G9), B220 (RA3-6B2), CD19 (eBio1D3), CD25 (PC61.5), CD38 (90), CD4 (RM4-5), CD44 (IM7), CD5 (53-7.3), CD62L (MEL-14), CD8 (53-6.7), FoxP3 (FJK-16s), GR-1 (RB6-8C5), IgD (11-26), IgM (II/41), Mac-1 (M1/70), TCR-β (H57-597), CD95 (15A7), CD21 (7G6), c-kit (2B8), KLRG1 (2F1), CD127 (A7R34), CD122 (TM-b1), Tbet (eBio4B10), F4/80 (A3-1), CD115 (AFS98), CD45RB (C363.16A; all eBioscience), Siglec-F (E50-2440), CD138 (281-2), CXCR5 (2G8), CD11c (HL3), Vα11.1/11.2 (RR8-1), Vα2 (B20.1), Vα3.2 (RR.3-16), Vα8.3 (B21.14), TCR Vβ screening panel (all BD), and PNA (Vector Laboratories). Samples were acquired on FACSCalibur and FACS-CantoII (BD) machines and analyzed with FlowJo software (Tree Star). To evaluate the relative ICOS expression on T cell subsets of the different cell type-specific Roquin knockout mice, four sets of three genotypes (cre control, heterozygous knockout, and homozygous knockout) were analyzed. The ICOS mean fluorescence intensity (MFI) for the cre transgenic control cells was set to 1 for each set.

Cell culture. We generated primary and SV40 large T-immortalized *Rc3h1^{f/f}* and control embryonic fibroblasts and treated them by cre protein transduction with Histag-tat-NLS-cre (Peitz et al., 2007).

Western blot. To prepare whole-cell lysates, cells were lysed for 15 min on ice by RIPA buffer, 10 μg/ml aprotinin, 10 μg/ml leupeptin, 0.1 mM Na3VO4, 1 mM PMSF, 10 mM NaF, 1 mM DTT, and 8 mM β-glycerophosphate. Polyvinylidene fluoride membranes were blotted with the following antibodies: anti-Rc3h1 (Bethyl Laboratories, Inc.), antitubulin (clone YL1/2;

Millipore), antiactinin (clone AT6/172; Millipore), and anti-GAPDH (clone 6C5; EMD).

Immunofluorescence and immunohistochemistry. For immunofluorescence stainings, frozen 10- μ m sections were thawed, air dried, methanol fixed, and stained for 1 h at room temperature in a humidified chamber with FITC-conjugated B220 (eBioscience), biotinylated rat anti-CD3 (BD), and rabbit antilaminin (gift from M. Sixt, Institute of Science and Technology Austria, Klosterneuburg, Austria) followed by Alexa Fluor 488-conjugated anti-fluorescein (Invitrogen), Cy3-conjugated streptavidin (Jackson ImmunoResearch Laboratories, Inc.), and Cy5-conjugated anti-rabbit antibodies (Jackson ImmunoResearch Laboratories, Inc.). Images were acquired using an Axio Imager.Z1 fluorescent microscope (Carl Zeiss) with AxioCam MRc5 (Carl Zeiss) and analyzed with AxioVision Rel. 4.8 software (Carl Zeiss).

Histology. Whole embryos or newborn pups were fixed for 24 h in 4% paraformaldehyde and decalcified for 4 h in Osteosoft (Merck), and heads and whole embryos were cut sagittally at the midline. Dehydration and paraffin embedding were performed using a vacuum embedding system (VIP; Sakura). Paraffin slides were performed with 4- μ m thickness and stained with hematoxylin and eosin and periodic acid Schiff (PAS). Images were taken using a virtual slide microscopy system (dotslide 2.0; Olympus).

ELISA. Antinuclear autoantibodies to eight different autoantigens were detected using the Varelisa ANA 8 screen (Phadia). Serum from a 1-yr-old BXD2 mouse was used as positive control. The following ELISAs were performed as described previously (Lech et al., 2008). For antinucleosome antibodies, MaxiSorp ELISA plates (Thermo Fisher Scientific) were precoated with poly-L-lysine (Trevigen) and PBS (ratio 1:1) for 1 h. ELISA plates were washed with 50 mM Tris and 0.14 M NaCl buffer and incubated with mouse double-stranded DNA-histones (both 2 μ g/ml) in SSC buffer overnight at 4°C. For anti-Smith antibodies, MaxiSorp ELISA plates were coated with Smith antigen (Immunovision) in 0.05 M carbonate-bicarbonate buffer overnight at 4°C. For rheumatoid factor, ELISA plates were coated with 10 μ g/ml rabbit IgG (Jackson ImmunoResearch Laboratories, Inc.) in 0.05 M carbonate-bicarbonate buffer overnight at 4°C. Serum samples were diluted 1:10 for all IgG ELISAs. 24-wk C57BL/6 wild-type and antibody-poor (IRF-4^{-/-}BL/6lpr) serum was used as negative controls. C57BL/6-lpr and MRL-lpr 24-wk mouse serum was used as positive control. Specific IgGs were detected by horseradish peroxidase-conjugated goat anti-mouse IgG (Bethyl Laboratories, Inc.).

Transplantation of thymic epithelial cells. Embryonic thymic lobes (E16.5) were placed onto Isopore membrane filters (Millipore), floating on 3 ml dGuo medium (IMDM) supplemented with 1.35 mM deoxyguanosine (Sigma-Aldrich) and 10% vol/vol FCS (Invitrogen) and cultured for 5 d. After dGuo treatment, the lobes were washed in PBS and transplanted underneath the kidney capsules of athymic C57BL/6 nude mice (Taconic).

Statistics. Statistical analysis of the results was performed by one-way analysis of variance (ANOVA) followed by Tukey's test or by Student's *t* test. P-values are presented in figure legends where a statistically significant difference was found.

Online supplemental material. Fig. S1 shows the targeting strategy for the *Rc3h1^{FL}* allele and ablation of Roquin in T cells. Figs. S2, S3, and S4 show the effects of T cell (Fig. S2)-, hematopoietic system (Figs. S3 and S4)-, and B cell-specific (Fig. S4) ablation of Roquin. Fig. S5 shows T cell development and selection in nude mice transplanted with *Rc3h1^{-/-}* and control fetal thymic epithelial cells. Fig. S6 shows that outbred CD1 Roquin^{-/-} mice display growth retardation and immune deregulation. Supplemental material and methods describe the preparation and staining of cytopins and ELISA. Online supplemental material is available at <http://www.jem.org/cgi/content/full/jem.20110578/DC1>.

We thank Christoph Vahl for cell sorting and Vigo Heissmeyer for advice. We are grateful to Reinhard Fässler for support. We wish to thank Julia Knogler, Barbara Habermehl, and Elenore Samson for technical assistance. We are indebted to Vigo Heissmeyer, Klaus Heger, Christoph Vahl, and Yuanyuan Chu for critical reading of the manuscript.

This study was supported by Emmy Noether grant SCHM2440 from the Deutsche Forschungsgemeinschaft (DFG) and a grant from the Thyssen Foundation to M. Schmidt-Suppran. H.-J. Anders was supported by DFG grant AN372/10-1, and M. Aichinger and L. Klein were supported by DFG grant KL1228/2-1.

The authors have no conflicting financial interests.

Submitted: 23 March 2011

Accepted: 21 July 2011

REFERENCES

- Athanasopoulos, V., A. Barker, D. Yu, A.H. Tan, M. Srivastava, N. Contreras, J. Wang, K.P. Lam, S.H. Brown, C.C. Goodnow, et al. 2010. The ROQUIN family of proteins localizes to stress granules via the ROQ domain and binds target mRNAs. *FEBS J.* 277:2109–2127. doi:10.1111/j.1742-4658.2010.07628.x
- Betz, U.A., C.A. Voshenrich, K. Rajewsky, and W. Müller. 1996. Bypass of lethality with mosaic mice generated by Cre-loxP-mediated recombination. *Curr. Biol.* 6:1307–1316. doi:10.1016/S0960-9822(02)70717-3
- de Boer, J., A. Williams, G. Skavdis, N. Harker, M. Coles, M. Tolaini, T. Norton, K. Williams, K. Roderick, A.J. Potocnik, and D. Kioussis. 2003. Transgenic mice with hematopoietic and lymphoid specific expression of Cre. *Eur. J. Immunol.* 33:314–325. doi:10.1002/immu.200310005
- Glasmacher, E., K.P. Hoefig, K.U. Vogel, N. Rath, L. Du, C. Wolf, E. Kremmer, X. Wang, and V. Heissmeyer. 2010. Roquin binds inducible costimulator mRNA and effectors of mRNA decay to induce microRNA-independent post-transcriptional repression. *Nat. Immunol.* 11:725–733. doi:10.1038/ni.1902
- Goodnow, C.C. 2007. Multistep pathogenesis of autoimmune disease. *Cell.* 130:25–35. doi:10.1016/j.cell.2007.06.033
- Harris, M.J., and D.M. Juriloff. 2007. Mouse mutants with neural tube closure defects and their role in understanding human neural tube defects. *Birth Defects Res. A Clin. Mol. Teratol.* 79:187–210. doi:10.1002/bdra.20333
- King, C., S.G. Tangye, and C.R. Mackay. 2008. T follicular helper (TFH) cells in normal and dysregulated immune responses. *Annu. Rev. Immunol.* 26:741–766. doi:10.1146/annurev.immunol.26.021607.090344
- Kyewski, B., and L. Klein. 2006. A central role for central tolerance. *Annu. Rev. Immunol.* 24:571–606. doi:10.1146/annurev.immunol.23.021704.115601
- Lech, M., O.P. Kulkarni, S. Pfeiffer, E. Savarese, A. Krug, C. Garlanda, A. Mantovani, and H.J. Anders. 2008. Tir8/SigIRR prevents murine lupus by suppressing the immunostimulatory effects of lupus autoantigens. *J. Exp. Med.* 205:1879–1888. doi:10.1084/jem.20072646
- Lee, P.P., D.R. Fitzpatrick, C. Beard, H.K. Jessup, S. Lehar, K.W. Makar, M. Pérez-Melgosa, M.T. Sweetser, M.S. Schlissel, S. Nguyen, et al. 2001. A critical role for Dnmt1 and DNA methylation in T cell development, function, and survival. *Immunity.* 15:763–774. doi:10.1016/S1074-7613(01)00227-8
- Linterman, M.A., R.J. Rigby, R. Wong, D. Silva, D. Withers, G. Anderson, N.K. Verma, R. Brink, A. Hutloff, C.C. Goodnow, and C.G. Vinuesa. 2009a. Roquin differentiates the specialized functions of duplicated T cell costimulatory receptor genes CD28 and ICOS. *Immunity.* 30:228–241. doi:10.1016/j.immuni.2008.12.015
- Linterman, M.A., R.J. Rigby, R.K. Wong, D. Yu, R. Brink, J.L. Cannons, P.L. Schwartzberg, M.C. Cook, G.D. Walters, and C.G. Vinuesa. 2009b. Follicular helper T cells are required for systemic autoimmunity. *J. Exp. Med.* 206:561–576. doi:10.1084/jem.20081886
- Peitz, M., R. Jäger, C. Patsch, A. Jäger, A. Egert, H. Schorle, and F. Edenhofer. 2007. Enhanced purification of cell-permeant Cre and germline transmission after transduction into mouse embryonic stem cells. *Genesis.* 45:508–517. doi:10.1002/dvg.20321
- Rickert, R.C., J. Roes, and K. Rajewsky. 1997. B lymphocyte-specific, Cre-mediated mutagenesis in mice. *Nucleic Acids Res.* 25:1317–1318. doi:10.1093/nar/25.6.1317

- Rodríguez, C.I., F. Buchholz, J. Galloway, R. Sequerra, J. Kasper, R. Ayala, A.F. Stewart, and S.M. Dymecki. 2000. High-efficiency deleter mice show that FLPe is an alternative to Cre-loxP. *Nat. Genet.* 25:139–140. doi:10.1038/75973
- Schmidt-Supprian, M., W. Bloch, G. Courtois, K. Addicks, A. Israël, K. Rajewsky, and M. Pasparakis. 2000. NEMO/IKK gamma-deficient mice model incontinentia pigmenti. *Mol. Cell.* 5:981–992. doi:10.1016/S1097-2765(00)80263-4
- Vinuesa, C.G., M.C. Cook, C. Angelucci, V. Athanasopoulos, L. Rui, K.M. Hill, D. Yu, H. Domaschensz, B. Whittle, T. Lambe, et al. 2005. A RING-type ubiquitin ligase family member required to repress follicular helper T cells and autoimmunity. *Nature.* 435:452–458. doi:10.1038/nature03555
- Yu, D., and C.G. Vinuesa. 2010. Multiple checkpoints keep follicular helper T cells under control to prevent autoimmunity. *Cell. Mol. Immunol.* 7:198–203. doi:10.1038/cmi.2010.18
- Yu, D., A.H. Tan, X. Hu, V. Athanasopoulos, N. Simpson, D.G. Silva, A. Hutloff, K.M. Giles, P.J. Leedman, K.P. Lam, et al. 2007. Roquin represses autoimmunity by limiting inducible T-cell co-stimulator messenger RNA. *Nature.* 450:299–303. doi:10.1038/nature06253

SUPPLEMENTAL MATERIAL

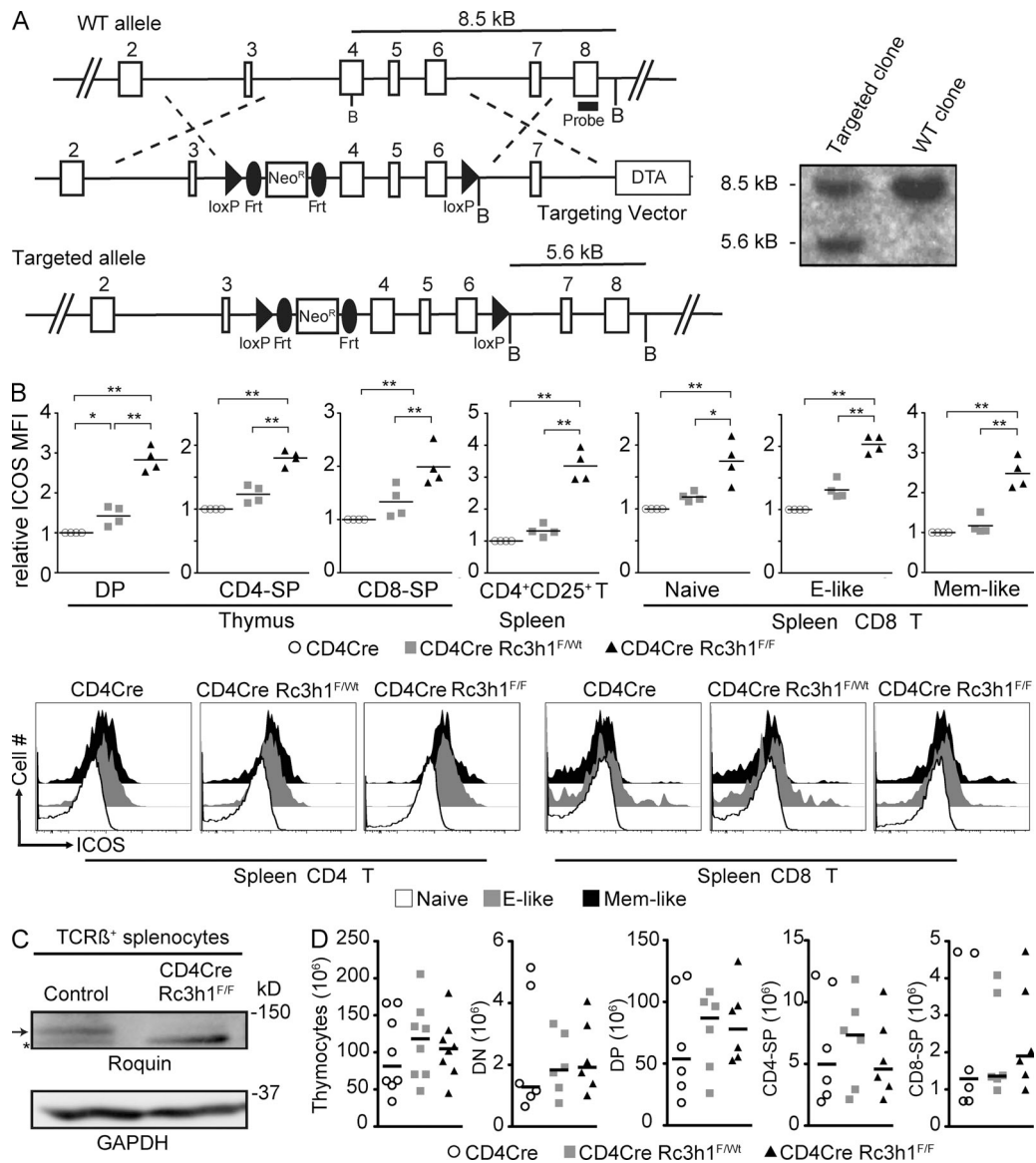
Bertossi et al., <http://www.jem.org/cgi/content/full/jem.20110578/DC1>

Figure S1. Conditional targeting strategy of the *Rc3h1* allele and ablation of Roquin in T cells. (A) Schematic representation of the gene targeting construct, the screening strategy used to generate the loxP-flanked *rc3h1* allele (left), and Southern blot of BamHI-digested ES cell DNA showing the targeted allele (right). (B, top) Relative ICOS MFI in different T cell subsets. Thymocyte subsets (top left): DP, CD4/CD8 double positive; SP, single positive. Splenic T cells (top right): naive, CD44^{lo}CD62L^{hi}; effector (E)-like, CD44^{hi}CD62L^{lo}; memory (Mem)-like, CD44^{hi}CD62L^{hi}. Bars indicate medians. (bottom) Representative histograms showing ICOS levels on the indicated splenic T cell subsets. (C) Western blot for Roquin in sorted TCRβ⁺ splenocytes of mice of the indicated genotypes. The arrow indicates Roquin, and the asterisk indicates an unspecific band. (D) Absolute numbers of thymocyte subsets calculated from six to eight mice per genotype: DN, CD4/CD8 double negative; DP, double positive; SP, single positive. Bars represent medians. *, P < 0.05; **, P < 0.001; one-way ANOVA.

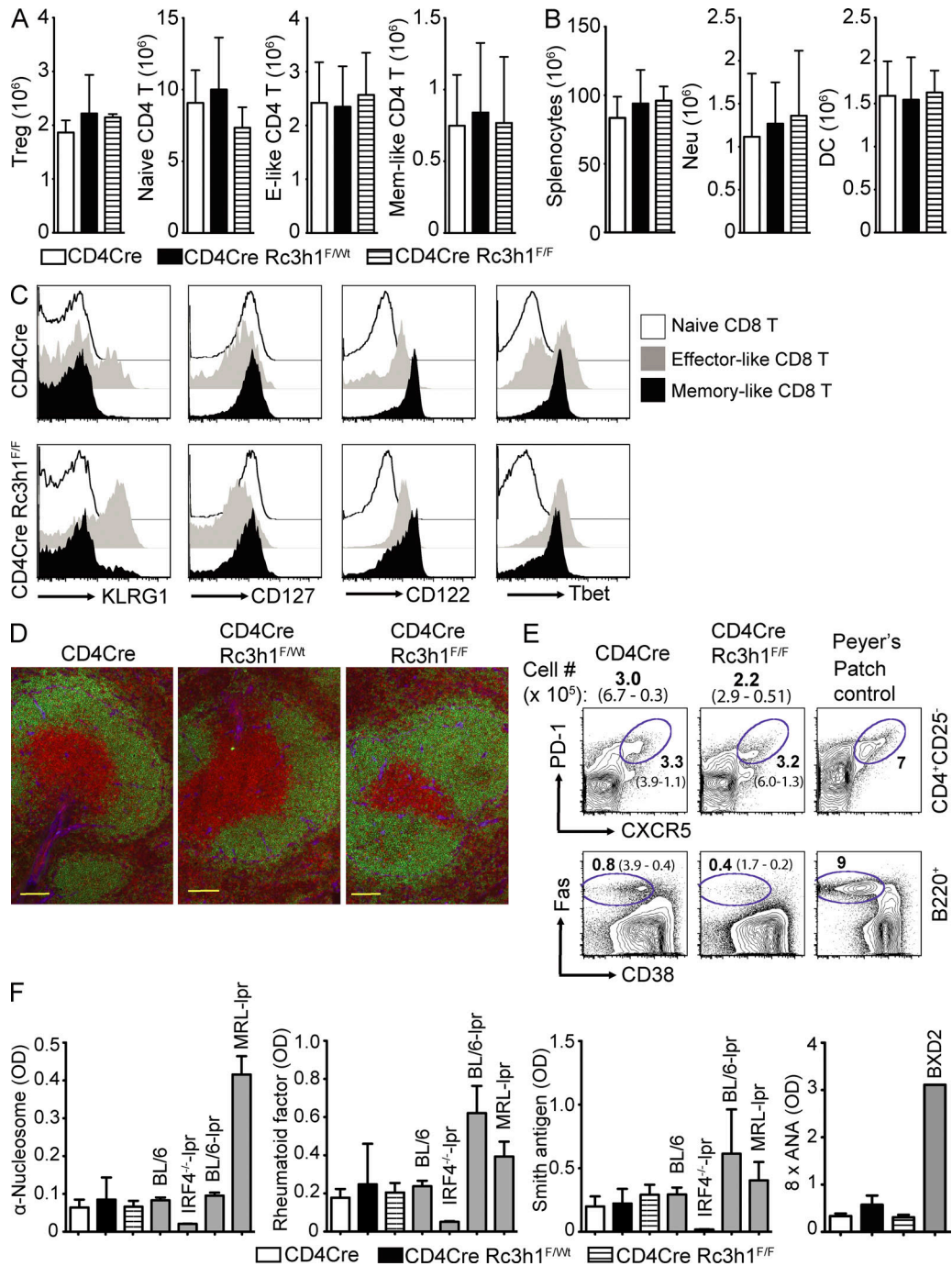


Figure S2. Effects of T cell-specific ablation of Roquin. (A) Bar charts of absolute numbers of splenic CD4 T cell subsets: T_{reg} cells, FoxP3⁺; naive, CD25⁻CD44^{lo}CD62L^{hi}; effector (E)-like, CD25⁻CD44^{hi}CD62L^{lo}; memory (Mem)-like, CD25⁻CD44^{hi}CD62L^{hi}. Columns and error bars represent means ± SD of four to nine mice per genotype. (B) Bar charts of absolute numbers of splenocytes, neutrophils (Neu; Mac1⁺Gr1^{hi}SiglecF⁻), and DCs (CD11c⁺) calculated from six to eight mice of the indicated genotypes. Columns and error bars represent means ± SD. (C) Representative histograms showing KLRG1, CD127, CD122, and Tbet expression levels on the indicated splenic CD8 T cell subsets (*n* = 4–5). (D) Immunofluorescence of spleen sections: green, α-B220; red, α-CD3; blue, α-laminin. Bars, 100 μm. (E) Contour plots of the proportions of follicular T helper cells (PD-1^{hi}CXCR5^{hi}; *n* = 5) in CD4 T cells and of germinal center B cells (GCB; Fas^{hi}CD38^{lo}; *n* = 5) in B cells; *n* refers to the number of mice per genotype analyzed. Numbers next to the gates indicate medians, and numbers in parentheses indicate upper and lower limits. Cell # indicates median of absolute cell numbers of follicular T helper cells in spleens of mice of the indicated genotypes, and numbers in parentheses indicate upper and lower limits (*n* = 5). Peyer's patches from BL/6 mice were used as staining positive control. (F) Titers of autoantibodies against nucleosomes, endogenous IgG (rheumatoid factor), Smith antigen (RNA), and eight different nuclear autoantigens (8x ANA) were determined in the serum of 3–10-mo-old mice of the indicated genotypes by ELISA. Columns and error bars represent means ± SD of 9–12 mice per group. Sera from BL/6, IRF4^{-/-}-lpr, BXD2, BL/6-lpr, and MRL-lpr mice were used as positive or negative controls.

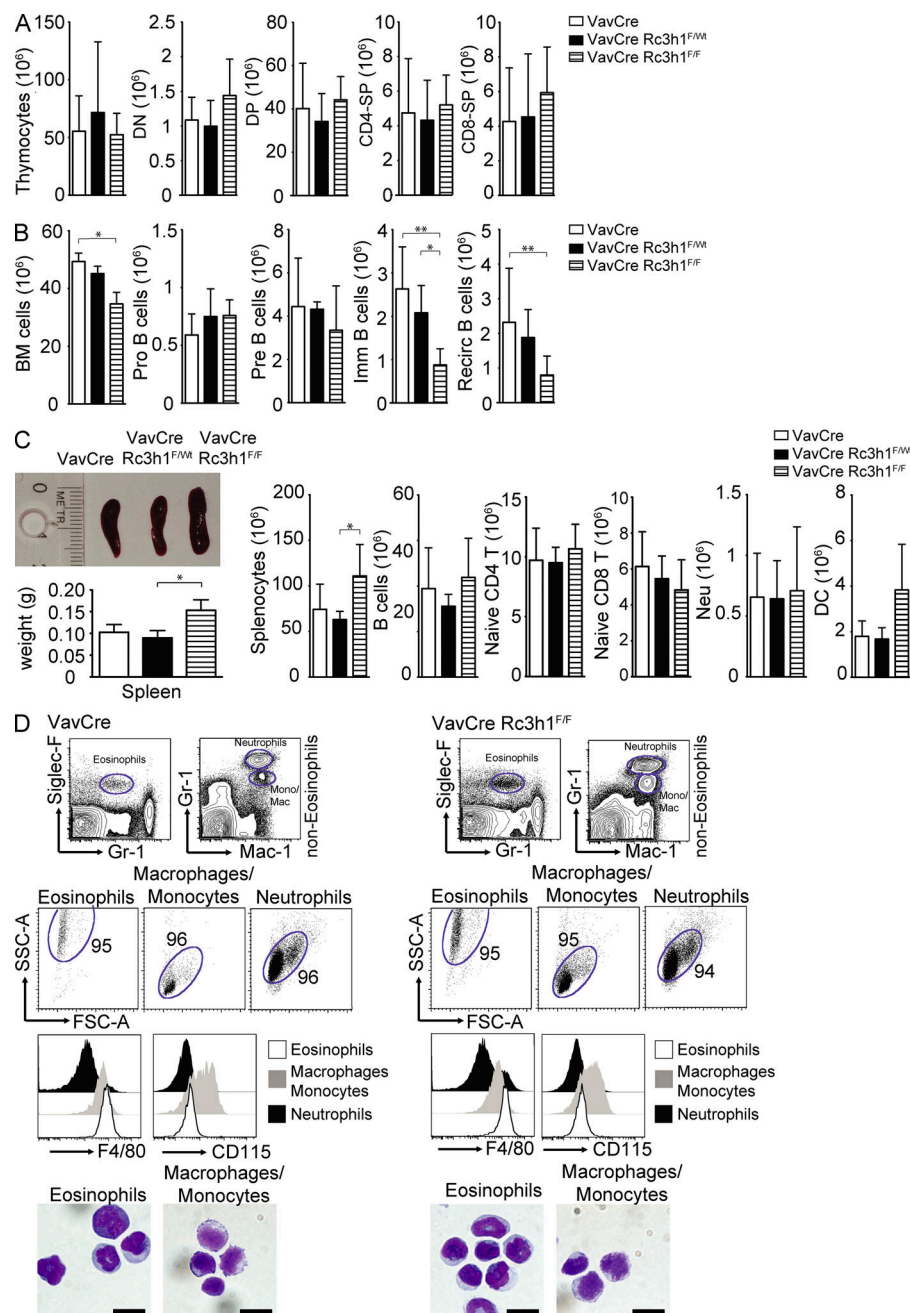


Figure S3. Effects of a Roquin-deficient hematopoietic system. (A and B) Absolute cell numbers of total thymocytes and of thymocyte subsets (A) and of total BM cells and BM B cell subsets (B) calculated from five to nine mice per genotype. DN, CD4/CD8 double negative; DP, double positive; SP, single positive; pro B, B220^{lo}IgM⁻CD25⁻c-Kit⁺; pre B, B220^{lo}IgM⁻CD25⁺c-Kit⁻; immature (Imm) B, B220^{lo}IgM⁺; recirculating (Recirc) B, B220^{hi}IgM⁺. Columns and error bars represent means \pm SD. (C) Representative spleen sizes (top left) and weight calculated from seven to nine mice per genotype (bottom left). (right) Total splenocyte ($n = 9-11$), B cell (B220⁺; $n = 9-11$), naive CD4 and CD8 T cell (CD44^{lo}CD62L^{hi}; $n = 9-7$), neutrophil (Neu; Mac1⁺Gr1^{hi}SiglecF⁻; $n = 4-6$), and DC (CD11c⁺; $n = 4-6$) numbers in spleens of mice of the indicated genotypes. Error bars indicate SD. (D) Representative contour plots (top) showing the gating strategy for eosinophils (Gr1^{int}SiglecF⁺), neutrophils (Mac1⁺Gr1^{hi}SiglecF⁻), and monocytes/macrophages (Mono/Mac; Gr1^{int}Mac1⁺SiglecF⁻). Representative histograms (third row) showing F4/80 and CD115 expression levels on the indicated cell subsets. SSC-A/FSC-A dot plot (second row) of eosinophils, macrophages/monocytes and neutrophils. Numbers next to gates indicate percentage; data are representative for four mice per genotype. (bottom) Cytopin of FACS-sorted eosinophils (Gr1^{int}SiglecF^{hi}) and macrophages/monocytes (Gr1^{int}Mac1⁺SiglecF⁻) from spleens of mice of the indicated genotypes stained using Hemacolor rapid staining. Bars, 10 μ m. *, $P < 0.05$; **, $P < 0.001$; one-way ANOVA.

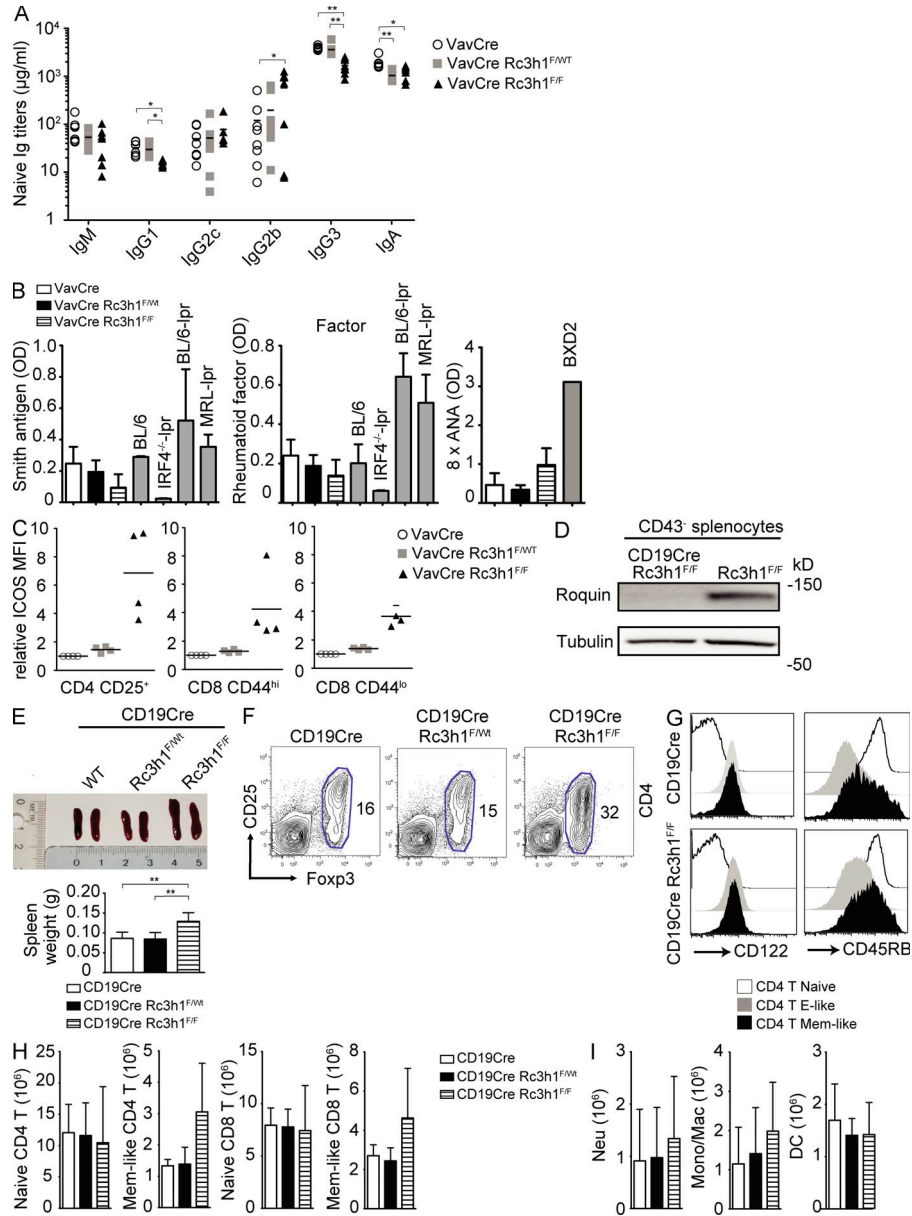


Figure S4. Roquin-deficient B cells cause deregulation of immune homeostasis. (A) Total levels of the indicated Igs in serum of naive mice of the indicated genotypes. Bars indicate mean of five to eight mice per genotype. (B) Titers of antibodies against Smith antigen ($n = 8-10$), rheumatoid factor ($n = 8-10$), and eight different nuclear autoantigens (8x ANA; $n = 4-6$) in serum from 2-7-mo-old mice of the indicated genotype. Sera from BL/6, IRF4^{-/-}-lpr, BXD2, BL/6-lpr, and MRL-lpr mice were used as positive or negative controls. Error bars indicate SD. (C) Relative ICOS MFI on the indicated splenic T cells subsets. Mice were analyzed in four sets of three genotypes, and the ICOS MFI for the VavCre control cells was set to 1 for each set. Bars indicate the median. (D) Western blot for Roquin protein levels in CD43⁺ splenocytes of mice of the indicated genotypes. (E) Representative spleen sizes (top) and spleen weight (bottom) calculated from eight mice per group. Columns and error bars indicate means \pm SD. (F) Contour plots showing the proportions of T_{reg} cells (FoxP3⁺) of CD4 T cells in the spleens of the indicated mice. (G) Representative histograms showing CD122 and CD45RB expression levels on the indicated subsets of splenocytes from control (top) or B ^{Δ Rc3h1} (bottom) mice ($n = 4$). (H and I) Absolute cell numbers of naive (CD44^{lo}CD62L^{hi}) and memory (Mem)-like (CD44^{hi}CD62L^{lo}) CD4 (H, left) and CD8 (H, right) T cells and splenic myeloid cells (I); Neu, neutrophils (Mac1⁺Gr1^{hi}SiglecF⁻); Mono/Mac, monocytes/macrophages (Gr1^{int}Mac1⁺SiglecF⁻); DC, CD11c⁺. Columns and error bars indicate means \pm SD of four to eight mice per genotype. *, $P < 0.05$; **, $P < 0.001$; one-way ANOVA.

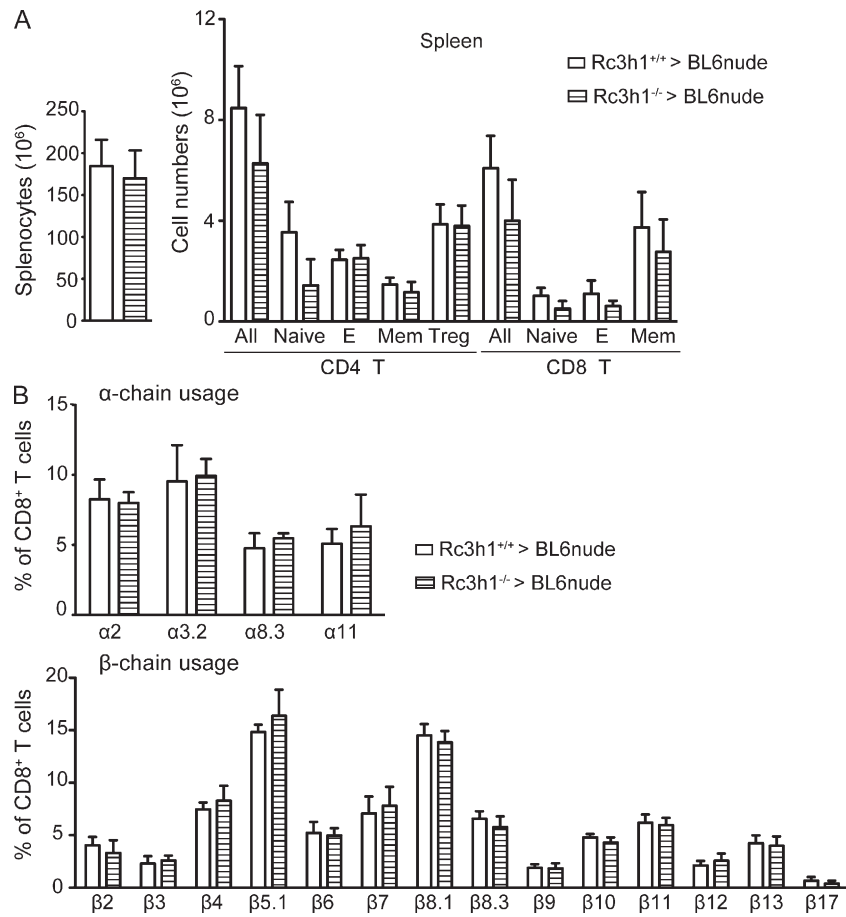


Figure S5. Normal T cell development and selection in nude mice transplanted with *Rc3h1*^{-/-} fetal thymic epithelial cells. (A) Absolute numbers of splenocytes and splenic CD4 and CD8 T cells subsets calculated from five to six mice per genotype. T_{reg} cells, CD4⁺FoxP3⁺; naive, CD44^{lo}CD62L^{hi}; effector (E)-like, CD44^{hi}CD62L^{lo}; memory (Mem)-like, CD44^{hi}CD62L^{hi}. (B) Proportions of α - (top) and β - (bottom) TCR chain usage in splenic CD8 T cells. (A and B) Columns and error bars represent means \pm SD of five to six mice per group.

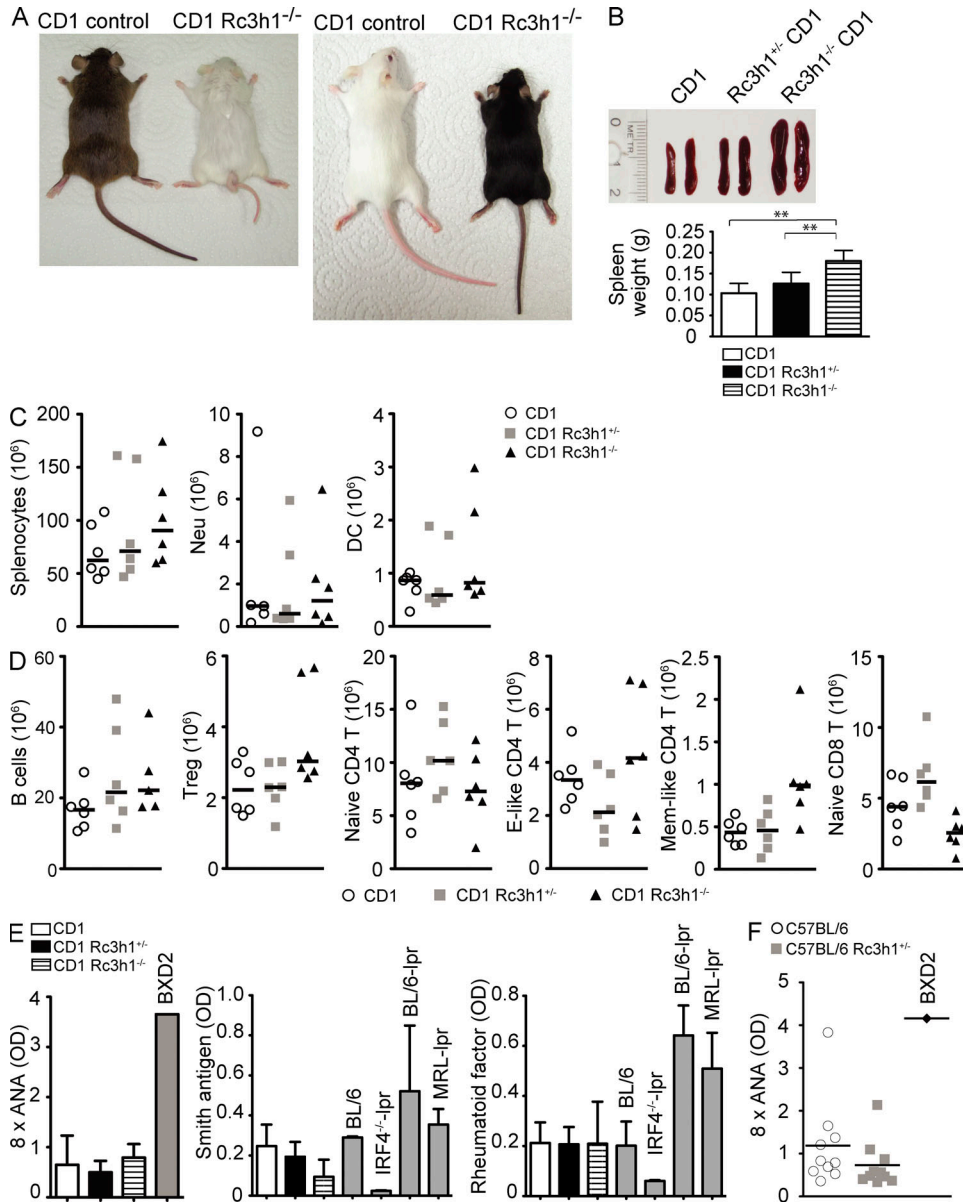


Figure S6. Growth retardation and immune phenotypes of CD1 Rc3h1^{-/-} mice. (A) Pictures of 3-mo-old CD1 Rc3h1^{-/-} mice and littermate controls. (B) Representative spleen sizes of 2–3-mo-old mice (top). Mean spleen weight calculated from six mice of the indicated genotypes (bottom). Error bars indicate SD. (C and D) Absolute cell numbers of splenocytes, neutrophils (Neu; Mac1⁺Gr1^{hi}Siglec-F⁻), and DCs (CD11c⁺); (C) and B cells, CD4 T cells subsets (T_{reg} cells, CD4⁺FoxP3^{hi}; naive, CD25⁻CD44^{lo}CD62L^{hi}; effector [E]-like, CD25⁻CD44^{hi}CD62L^{lo}; memory [Mem]-like, CD25⁻CD44^{hi}CD62L^{hi}) and naive (CD44^{lo}CD62L^{hi}) CD8 T cells (D) in five to six mice of the indicated genotype. Bars represent medians. (E) Serum titers of antibodies against eight prevalent nuclear autoantigens (8x ANA), Smith antigen, and endogenous IgG (rheumatoid factor) were determined in 2.5–3.5-mo-old mice of the indicated genotype by ELISA. Columns and error bars represent means ± SD of eight to nine mice per group. Sera from BL/6, IRF4^{-/-}-lpr, BXD2, BL/6-lpr, and MRL-lpr were used as positive or negative controls. (F) Serum titers of antibodies against eight prevalent nuclear autoantigens in 10 C57BL/6 (four males at 5–15 mo and six females at 3–9 mo) and 10 C57BL/6 Roquin^{+/-} mice (seven males at 3–8 mo and three females at 4–6 mo). Sera from a BXD2 mouse was used as a positive control. Bars indicate the mean. **, P < 0.001; one-way ANOVA.

SUPPLEMENTAL MATERIALS AND METHODS

Cytology. A cytospin was prepared by using Shandon Cytospin4 (Thermo Fisher Scientific). The staining was performed by using Hemacolor Stain Solution (Merck) according to the manufacturer's instructions. Images were acquired using a microscope (Axioskop; Carl Zeiss) with a camera (DC500; Leica).

ELISA. Serum Ig concentrations were determined by ELISA as described previously (Schmidt-Supprian et al., 2004).

REFERENCE

Schmidt-Supprian, M., J. Tian, H. Ji, C. Terhorst, A.K. Bhan, E.P. Grant, M. Pasparakis, S. Casola, A.J. Coyle, and K. Rajewsky. 2004. I kappa B kinase 2 deficiency in T cells leads to defects in priming, B cell help, germinal center reactions, and homeostatic expansion. *J. Immunol.* 173:1612–1619.